

## **Supplementary information**

**Hydroxynitrile lyase engineering for promiscuous asymmetric Henry reaction with enhanced conversion, enantioselectivity and catalytic efficiency**

Badipatla Vishnu Priya,<sup>a</sup> D. H. Sreenivasa Rao,<sup>a,b</sup> Ayon Chatterjee,<sup>a,b</sup> and Santosh Kumar

Padhi\*<sup>a</sup>

## **Table of contents**

1. Materials and methods.....	3
2. Supporting figures and spectra.....	5
3. Supporting tables.....	77
4. References.....	87

## 1. Materials and methods

### 1.1. Chemicals and materials

*AtHNL* (UniProt accession ID: Q9LFT6) synthetic gene cloned in pET28a was obtained from Abgenex Pvt. Ltd, India. Culture media and kanamycin were procured from HiMedia laboratory Pvt. Ltd, India. Isopropyl- $\beta$ -D-1-thiogalactopyranoside (IPTG) was purchased from BR-BIOCHEM Pvt. Ltd, India. Chemicals such as aldehydes, nitromethane and mandelonitrile were purchased from Sigma Aldrich, AVRA, SRL and Alfa-Aesar. HPLC grade solvents were purchased from RANKEM, Molychem, FINAR, and SRL.

### 1.2. Primers employed in this work

Primers were synthesized by Eurofins Genomics India Pvt. Ltd., Hyderabad, India (Table S1).

### 1.3. Preparation of *AtHNL* variant library

The library of *AtHNL* variants used for screening in the current study was created by site saturation mutagenesis (SSM). At Tyr14, Phe179, two saturation libraries were prepared by SSM using protocol mentioned in our previous paper.<sup>1</sup>

### 1.4. Preparation of *AtHNL* double variants

To prepare Y14F-F179N, and Y14F-F179W, PCR composition and conditions were maintained similar to that described earlier,<sup>1</sup> F179N and F179W plasmids were taken as templates and forward and reverse primers for Y14F (Table S1) were used in the PCR. To prepare Y14M-F179N and Y14M-F179W, we used Y14M plasmid as a template with F179N and F179W forward and reverse primers (Table S1) with same PCR conditions as used earlier.<sup>1</sup>

### 1.5. Enzyme purification

Expression and purification of *AtHNL* wild type and its mutants was carried out using the protocol described earlier.<sup>2</sup>

### 1.6. HNL assay

The assay was performed in a 96 well microtiter plate and was monitored using a Multiskan GO UV–Visible spectrophotometer at 25°C. Each well contained reaction mixture of 160  $\mu$ L 50 mM citrate phosphate buffer (pH 5.5), 20  $\mu$ L purified enzyme (1 mg/mL), and 20  $\mu$ L substrate [racemic MN, 67 mM / racemic NPE, 20 mM] pre-dissolved in 1 mL of 5 mM citrate buffer (pH 3.15) making a total volume of 200  $\mu$ L. The control experiment was carried out identically except the enzyme is replaced with 20 mM KPb, pH 7.0. The assay was done in triplicates and the absorbance of the control resulting due to the spontaneous reaction was subtracted from the enzymatic reaction. The assay measured the formation of benzaldehyde resulting from enzymatic cleavage of MN or NPE at 280 nm. The activity was calculated using the molar extinction coefficient of benzaldehyde (1376 M<sup>-1</sup> cm<sup>-1</sup>).

### 1.7. Synthesis of racemic $\beta$ -nitro alcohols

Racemic synthesis of various  $\beta$ -nitro alcohols was carried out by addition of aldehydes to nitromethane in 1:10 molar ratio in the presence of 5 mol% of Ba(OH)<sub>2</sub> as a catalyst as per the procedure described earlier.<sup>2</sup> All the racemic  $\beta$ -nitroalcohols synthesized were confirmed by <sup>1</sup>H and <sup>13</sup>C NMR characterization.

### 1.8. Screening of AtHNL and its variants for (*R*)-NPE synthesis

A reaction mixture of 1 mL containing 125 units of purified variant enzyme and *n*-butyl acetate in equal v/v ratio along with 25  $\mu$ L of nitromethane and 12.5  $\mu$ mol of the benzaldehyde was taken in a 2 mL glass vial. In the control, the enzyme was replaced by an equal volume of 20 mM potassium phosphate buffer (KPB). The reaction mixture was placed on a thermomixer at 1,200 rpm for 3 h at 30 °C. After every hour, 100  $\mu$ L of aliquot was taken and extracted with 150  $\mu$ L of diethyl ether. To this, a pinch of sodium sulfate was added and vortexed. After centrifugation at 10,000 rpm for 2 min at 4°C, the upper layer was taken and this step was repeated one more time. Finally, 20  $\mu$ L of the upper organic layer was taken and analyzed in an HPLC (Agilent) using Chiralpak® IB chiral column using 1 mL/min flow rate and 90:10 of hexane: isopropanol. The % conversion represents the absolute amount of (*R*)-NPE, and was calculated by the equation % C= 
$$\left[ \frac{S-NPE + R-NPE}{S-NPE + R-NPE + \text{benzaldehyde} \cdot \text{conversion factor}} \right]$$
 and % ee = 
$$\left[ \frac{R-S}{S+R} \right] * 100.$$

### 1.9. AtHNL variant catalyzed preparation of various (*R*)- $\beta$ -nitroalcohols using nitroaldol reaction

A reaction mixture consisting of 62.5 or 125 units of purified variant enzyme and *n*-butyl acetate in equal v/v ratio along with 1.75 M of nitromethane and 20 mM of aldehyde was taken in a 2 mL glass vial. After the reaction, the remaining protocols for extraction and HPLC analysis are the same as mentioned above.

### 1.10. Preparative scale synthesis of (*R*)-1-(4-methoxyphenyl)-2-nitroethanol

AtHNL-Y14M-F179W catalysed preparative scale synthesis of (*R*)-1-(4-methoxyphenyl)-2-nitroethanol was carried out using crude cell lysates (12.06 $\pm$ 0.4 U/mg). Ten mini preparative scale reactions each containing 1000 U (680  $\mu$ L, 123 mg/mL) of Y14M-F179W cell lysate along with equal v/v of *n*-butyl acetate (680  $\mu$ L), 1.75 M of nitromethane (144.5  $\mu$ L), 100 mM of 4-methoxybenzaldehyde (18.18  $\mu$ L, 150 mmol), and 23  $\mu$ L double distilled water were taken in a 2 mL microcentrifuge tube. The total reaction volume of each reaction was 1.5 mL. Reactions were incubated in a thermoshaker at 1200 rpm, 30 °C for 18 h. At the end of 18 h, reaction mixture was extracted with ethyl acetate, the organic layer was collected and dried over anhydrous sodium sulfate and concentrated in vacuum. The product was analysed by chiral HPLC as mentioned above. Column purification of the crude product was done using hexane: ethyl acetate to get pure (*R*)-1-(4-methoxyphenyl)-2-nitroethanol. The purified product was confirmed by <sup>1</sup>H and <sup>13</sup>C NMR.

### 1.11. Determination of the kinetic parameters purified AtHNL and its variants towards various substrates using Henry reaction

A reaction mixture of 0.5 mL consisting of 1 mg of purified enzyme in 20 mM KPB and *n*-butyl acetate in equal v/v ratio along with 1.75 M of nitromethane and 0.5-24 mM of aldehyde concentration was taken in a 2 mL glass vial. The reaction mixture was placed on a thermomixer at 1,200 rpm for 30 minutes (40 minutes for 2,4-dimethoxybenzaldehyde and 3,4,5-trimethoxybenzaldehyde, 1 h for *trans* cinnamaldehyde) at 30 °C. After the reaction, the remaining protocols for extraction and HPLC analysis are the same as mentioned in the screening section above. In the control, the enzyme was replaced by an equal volume of 20 mM potassium phosphate buffer (KPB) and all the reaction are done in triplicates. Rate of the reaction against each substrate concentration was determined from the HPLC analysis based on the amount of product formed. Solver function in Microsoft excel was used to best fit the data to Michaelis – Menten equation.

## 2. Supporting figures and spectra

### NMR characterization of racemic $\beta$ -nitroalcohols

Six racemic  $\beta$ -nitroalcohols, **2a**, **2d**, **2e**, **2g**, **2j** and **2l** were used by us in a previous study and their  $^1\text{H}$  and  $^{13}\text{C}$  NMR are given in the Supporting information of the Adv. Synth. Catal. 2021, 363, 5310–5318, section 4.2.<sup>3</sup>  $^1\text{H}$  and  $^{13}\text{C}$  NMR of the remaining racemic  $\beta$ -nitroalcohols used in this study are given below.

#### (*E*)-1-nitro-4-phenylbut-3-en-2-ol **2b**<sup>4</sup>

$^1\text{H}$  NMR (400 MHz,  $\text{CDCl}_3$ )  $\delta$  7.43 – 7.27 (m, 5H), 6.78 (dd,  $J = 15.9, 1.4$  Hz, 1H), 6.14 (dd,  $J = 15.9, 6.3$  Hz, 1H), 5.04 (dt,  $J = 7.8, 5.8$  Hz, 1H), 4.51 (d,  $J = 6.5$  Hz, 2H), 2.77 (s, 1H);  $^{13}\text{C}$  NMR (101 MHz,  $\text{CDCl}_3$ )  $\delta$  135.99, 133.96, 128.91, 128.66, 126.95, 125.57, 80.22, 69.76.

#### 1-(4-Fluorophenyl)-2-nitroethanol **2c**<sup>4</sup>

$^1\text{H}$  NMR (500 MHz,  $\text{CDCl}_3$ )  $\delta$  7.42 – 7.33 (m, 2H), 7.14 – 7.03 (m, 2H), 5.44 (dd,  $J = 9.6, 3.0$  Hz, 1H), 4.57 (dd,  $J = 13.3, 9.6$  Hz, 1H), 4.48 (dd,  $J = 13.4, 3.1$  Hz, 1H), 3.07 (s, 1H);  $^{13}\text{C}$  NMR (126 MHz,  $\text{CDCl}_3$ )  $\delta$  164.00, 162.03, 134.07, 134.04, 127.94, 127.88, 116.21, 116.03, 81.24, 70.45.

#### 1-(2,4-Dimethoxyphenyl)-2-nitroethanol **2f**<sup>5</sup>

$^1\text{H}$  NMR (400 MHz,  $\text{CDCl}_3$ )  $\delta$  7.31 (d,  $J = 8.4$  Hz, 1H), 6.50 (dd,  $J = 8.4, 2.4$  Hz, 1H), 6.46 (d,  $J = 2.4$  Hz, 1H), 5.60 – 5.49 (m, 1H), 4.64 – 4.54 (m, 2H), 3.84 (s, 3H), 3.80 (s, 3H), 3.19 (d,  $J = 6.4$  Hz, 1H);  $^{13}\text{C}$  NMR (101 MHz,  $\text{CDCl}_3$ )  $\delta$  161.73, 157.67, 128.30, 119.24, 105.40, 99.31, 80.45, 67.90, 55.68, 55.66.

### 1-(3-Methylphenyl)-2-nitroethanol 2h<sup>6</sup>

<sup>1</sup>H NMR (500 MHz, CDCl<sub>3</sub>) δ 7.31 (1H, dd, *J* = 7.5, 4.0 Hz), 7.17-7.21 (3H, m), 5.40 (1H, d, *J* = 9.5 Hz), 4.56-4.60 (1H, m), 4.47-4.50 (1H, m), 3.13-3.19 (1H, m), 2.39 (3H, s); <sup>13</sup>C NMR (125 MHz, CDCl<sub>3</sub>) δ 138.8, 138.1, 129.6, 128.9, 126.6, 123.0, 81.2, 71.0, 21.3.

### 1-(4-Methylphenyl)-2-nitroethanol 2i<sup>6</sup>

<sup>1</sup>H NMR (500 MHz, CDCl<sub>3</sub>) δ 7.29 (2H, d, *J* = 8.5 Hz), 7.23 (2H, d, *J* = 8 Hz), 5.42 (1H, ddd, *J* = 3.0, 3.5, 9.5 Hz), 4.61 (1H, dd, *J* = 9.5, 13.0 Hz), 4.50 (1H, dd, *J* = 3.0, 13.0 Hz), 3.05 (1H, d, *J* = 3.5 Hz), 2.38 (3H, s); <sup>13</sup>C NMR (125 MHz, CDCl<sub>3</sub>) δ 138.9, 135.2, 129.7(X2), 125.9 (X2), 81.2, 70.8, 21.1.

### 1-(3,4,5-Trimethoxyphenyl)-2-nitroethanol 2k<sup>7</sup>

<sup>1</sup>H NMR (400 MHz, CDCl<sub>3</sub>) δ 6.57 (2H, d, 0.4 Hz), 5.38 (1H, d, *J* = 9.6 Hz), 4.62 (1H, dd, *J* = 9.6, 12.8 Hz), 4.51 (1H, d, *J* = 3.2, 12.8 Hz), 3.83 (6H, s), 3.79 (3H, s), 3.34 (1H, d, *J* = 2.4 Hz); <sup>13</sup>C NMR (125 MHz, CDCl<sub>3</sub>) δ 153.5, 137.9, 134.1, 102.8, 81.3, 71.1, 60.8, 56.1.

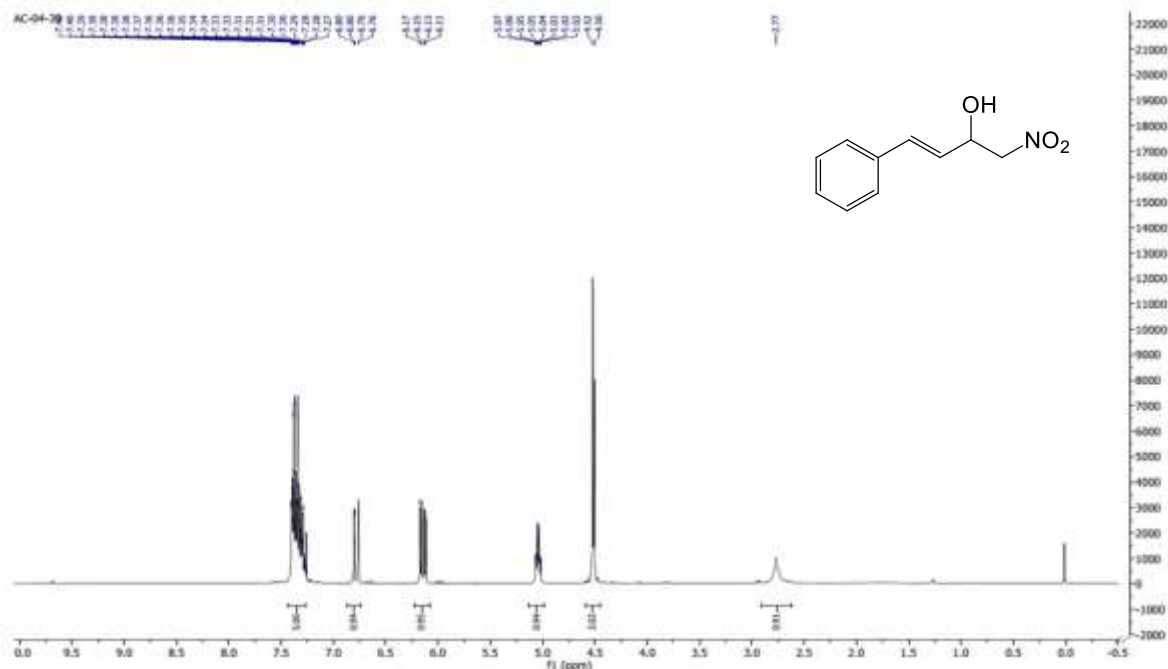


**Figure S1:** <sup>1</sup>H NMR spectrum of (*E*)-1-nitro-4-phenylbut-3-en-2-ol

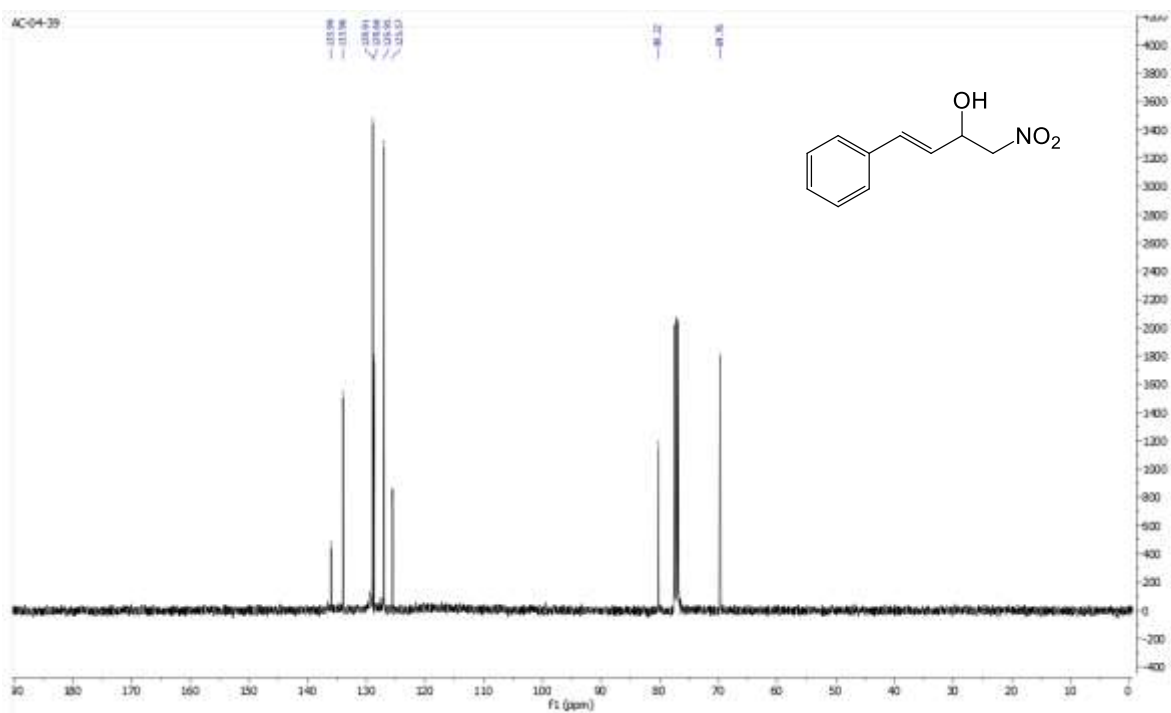


Figure S2:  $^{13}\text{C}$  NMR spectrum of (*E*)-1-nitro-4-phenylbut-3-en-2-ol

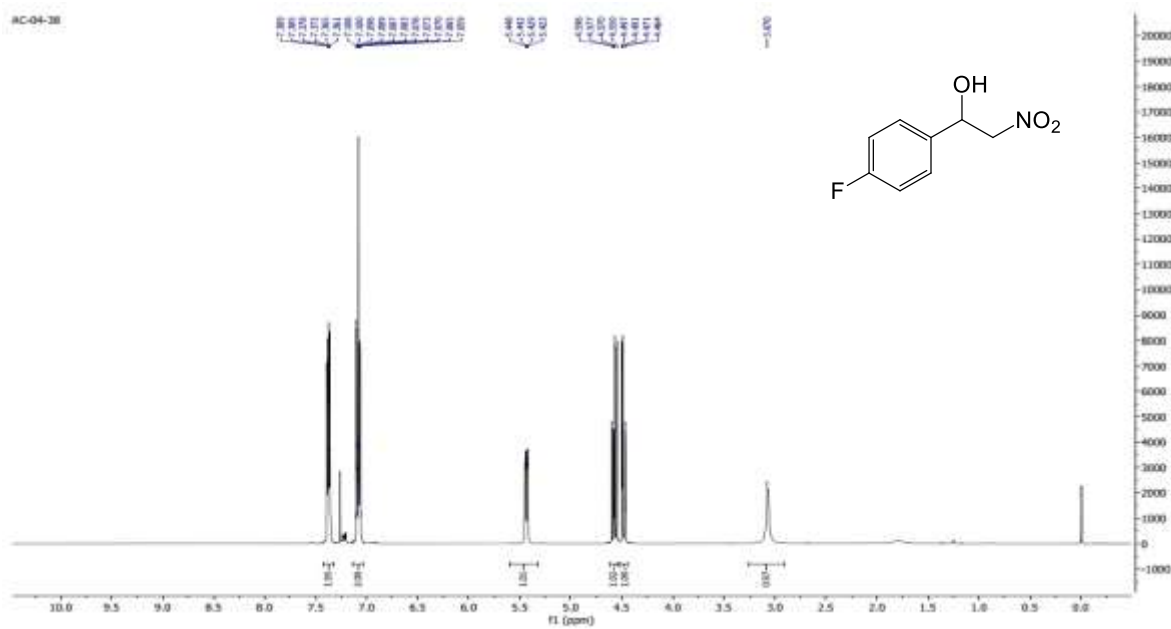
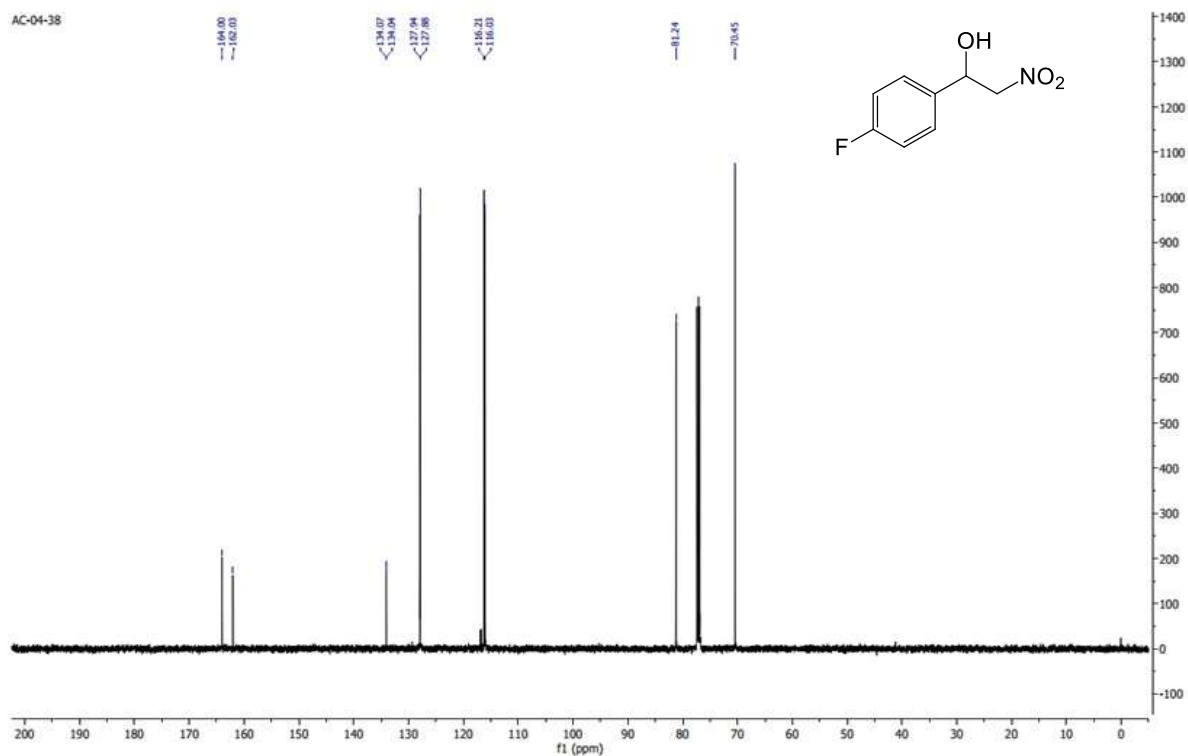
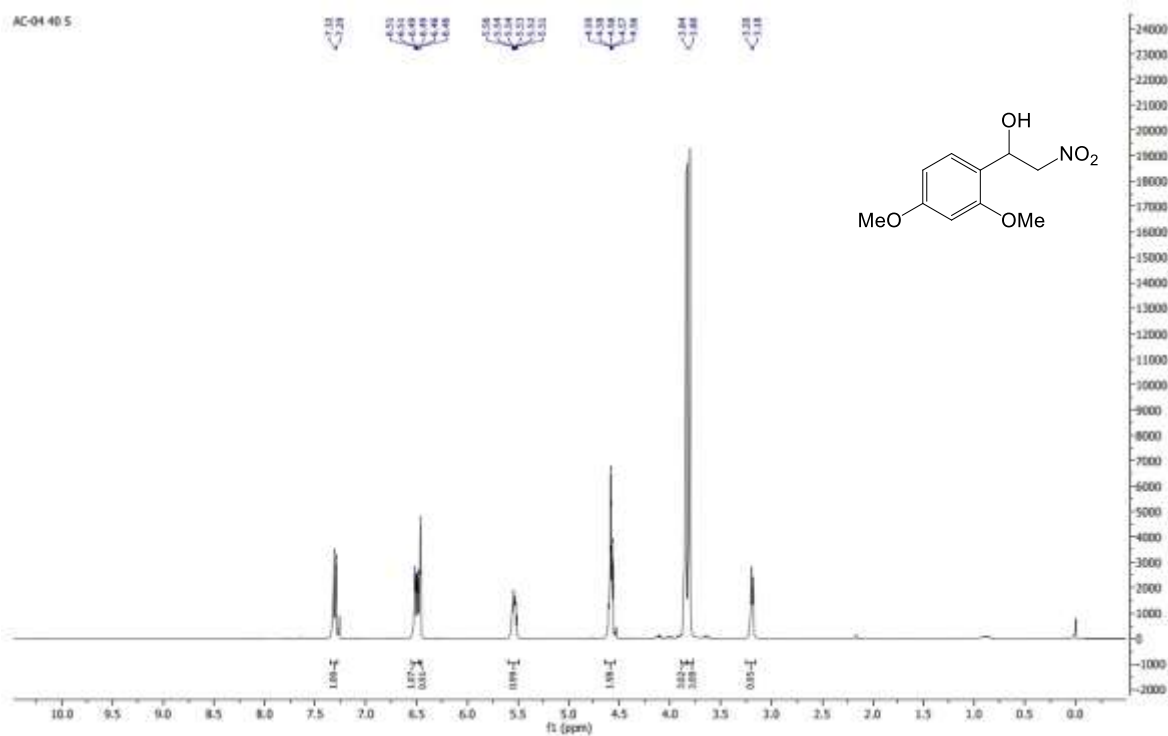


Figure S3:  $^1\text{H}$  NMR spectrum of 1-(4-fluorophenyl)-2-nitroethanol



**Figure S4:**  $^{13}\text{C}$  NMR spectrum of 1-(4-fluorophenyl)-2-nitroethanol



**Figure S5:**  $^1\text{H}$  NMR spectrum of 1-(2,4-Dimethoxyphenyl)-2-nitroethanol



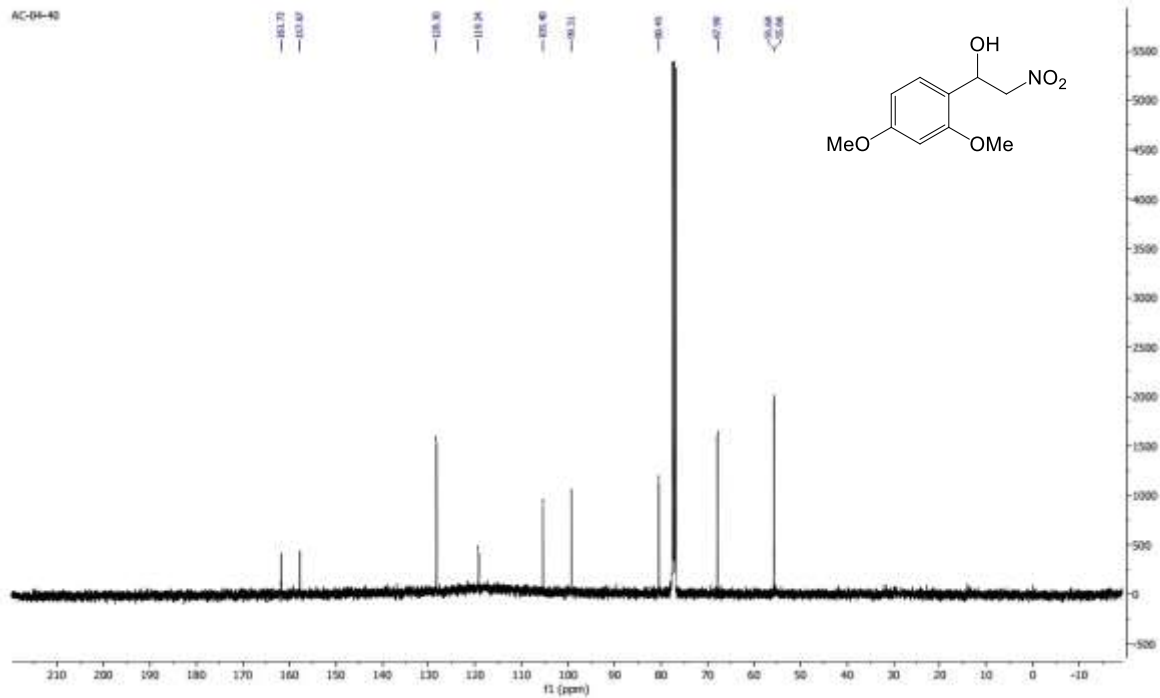


**Figure S6:**  $^{13}\text{C}$  NMR spectrum of 1-(2,4-Dimethoxyphenyl)-2-nitroethanol

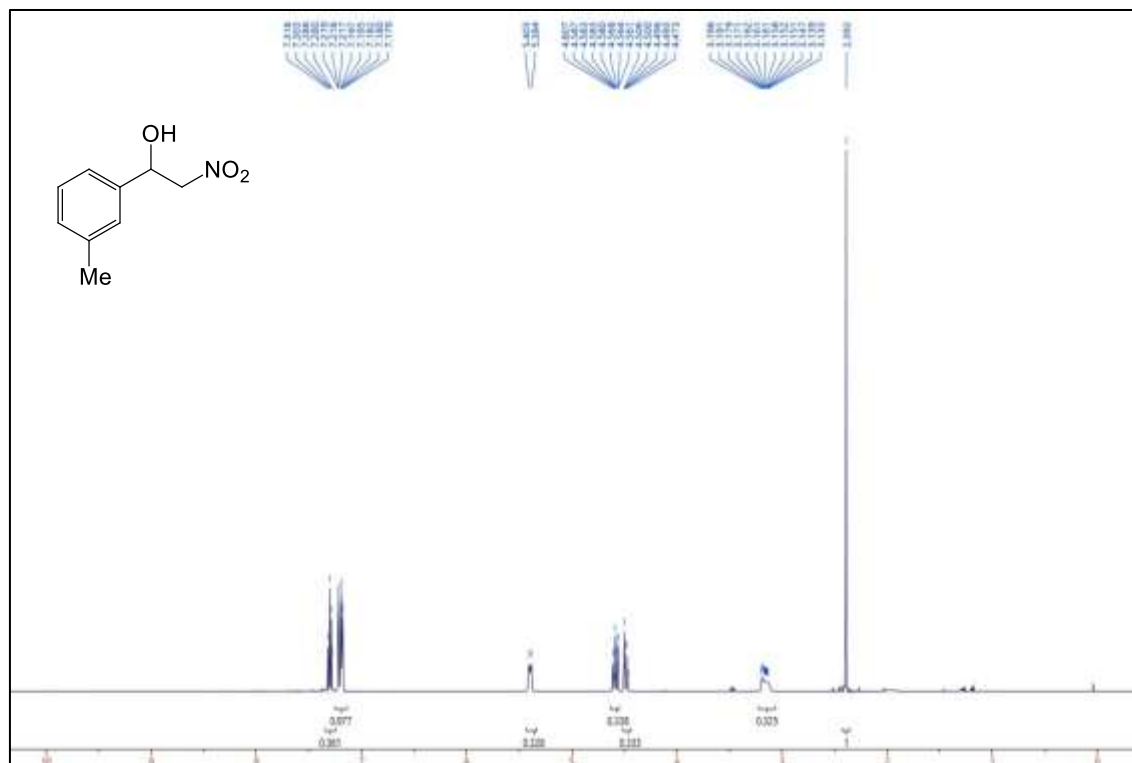


**Figure S7:**  $^1\text{H}$  NMR spectrum of 1-(3-methylphenyl)-2-nitroethanol

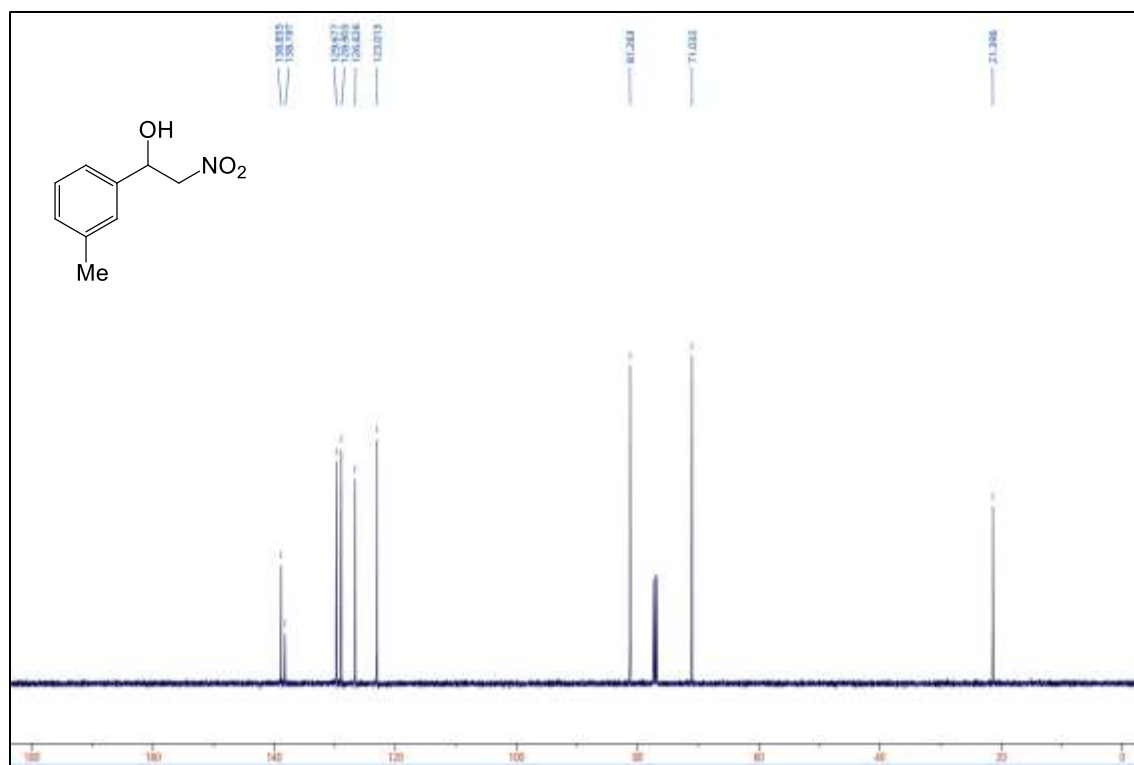


**Figure S8:** <sup>13</sup>C NMR spectrum of 1-(3-methylphenyl)-2-nitroethanol

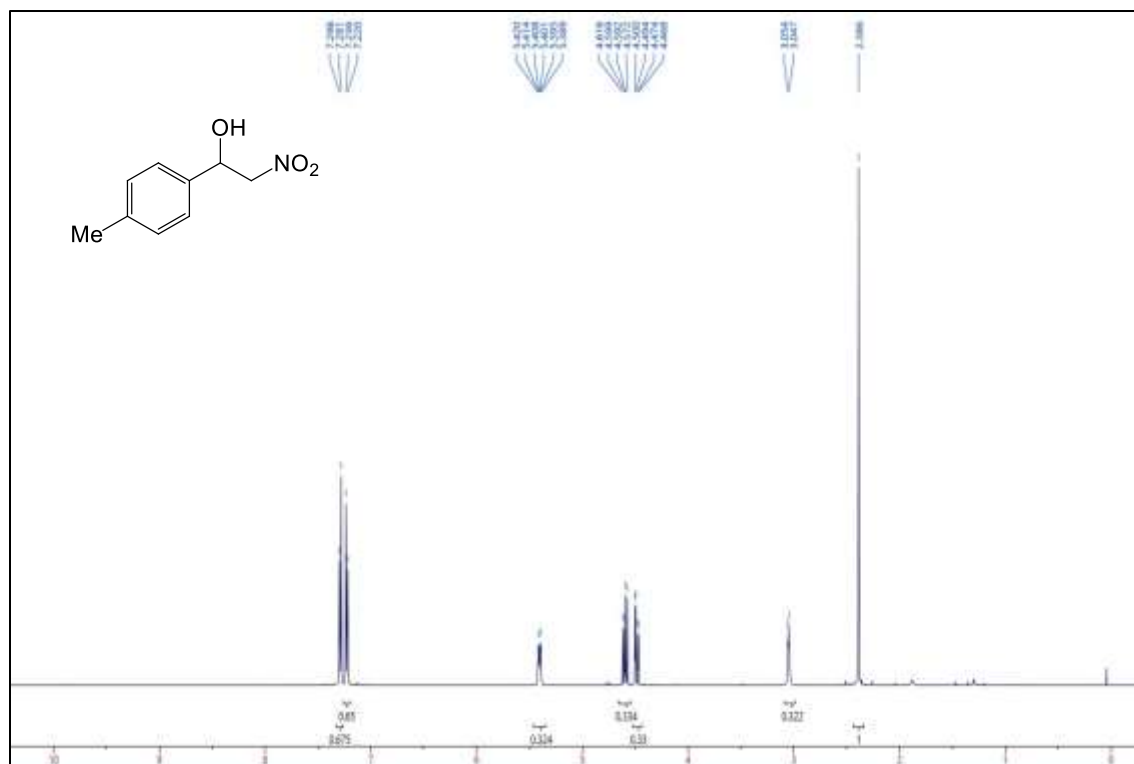


**Figure S9:** <sup>1</sup>H NMR spectrum of 1-(4-Methylphenyl)-2-nitroethanol



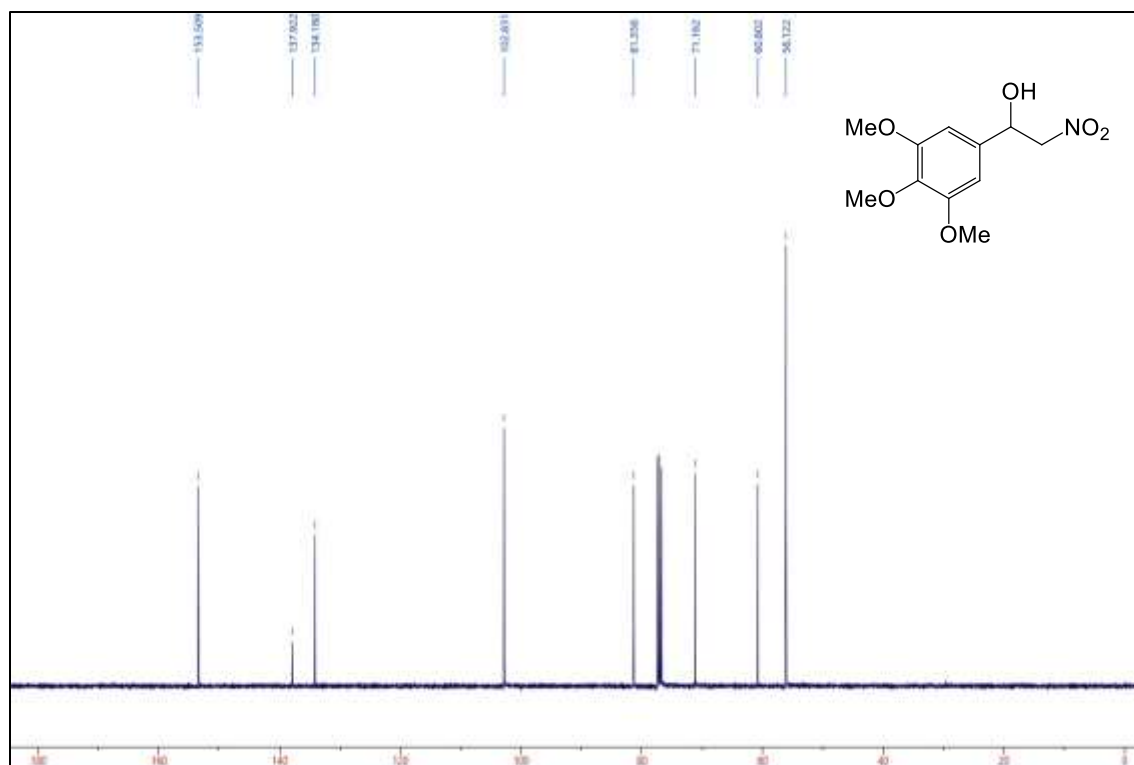


**Figure S12:**  $^{13}\text{C}$  NMR spectrum of 1-(3,4,5-trimethoxyphenyl)-2-nitroethanol

The racemic  $\beta$ -nitroalcohols characterized above were analyzed by chiral HPLC and compared with the biocatalysis products as described below.

**Figure S13 to S25:** Separation and chiral resolution of aldehyde and corresponding racemic  $\beta$ -nitroalcohols

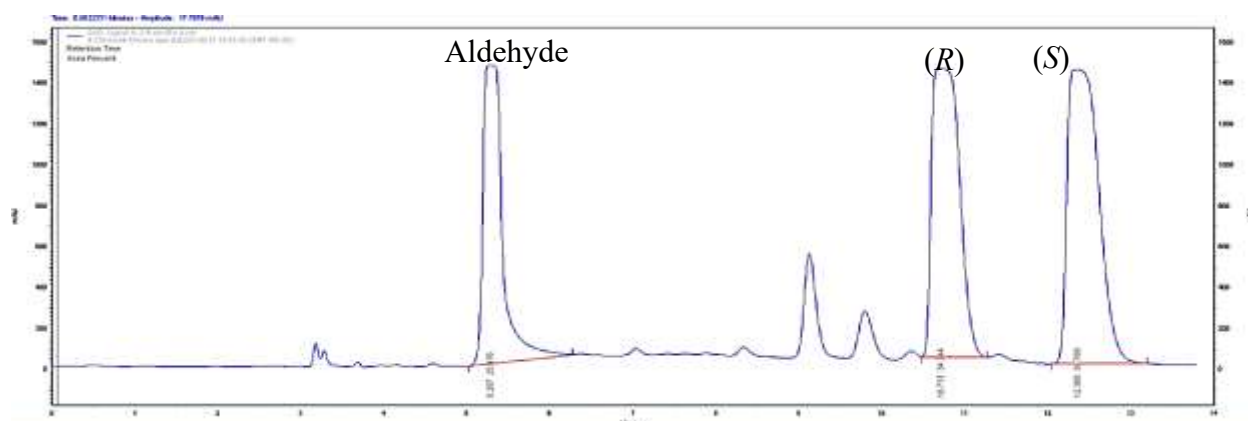


**Figure S13:** HPLC chromatogram of the standards: **1a**, and racemic **2a**.

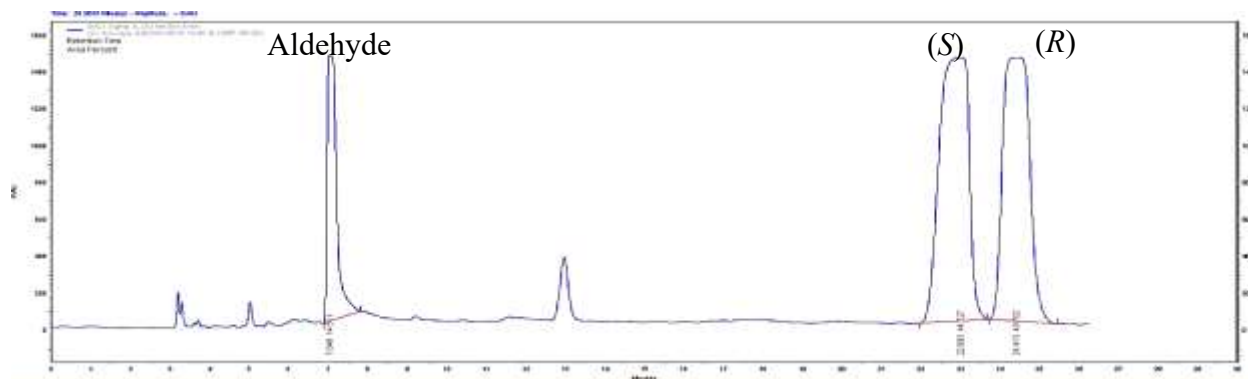


**Figure S14:** HPLC chromatogram of the standards: **1b**, and racemic **2b**.

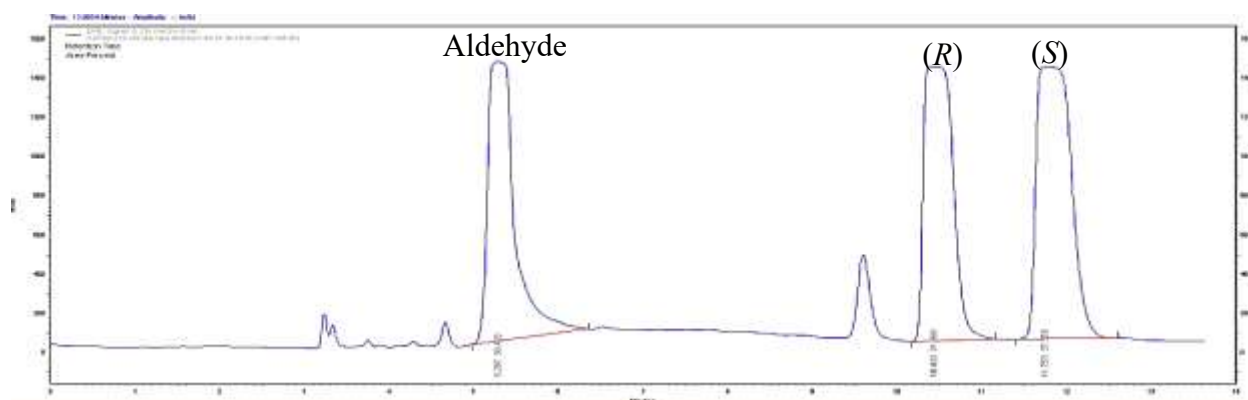


**Figure S15:** HPLC chromatogram of the standards: **1g**, and racemic **2g**.

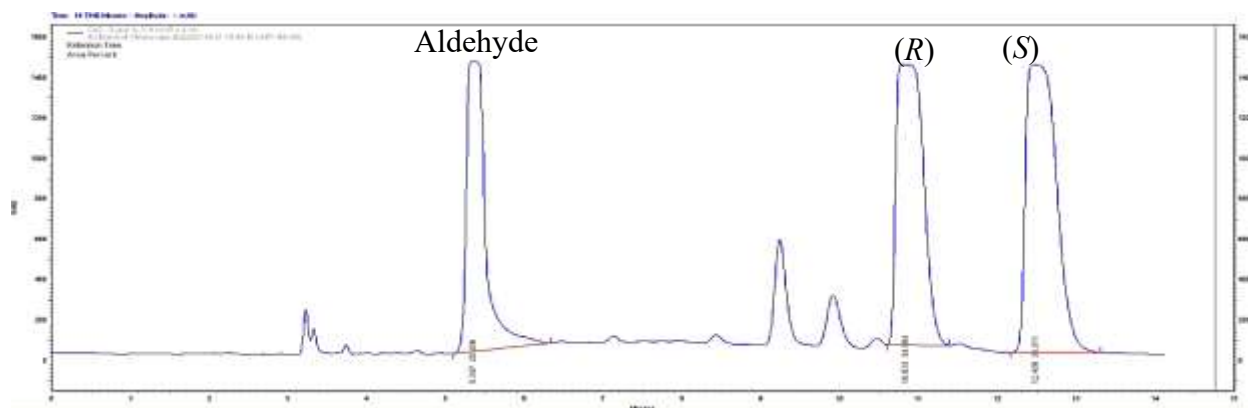


**Figure S16:** HPLC chromatogram of the standards: **1d**, and racemic **2d**.

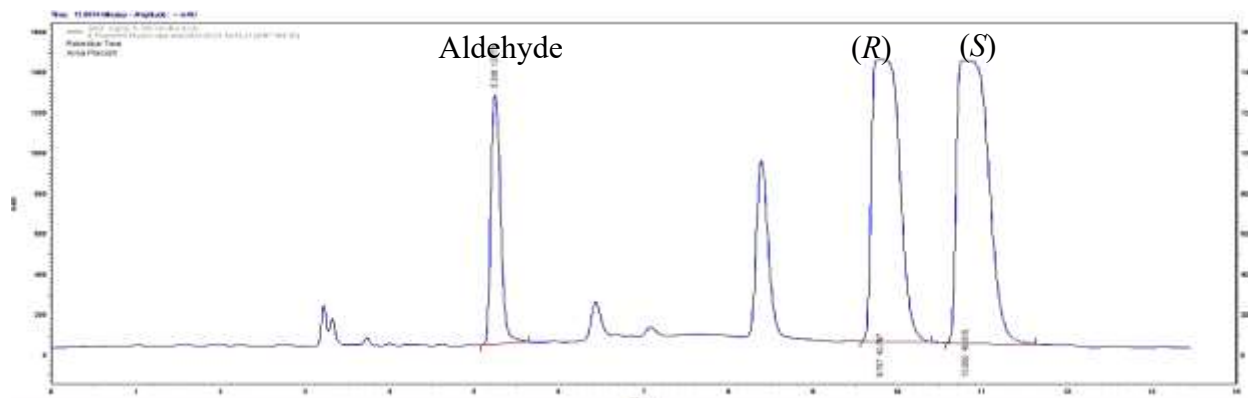


**Figure S17:** HPLC chromatogram of the standards: **1c**, and racemic **2c**.

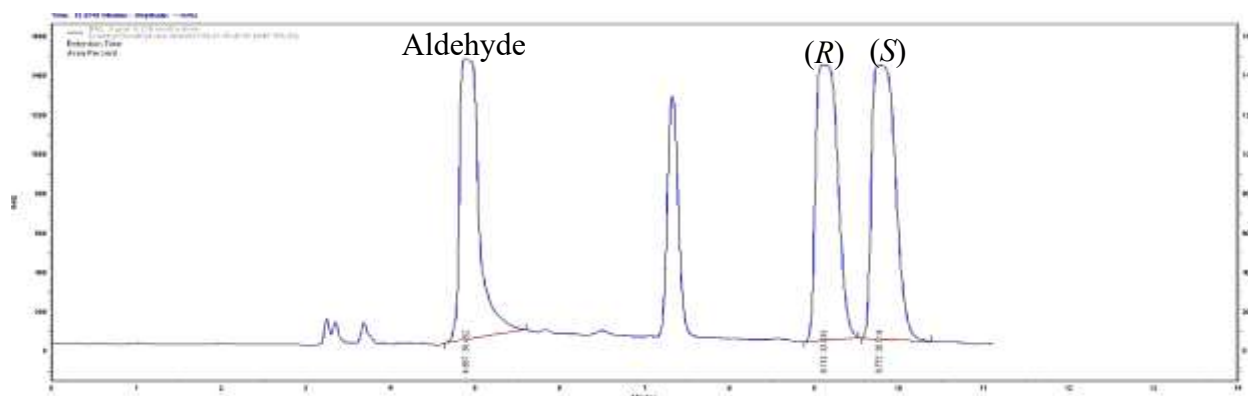


**Figure S18:** HPLC chromatogram of the standards: **1h**, and racemic **2h**.

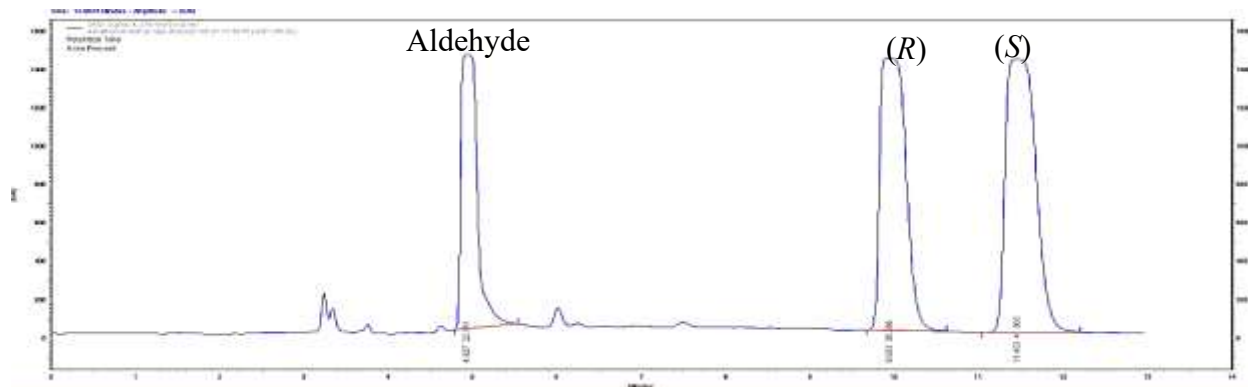


**Figure S19:** HPLC chromatogram of the standards: **1i**, and racemic **2i**.

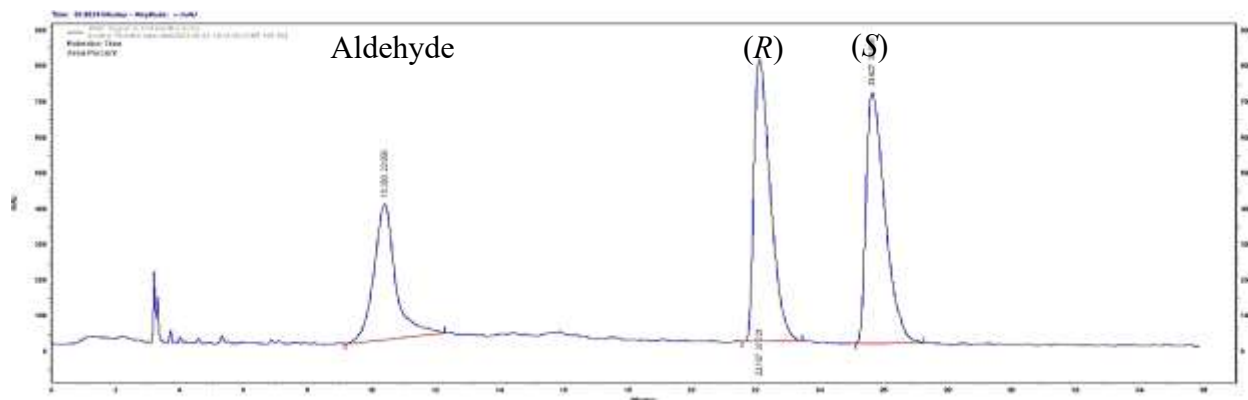


**Figure S20:** HPLC chromatogram of the standards: **1e**, and racemic **2e**.

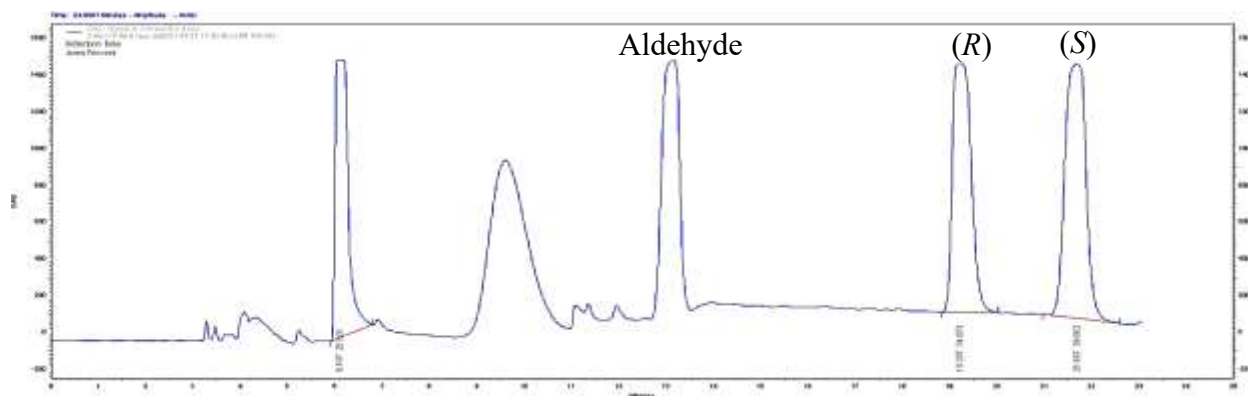


**Figure S21:** HPLC chromatogram of the standards: **1j**, and racemic **2j**.

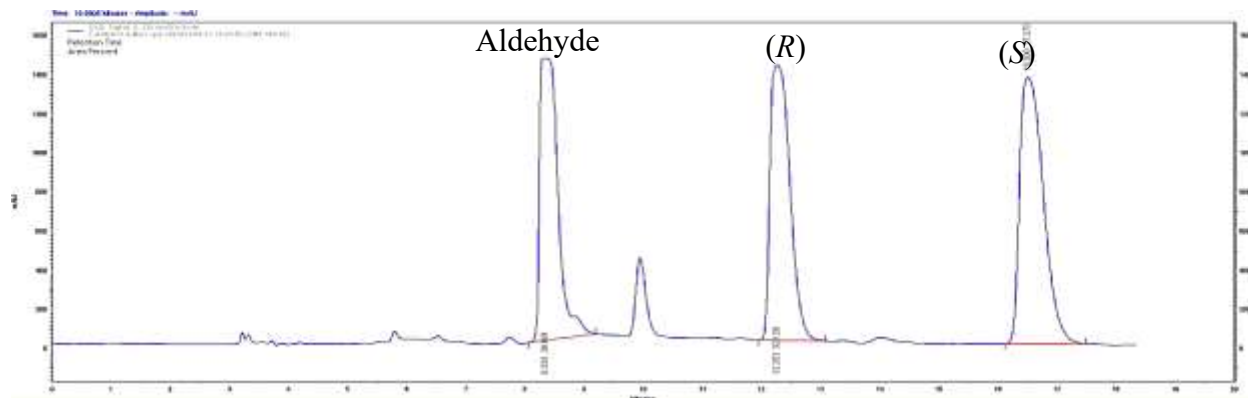


**Figure S22:** HPLC chromatogram of the standards: **1f**, and racemic **2f**.

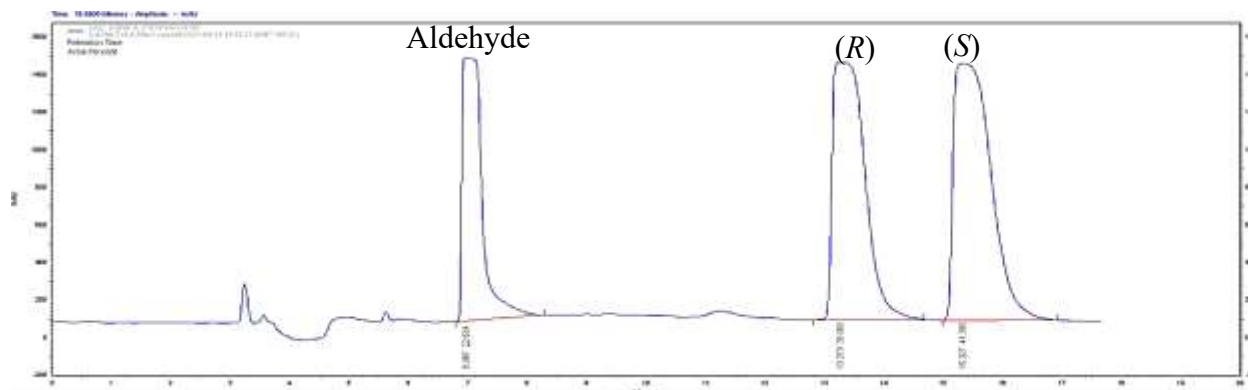


**Figure S23:** HPLC chromatogram of the standards: **1k**, and racemic **2k**.

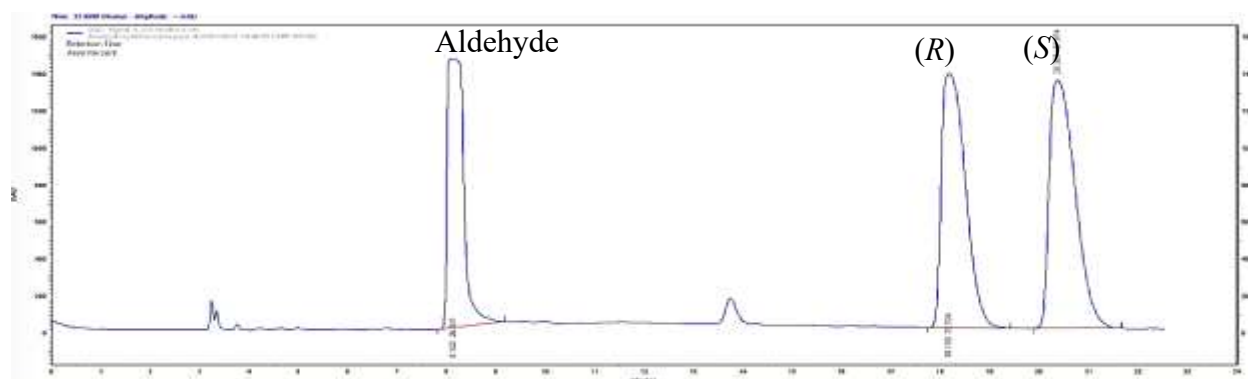


**Figure S24:** HPLC chromatogram of the standards: **1l**, and racemic **2l**.

**Figure S25 to S63:** Screening of AtHNL wt and variants in the enantioselective synthesis of **2a**.

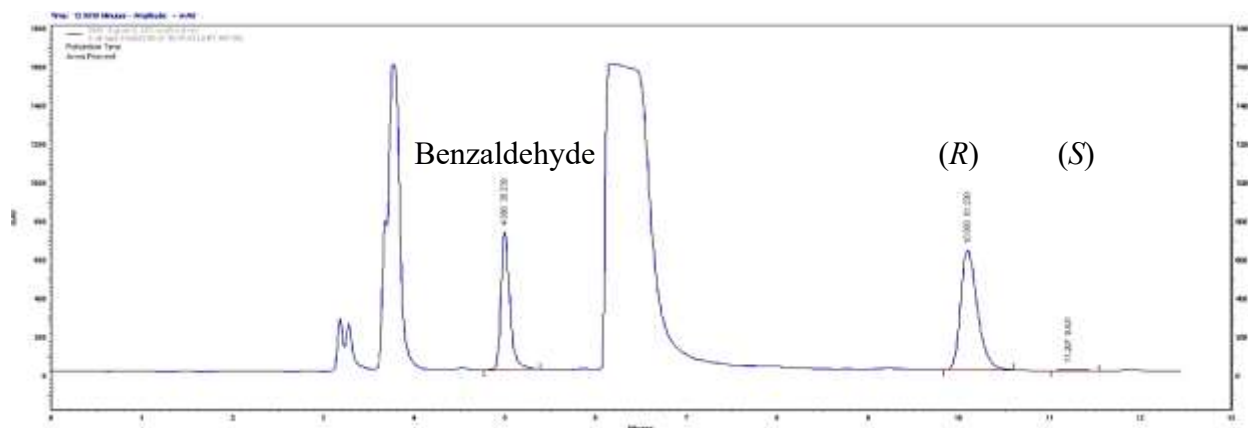


**Figure S25:** HPLC chromatogram of the WT showing enantioselective synthesis of (*R*)-**2a** at 2 h.



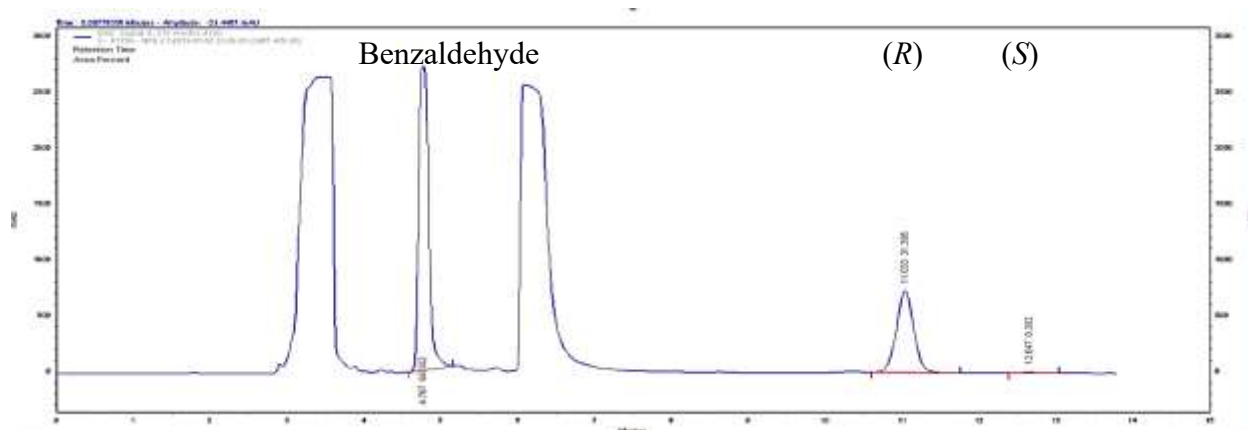


**Figure S26:** HPLC chromatogram of F179A showing enantioselective synthesis of (R)-2a at 2 h.

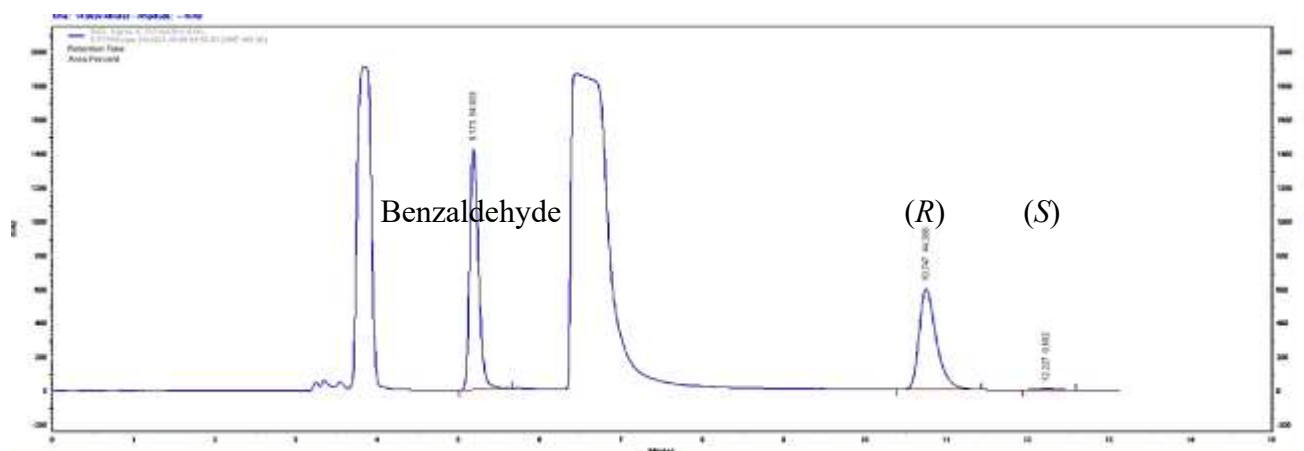


**Figure S27:** HPLC chromatogram of F179H showing enantioselective synthesis of (R)-2a at 2 h.

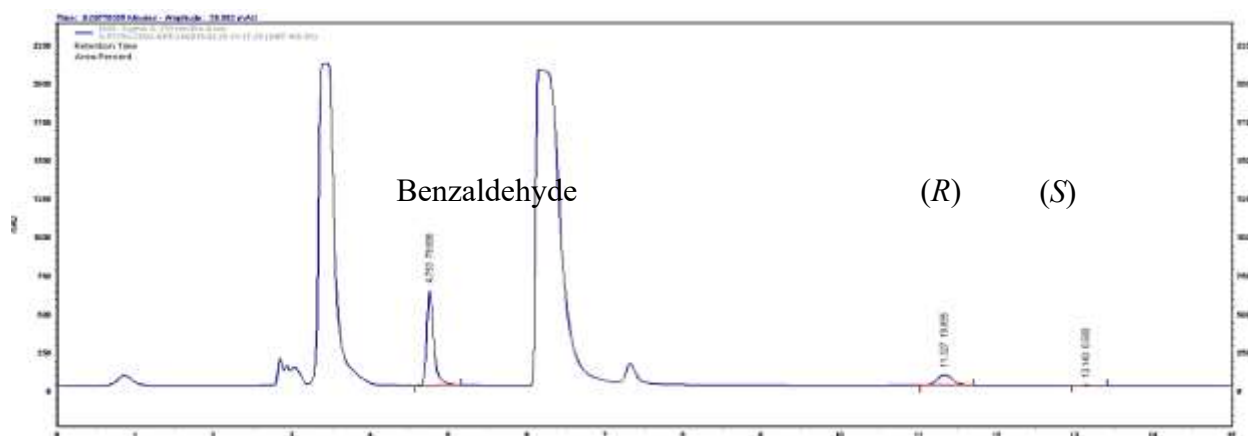


**Figure S28:** HPLC chromatogram of F179S showing enantioselective synthesis of (R)-2a at 2 h.

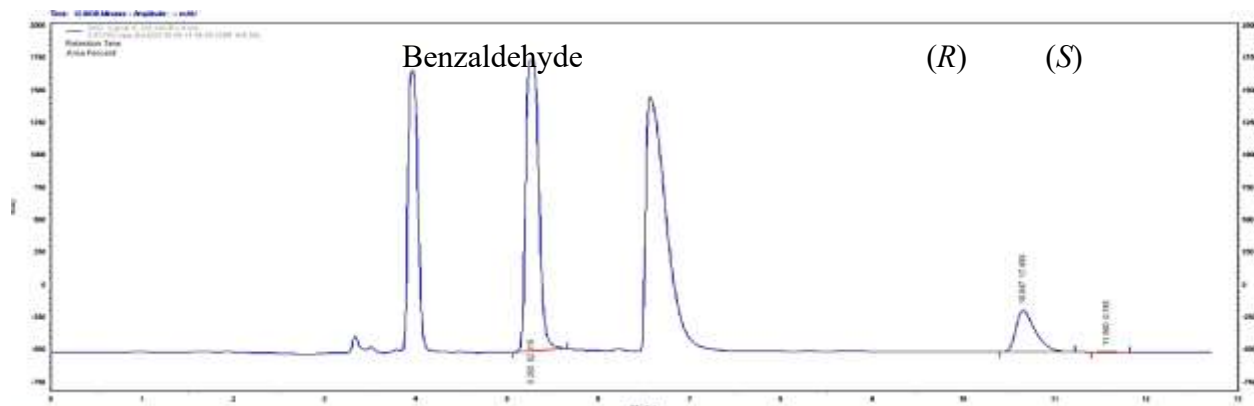


**Figure S29:** HPLC chromatogram of F179C showing enantioselective synthesis of (*R*)-**2a** at 2 h.

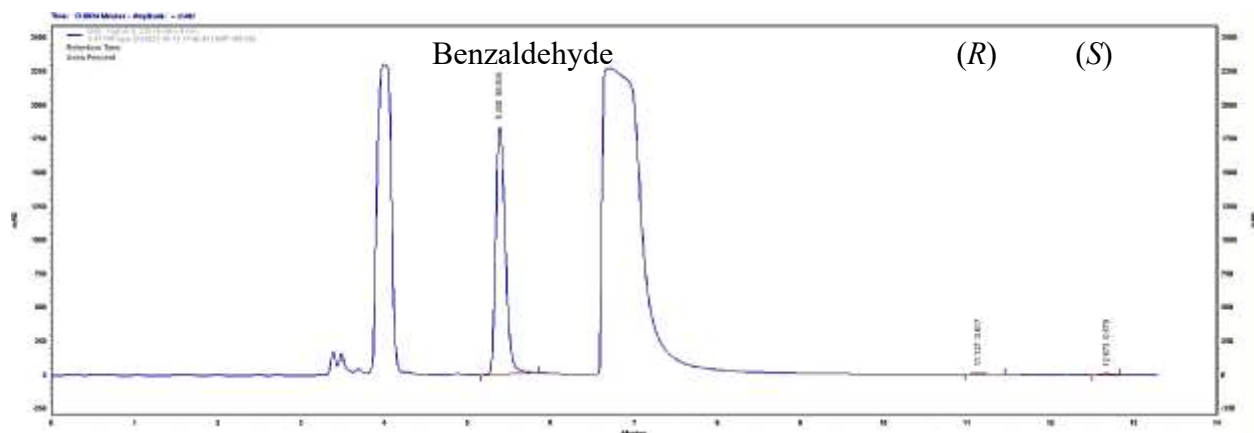


**Figure S30:** HPLC chromatogram of F179P showing enantioselective synthesis of (*R*)-**2a** at 2 h.

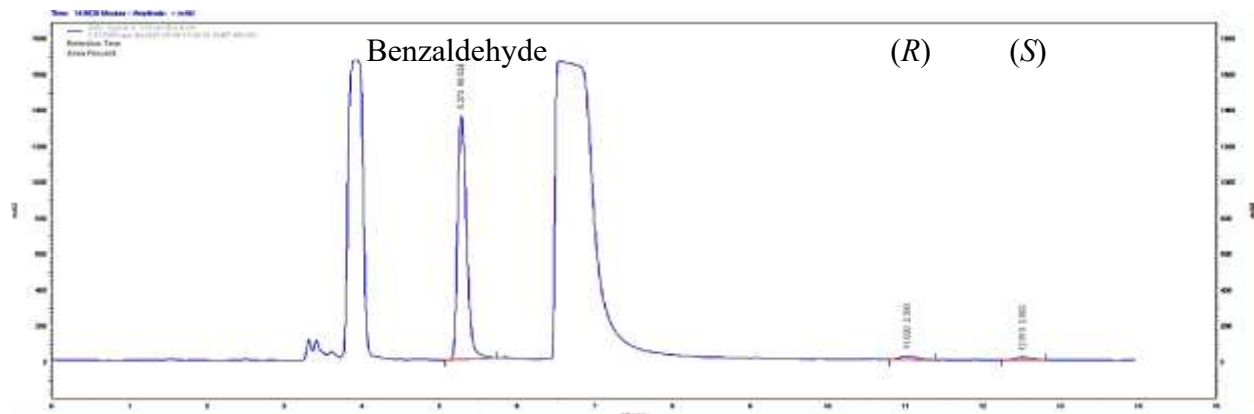


**Figure S31:** HPLC chromatogram of F179R showing enantioselective synthesis of (*R*)-**2a** at 2 h.

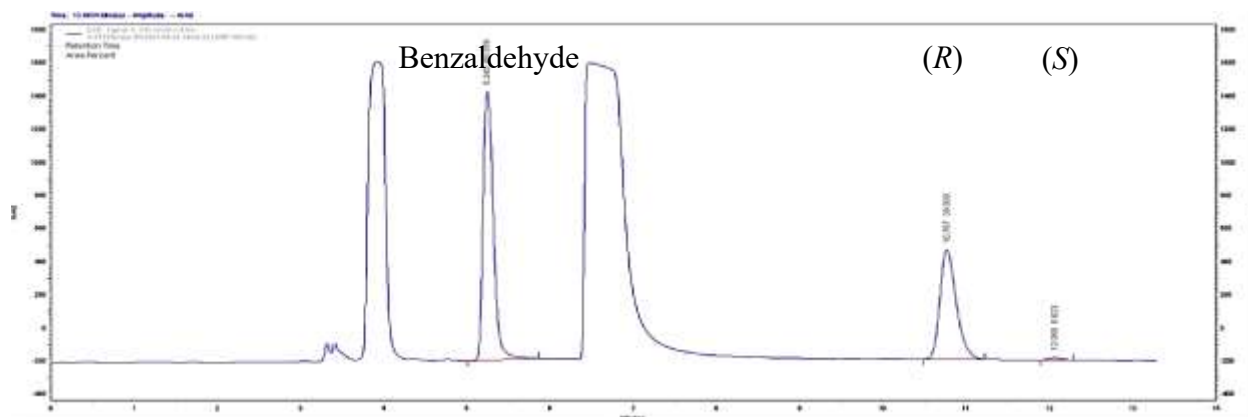


**Figure S32:** HPLC chromatogram of F179N showing enantioselective synthesis of (R)-2a at 2 h.

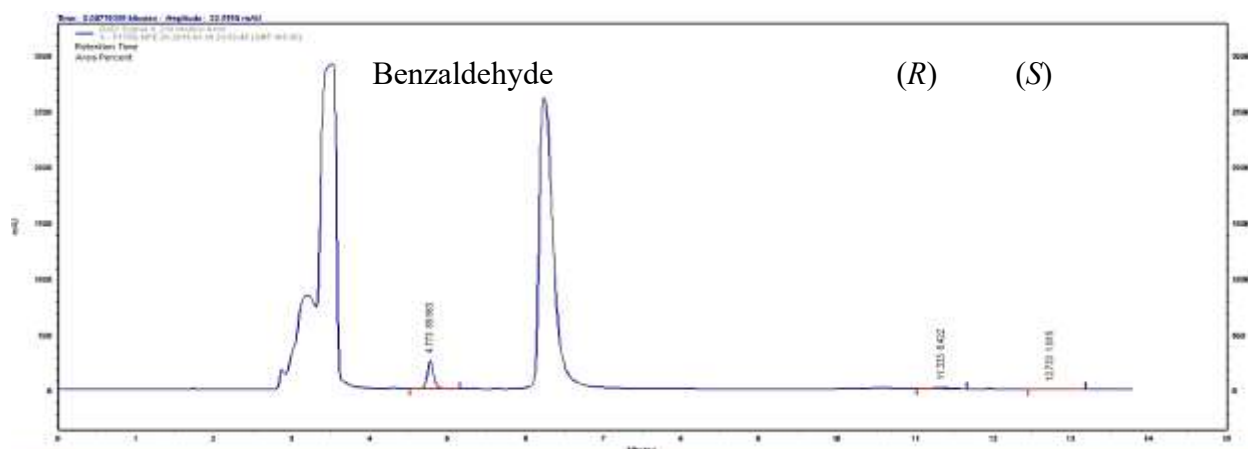


**Figure S33:** HPLC chromatogram of F179Q showing enantioselective synthesis of (R)-2a at 2 h.

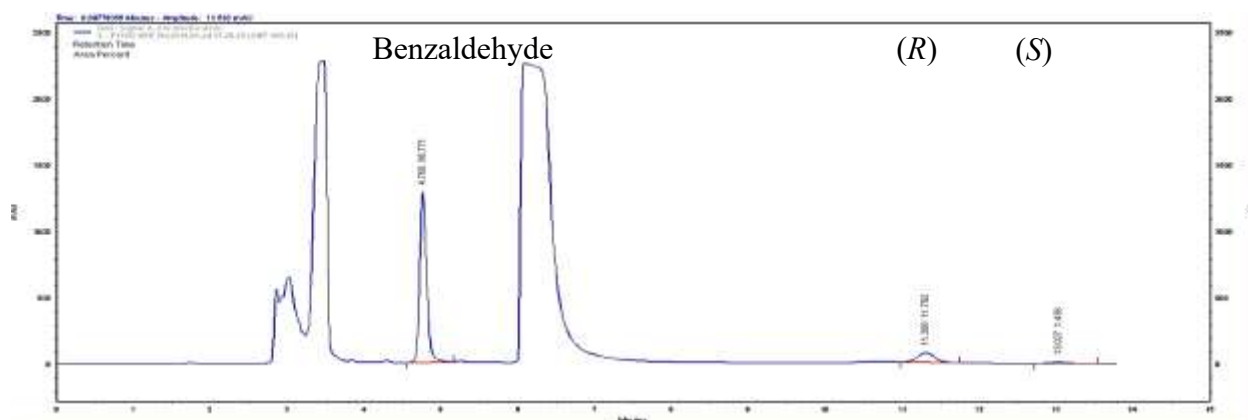


**Figure S34:** HPLC chromatogram of F179G showing enantioselective synthesis of (R)-2a at 2 h.

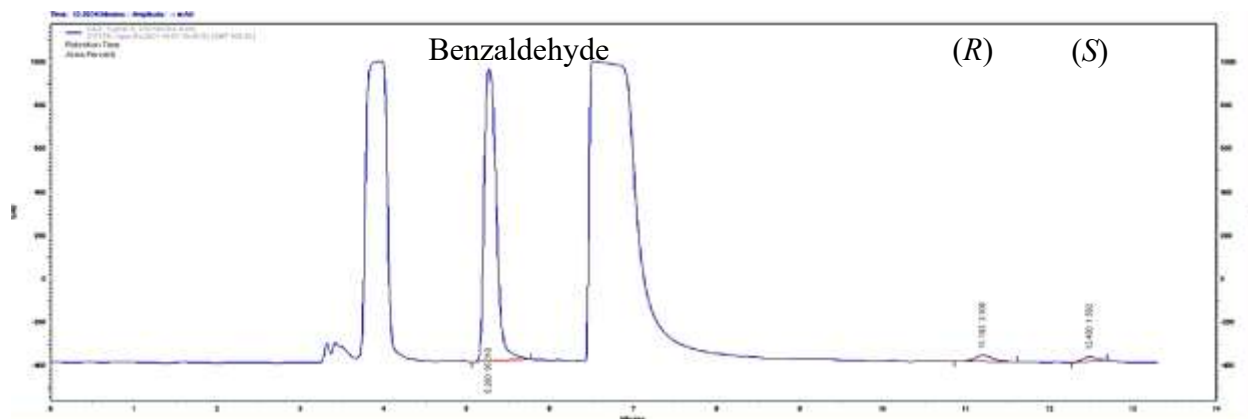


**Figure S35:** HPLC chromatogram of F179I showing enantioselective synthesis of (*R*)-**2a** at 2 h.

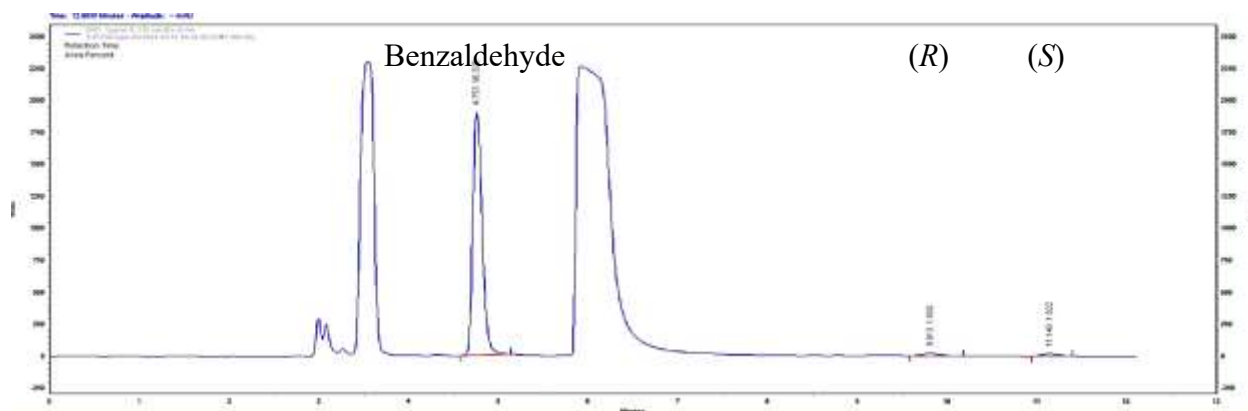


**Figure S36:** HPLC chromatogram of F179E showing enantioselective synthesis of (*R*)-**2a** at 2 h.

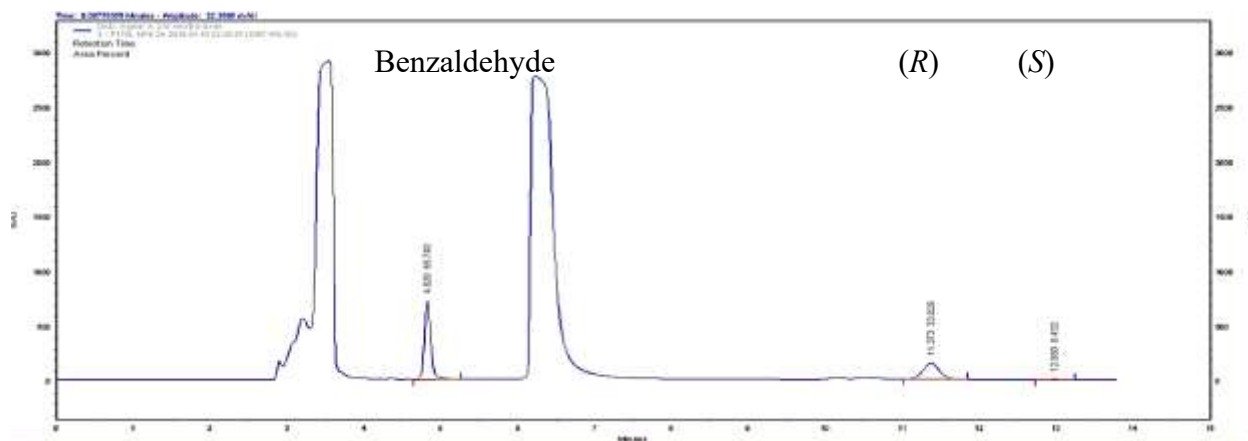


**Figure S37:** HPLC chromatogram of F179L showing enantioselective synthesis of (*R*)-**2a** at 2 h.

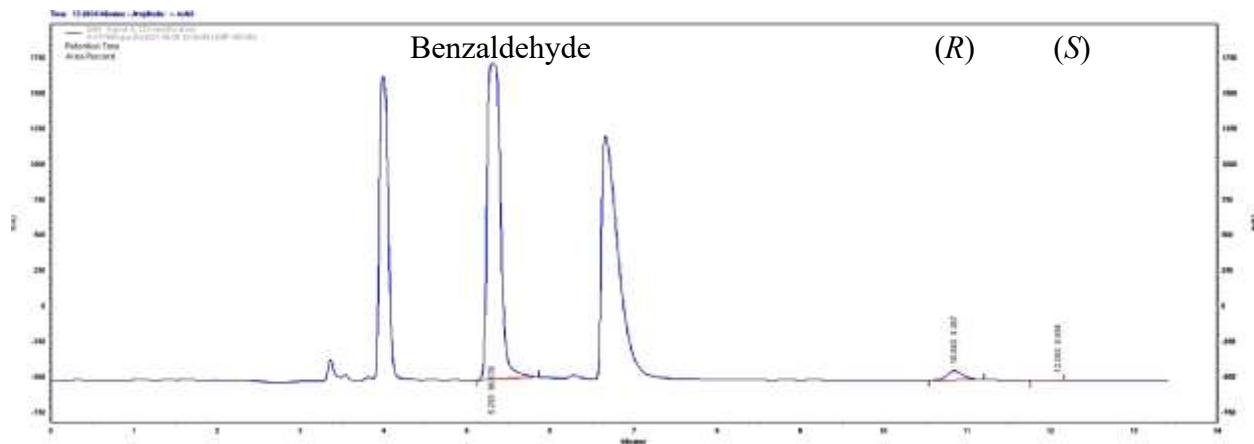


**Figure S38:** HPLC chromatogram of F179M showing enantioselective synthesis of (R)-2a at 2 h.

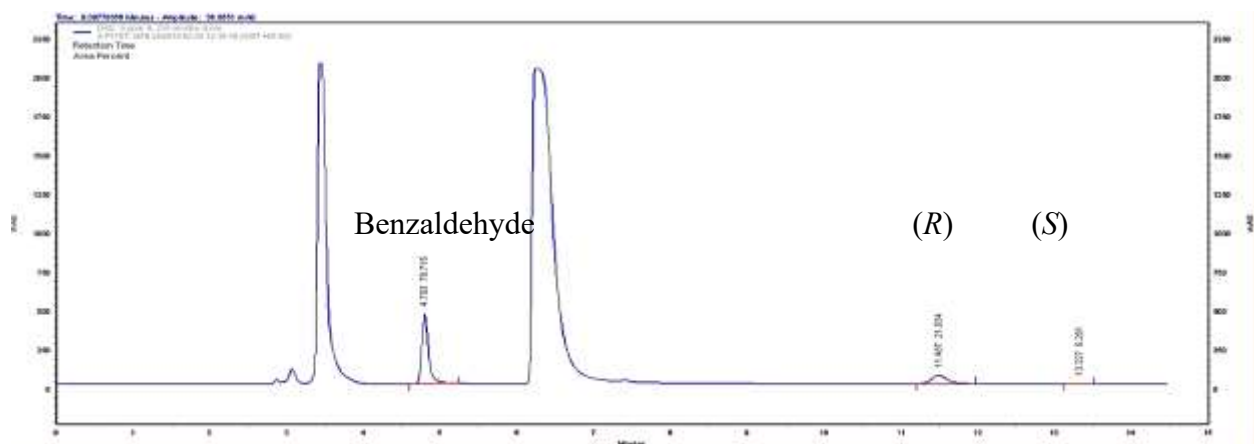


**Figure S39:** HPLC chromatogram of F179T showing enantioselective synthesis of (R)-2a at 2 h.

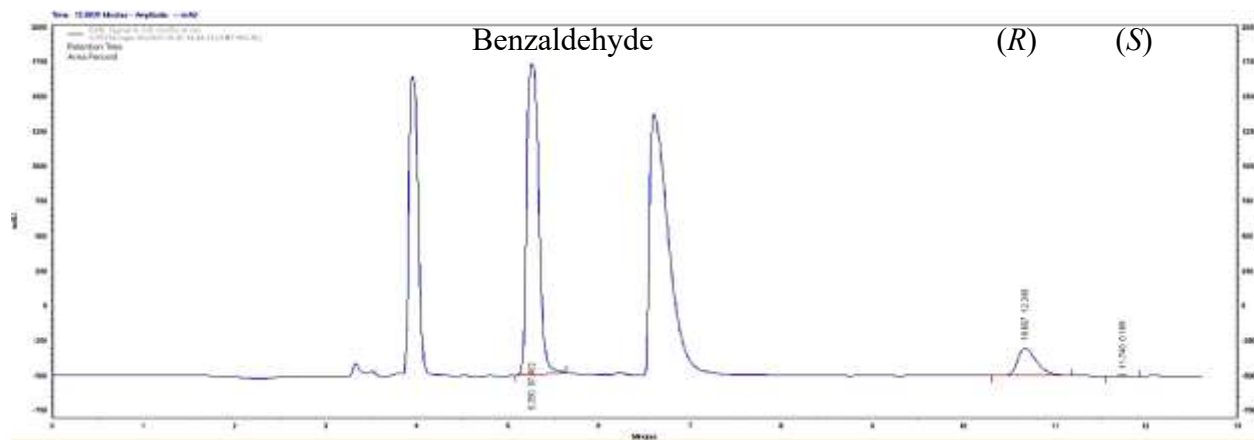


**Figure S40:** HPLC chromatogram of F179V showing enantioselective synthesis of (R)-2a at 2 h.

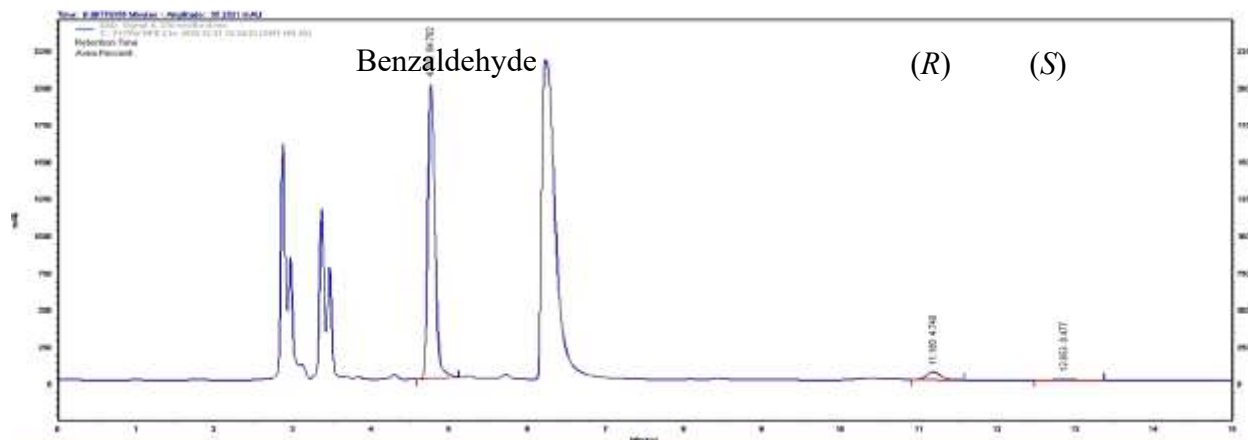


**Figure S41:** HPLC chromatogram of F179K showing enantioselective synthesis of (*R*)-**2a** at 2 h.

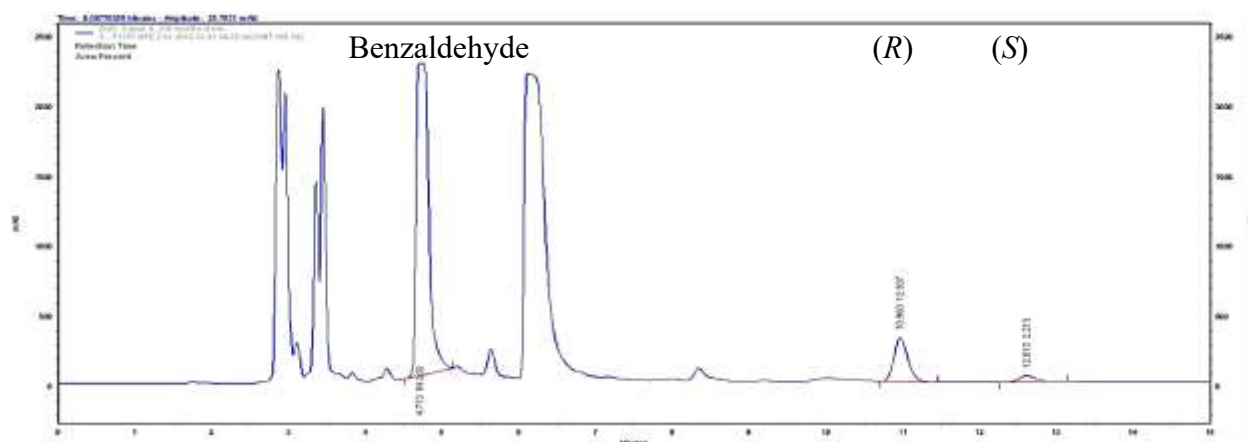


**Figure S42:** HPLC chromatogram of F179Y showing enantioselective synthesis of (*R*)-**2a** at 2 h.

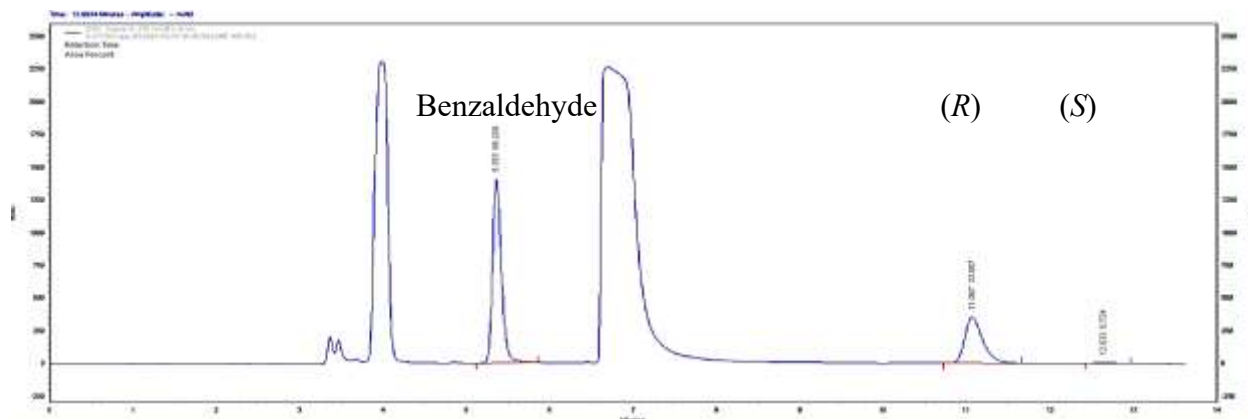


**Figure S43:** HPLC chromatogram of F179W showing enantioselective synthesis of (*R*)-**2a** at 2 h.

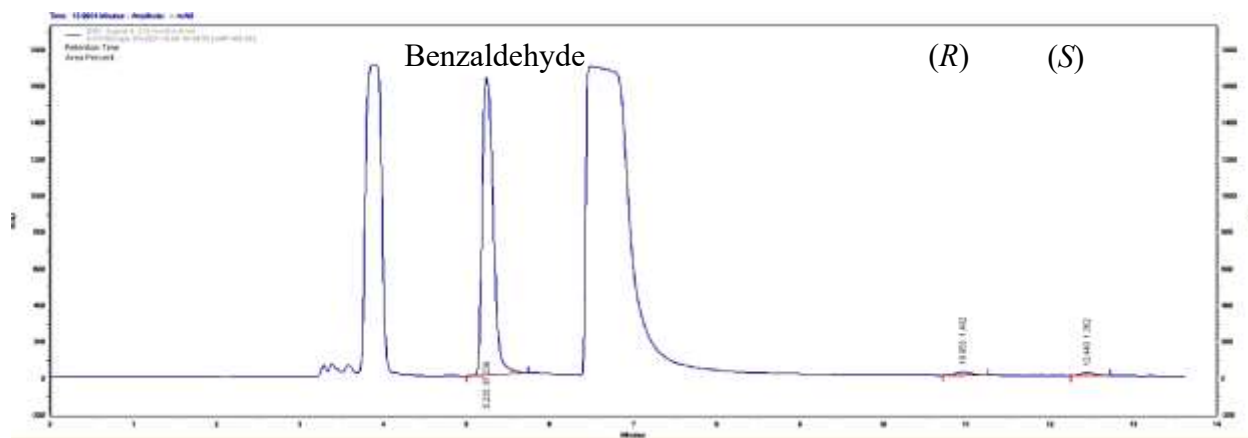


**Figure S44:** HPLC chromatogram of F179D showing enantioselective synthesis of (*R*)-**2a** at 2 h.

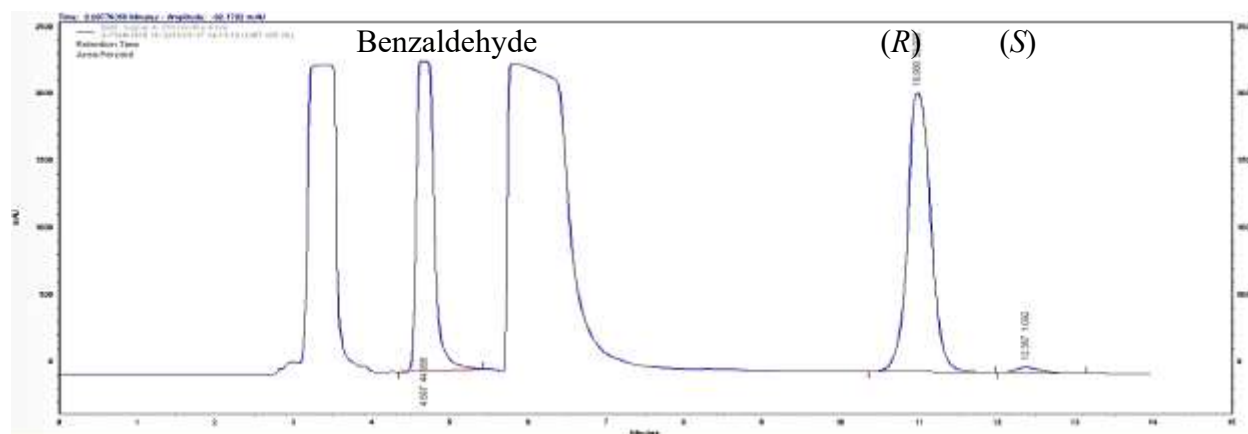


**Figure S45:** HPLC chromatogram of Y14A showing enantioselective synthesis of (*R*)-**2a** at 2 h.

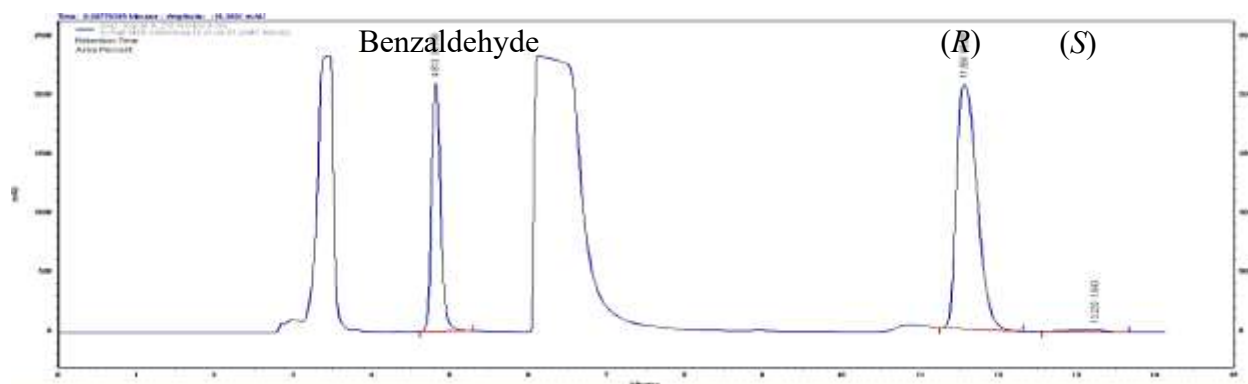


**Figure S46:** HPLC chromatogram of Y14C showing enantioselective synthesis of (*R*)-**2a** at 2 h.

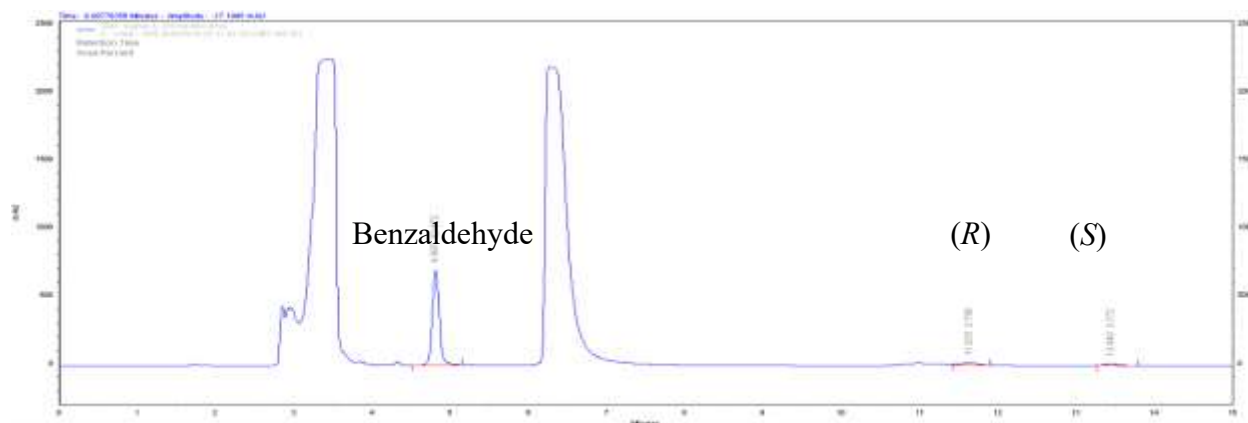


**Figure S47:** HPLC chromatogram of Y14Q showing enantioselective synthesis of (*R*)-**2a** at 2 h.

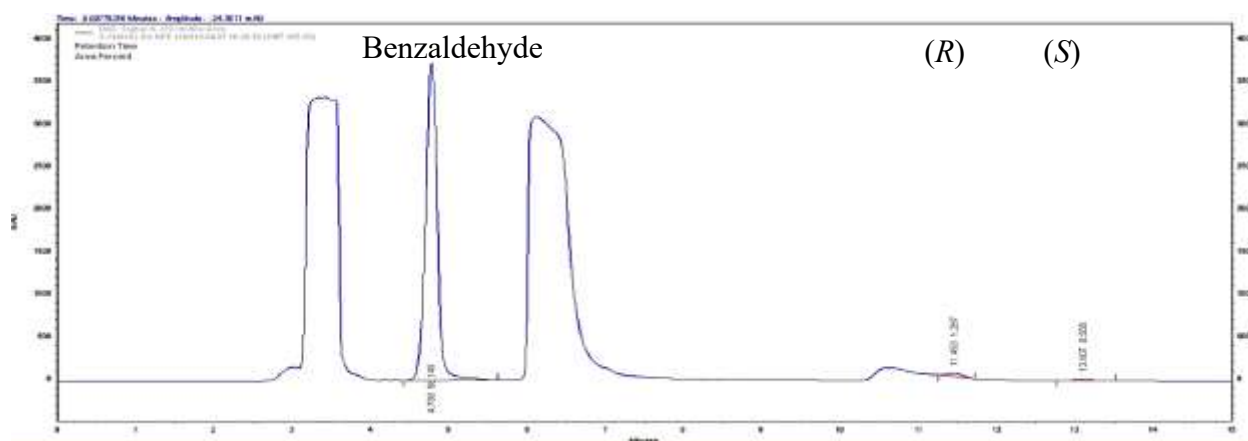


**Figure S48:** HPLC chromatogram of Y14H showing enantioselective synthesis of (*R*)-**2a** at 2 h.

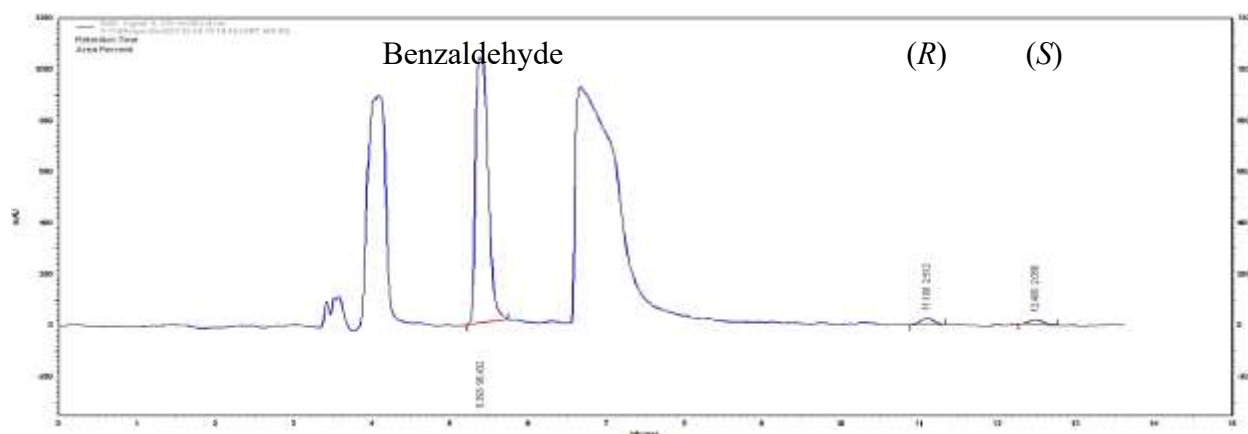


**Figure S49:** HPLC chromatogram of Y14N showing enantioselective synthesis of (*R*)-**2a** at 2 h.



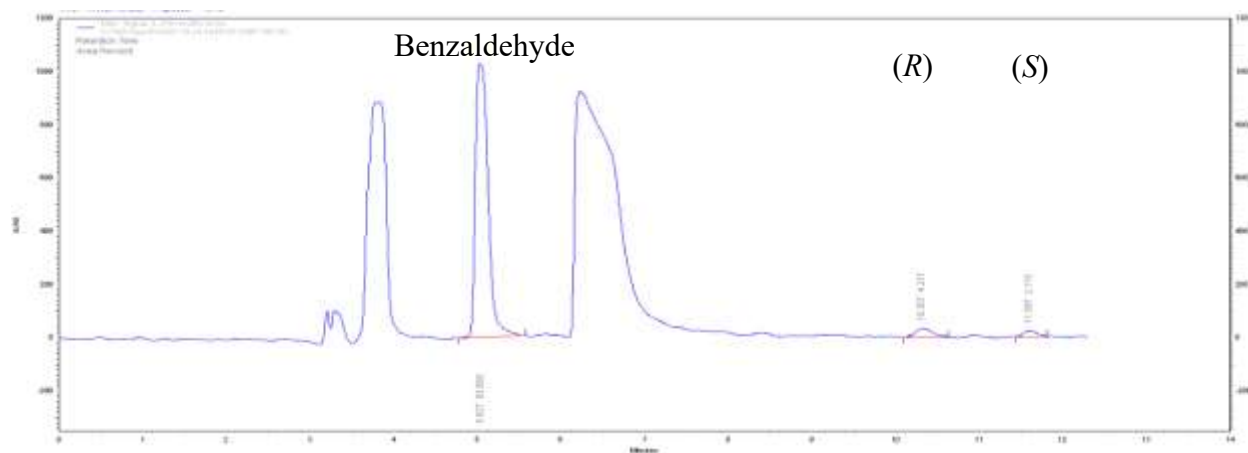


**Figure S50:** HPLC chromatogram of Y14P showing enantioselective synthesis of (*R*)-**2a** at 2 h.

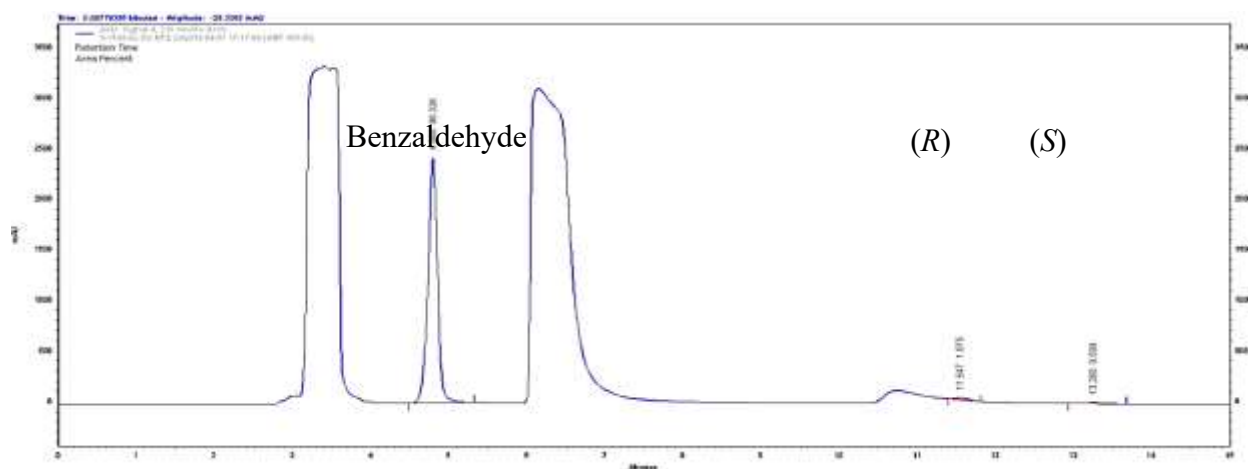


**Figure S51:** HPLC chromatogram of Y14S showing enantioselective synthesis of (*R*)-**2a** at 2 h.

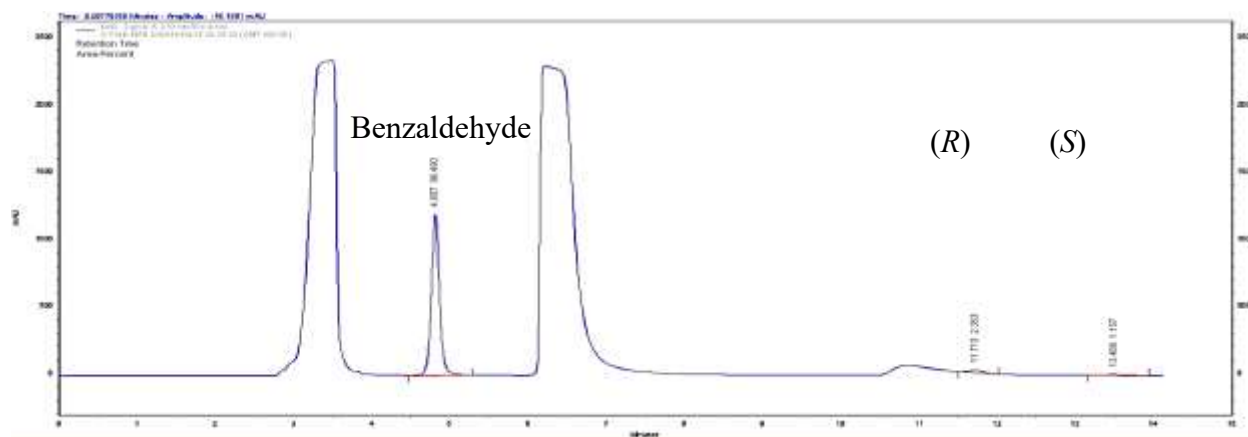


**Figure S52:** HPLC chromatogram of Y14D showing enantioselective synthesis of (*R*)-**2a** at 2 h.

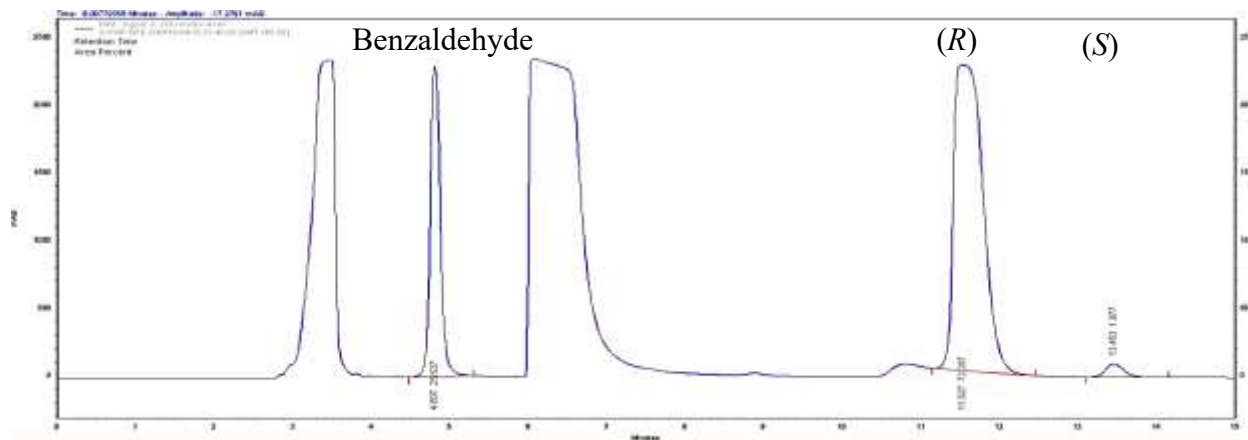


**Figure S53:** HPLC chromatogram of Y14F showing enantioselective synthesis of (*R*)-**2a** at 2 h.

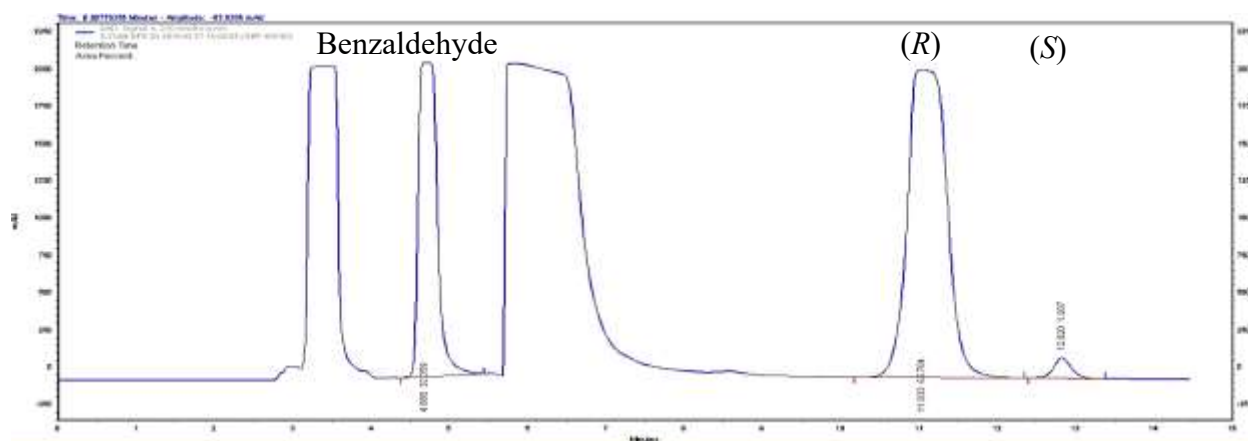


**Figure S54:** HPLC chromatogram of Y14M showing enantioselective synthesis of (*R*)-**2a** at 2 h.

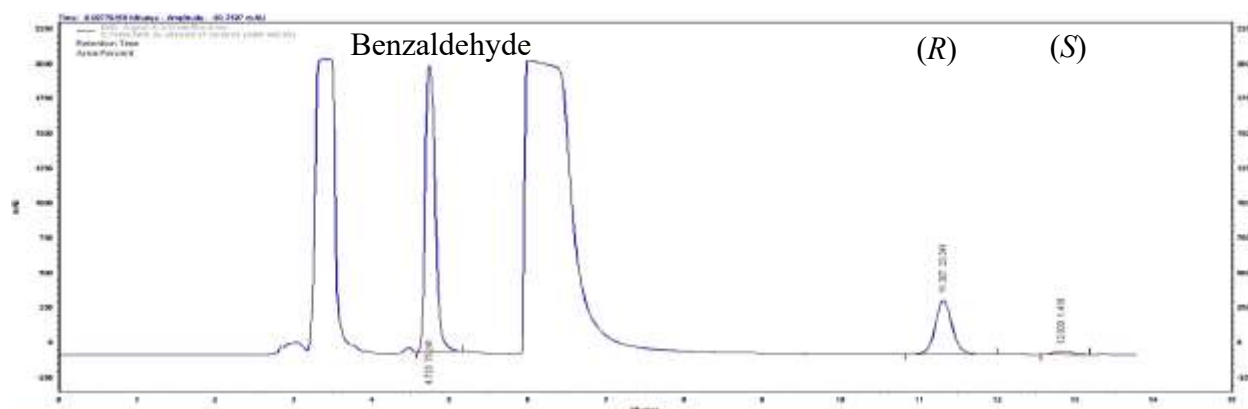


**Figure S55:** HPLC chromatogram of Y14V showing enantioselective synthesis of (*R*)-**2a** at 2 h.

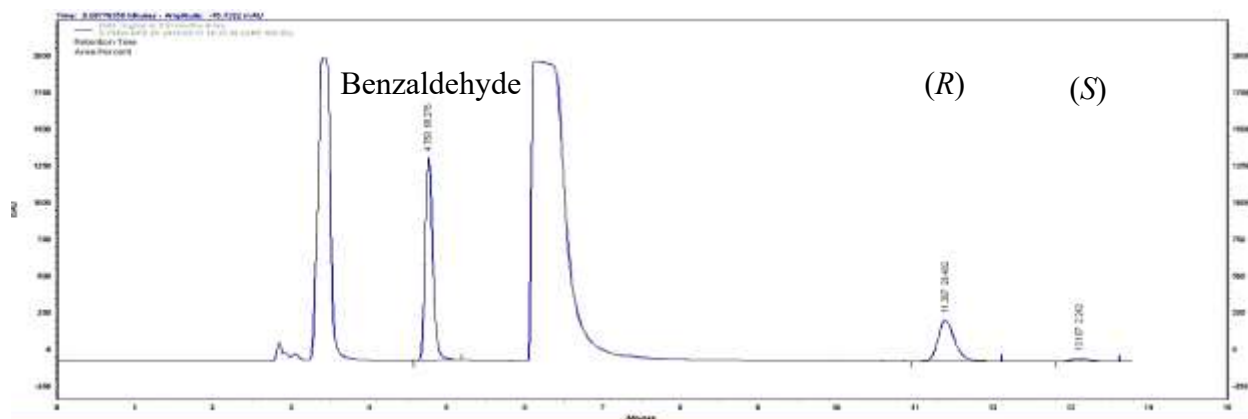


**Figure S56:** HPLC chromatogram of Y14W showing enantioselective synthesis of (R)-2a at 2 h.

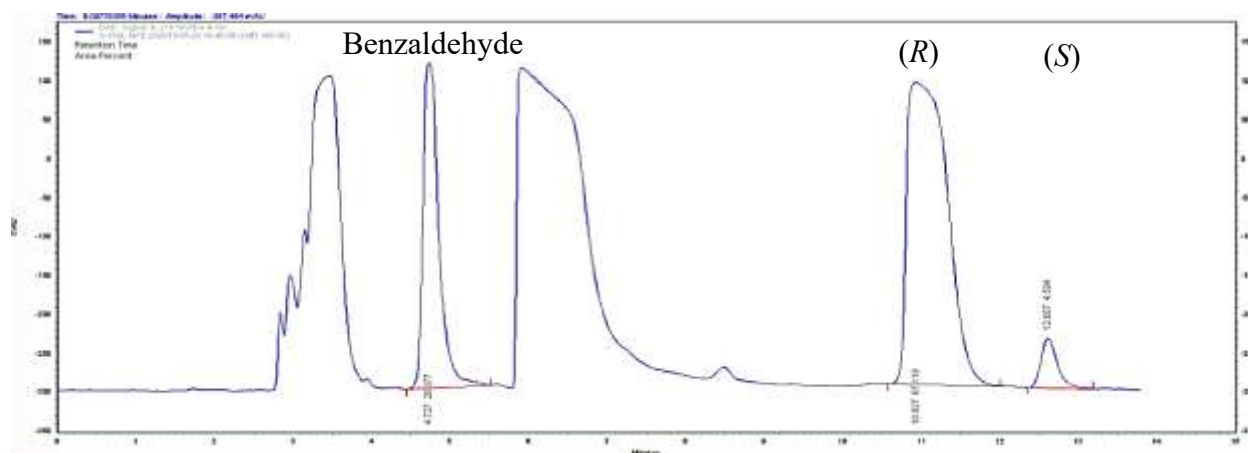


**Figure S57:** HPLC chromatogram of Y14L showing enantioselective synthesis of (R)-2a at 2 h.

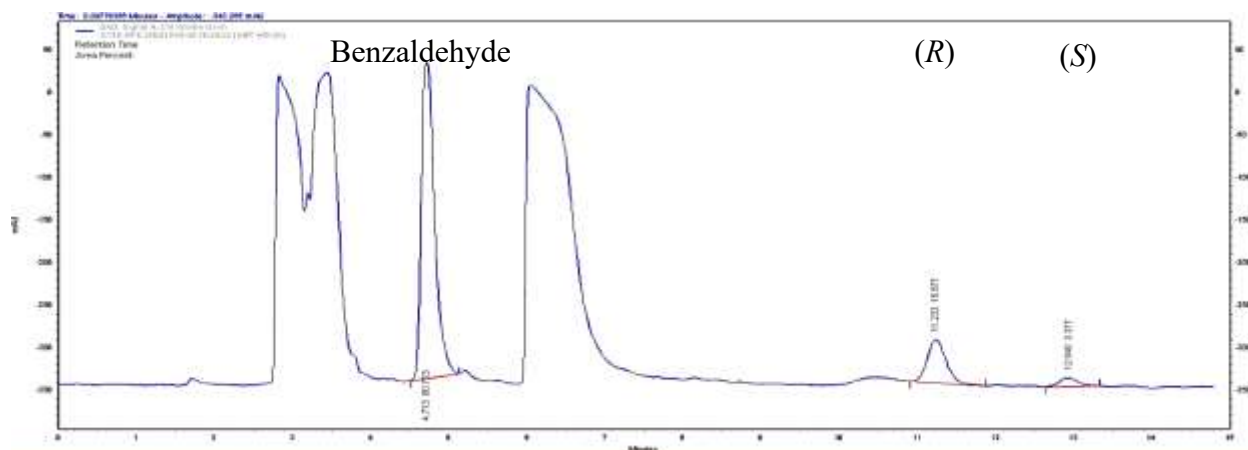


**Figure S58:** HPLC chromatogram of Y14E showing enantioselective synthesis of (R)-2a at 2 h.

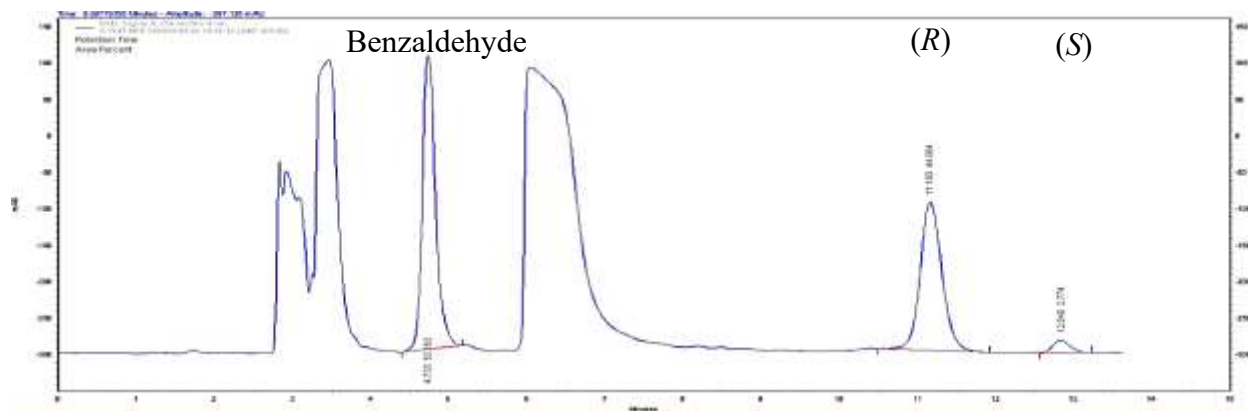


**Figure S59:** HPLC chromatogram of Y14T showing enantioselective synthesis of (*R*)-**2a** at 2 h.

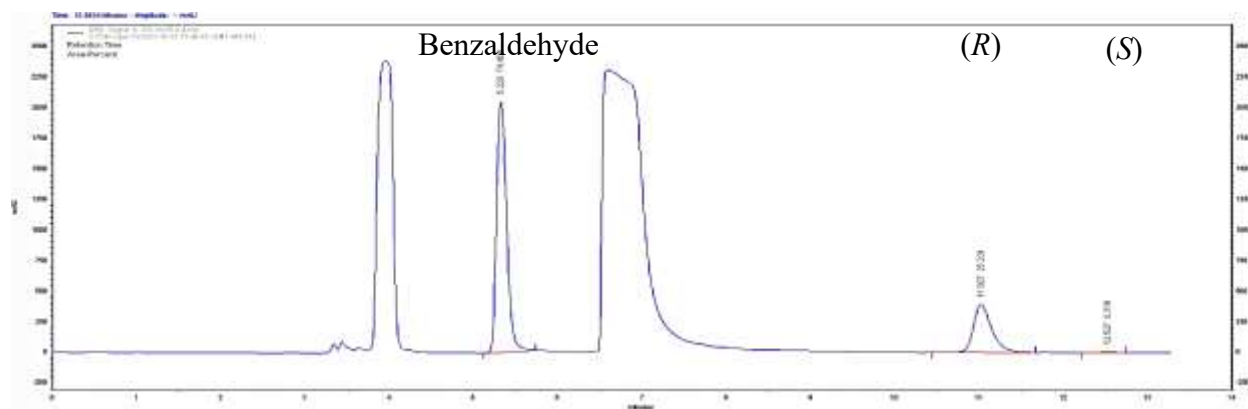


**Figure S60:** HPLC chromatogram of Y14K showing enantioselective synthesis of (*R*)-**2a** at 2 h.

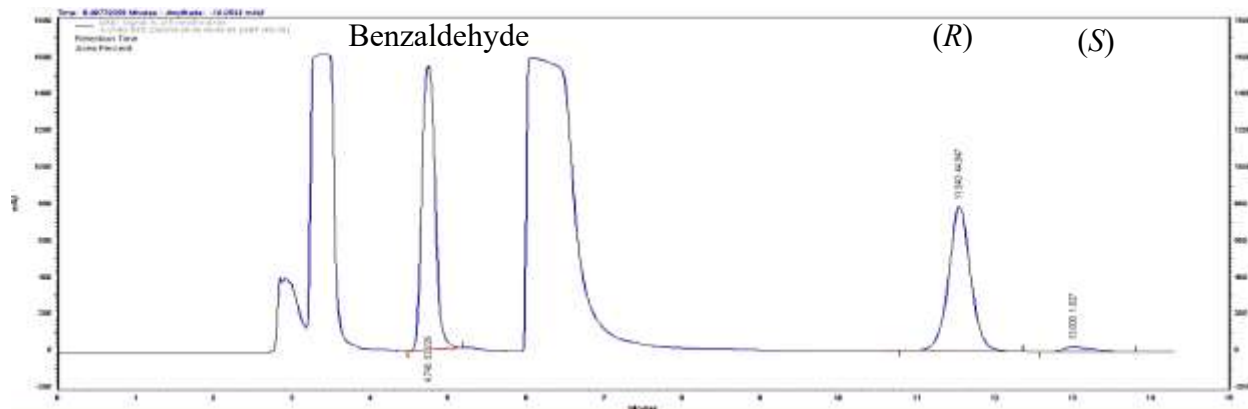


**Figure S61:** HPLC chromatogram of Y14G showing enantioselective synthesis of (*R*)-**2a** at 2 h.

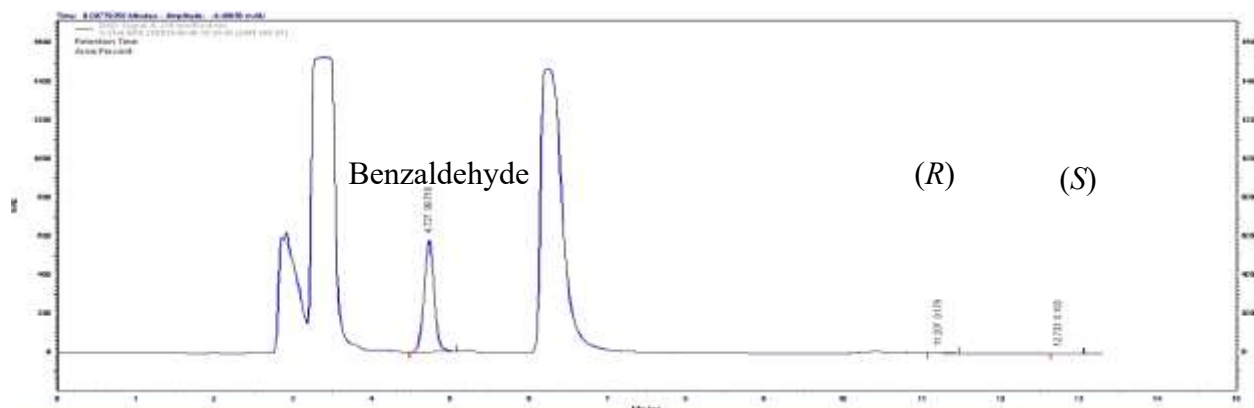


**Figure S62:** HPLC chromatogram of Y14I showing enantioselective synthesis of (*R*)-**2a** at 2 h.

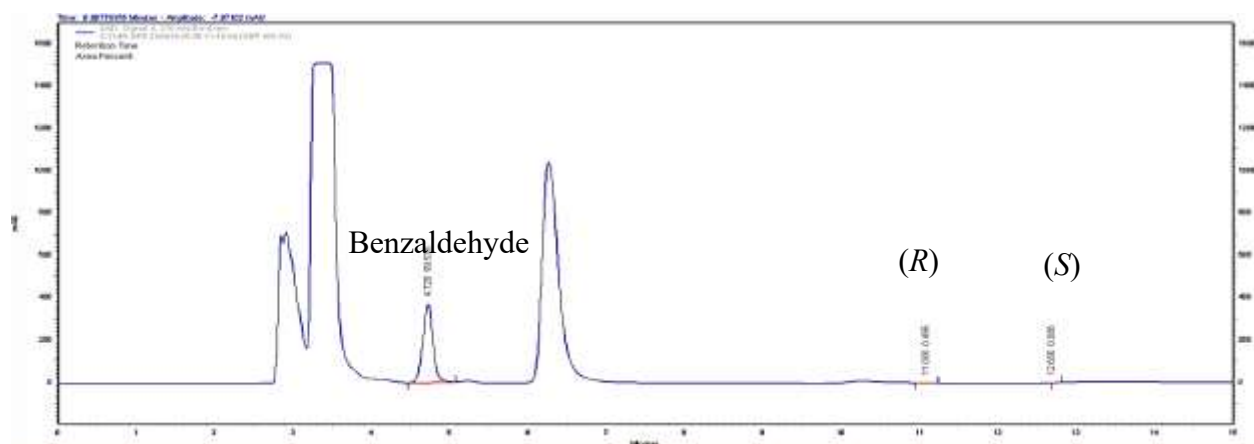


**Figure S63:** HPLC chromatogram of Y14R showing enantioselective synthesis of (*R*)-**2a** at 2 h.

**Figure S64-S135:** AtHNL variants (62.5U) in enantioselective synthesis of  $\beta$ -nitroalcohols and their substrate scope

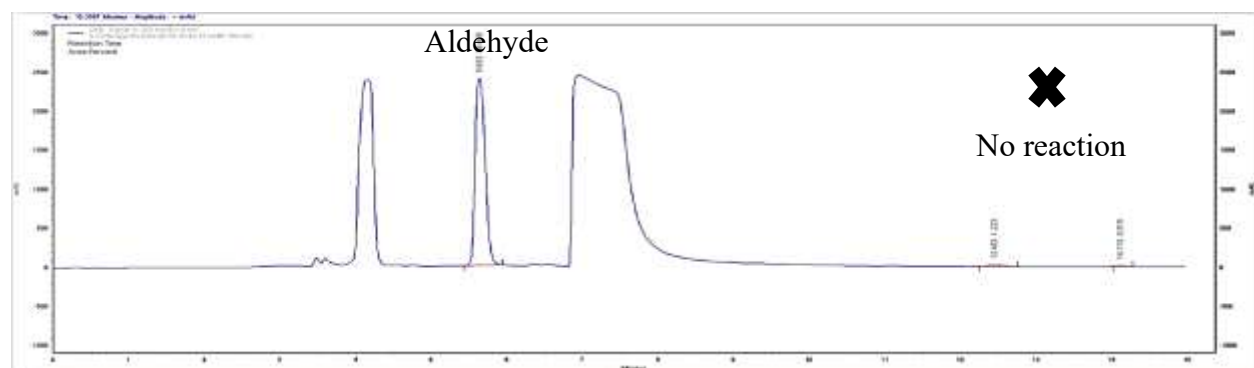


**Figure S64:** HPLC chromatogram of control reaction at 3 h where enzyme is replaced by 20 mM KPb and **1a** used as the substrate.

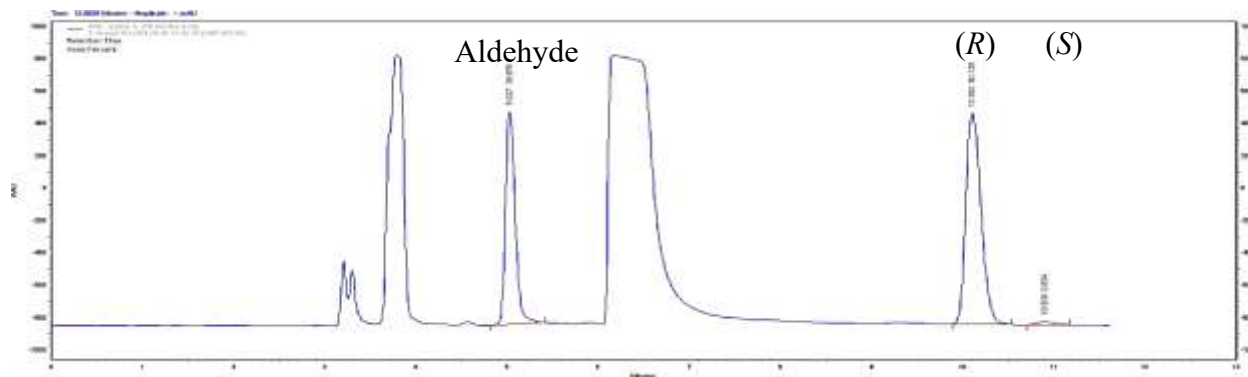


**Figure S65:** HPLC chromatogram of wild type *AtHNL* showing enantioselective synthesis of (*R*)-**2a** at 3 h using **1a** as the substrate.

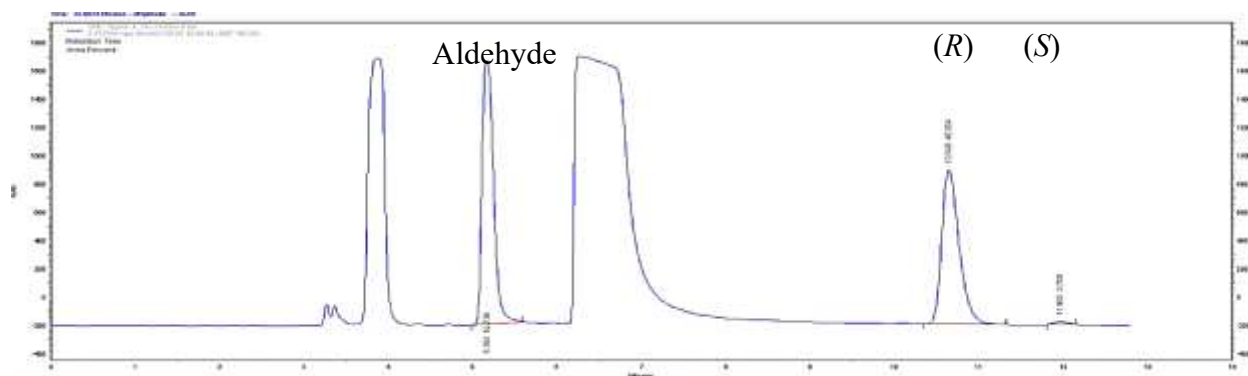


**Figure S66:** HPLC chromatogram of the F179W variant showing enantioselective synthesis of (*R*)-**2a** at 3 h using **1a** as the substrate.

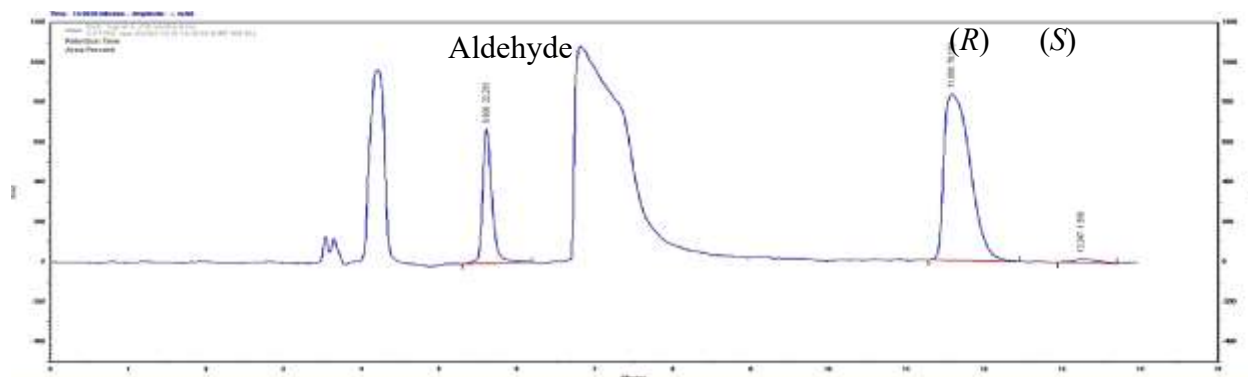


**Figure S67:** HPLC chromatogram of the F179N variant showing enantioselective synthesis of (*R*)-**2a** at 3 h using **1a** as the substrate.

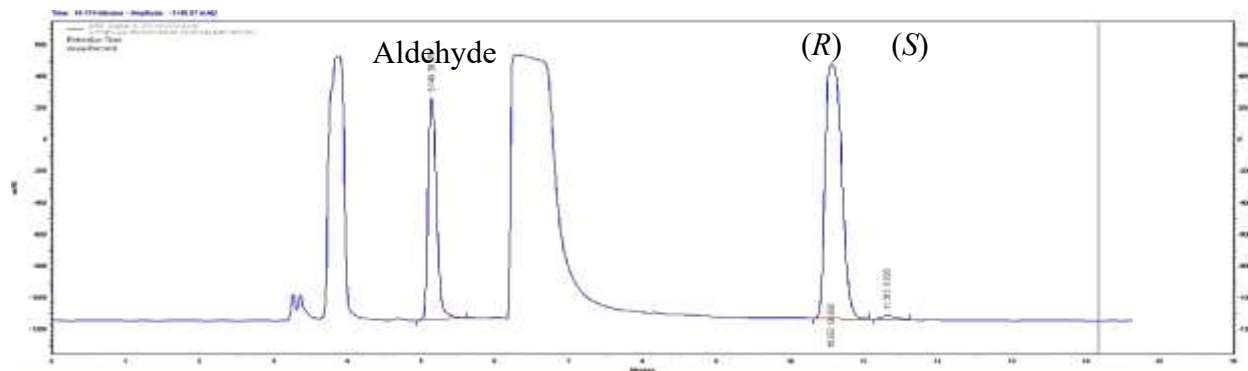


**Figure S68:** HPLC chromatogram of the Y14F variant showing enantioselective synthesis of (*R*)-**2a** at 3 h using **1a** as the substrate.

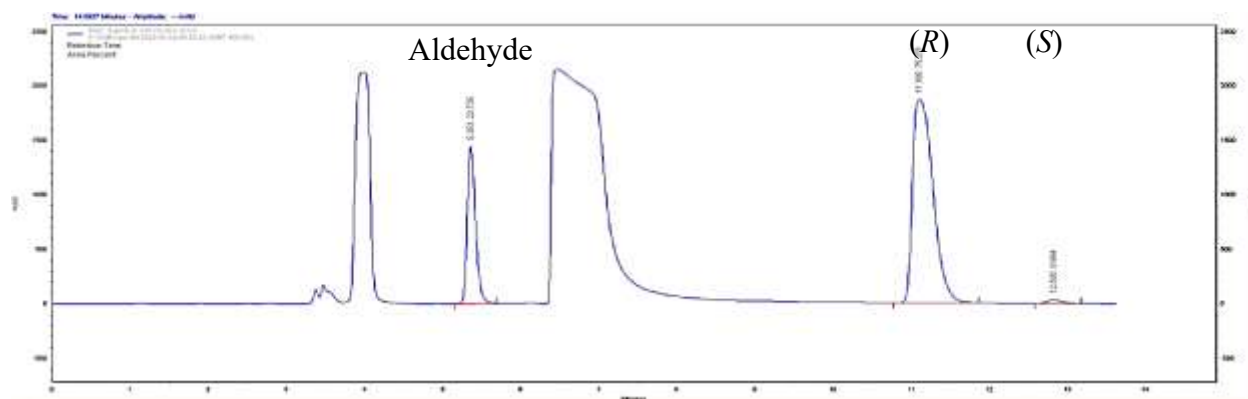


**Figure S69:** HPLC chromatogram of the Y14M variant showing enantioselective synthesis of (*R*)-**2a** at 3 h using **1a** as the substrate.

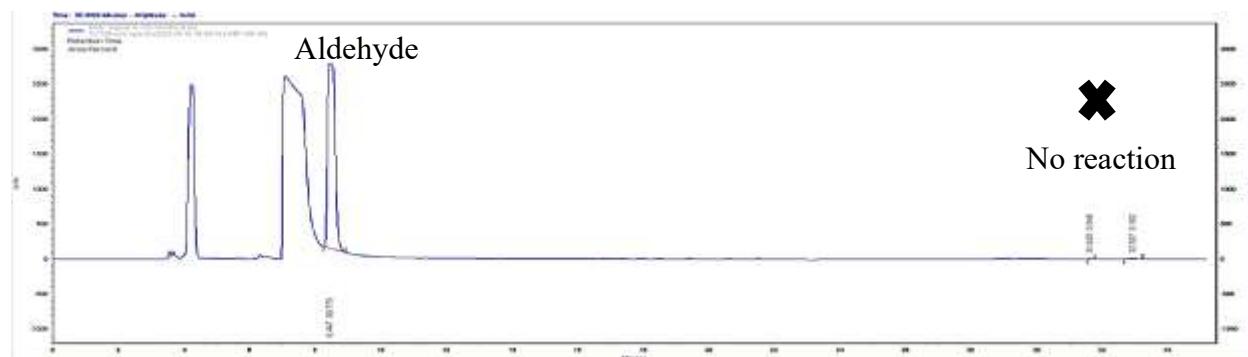


**Figure S70:** HPLC chromatogram of control reaction at 3 h where enzyme is replaced by 20 mM KPb and **1b** used as the substrate.

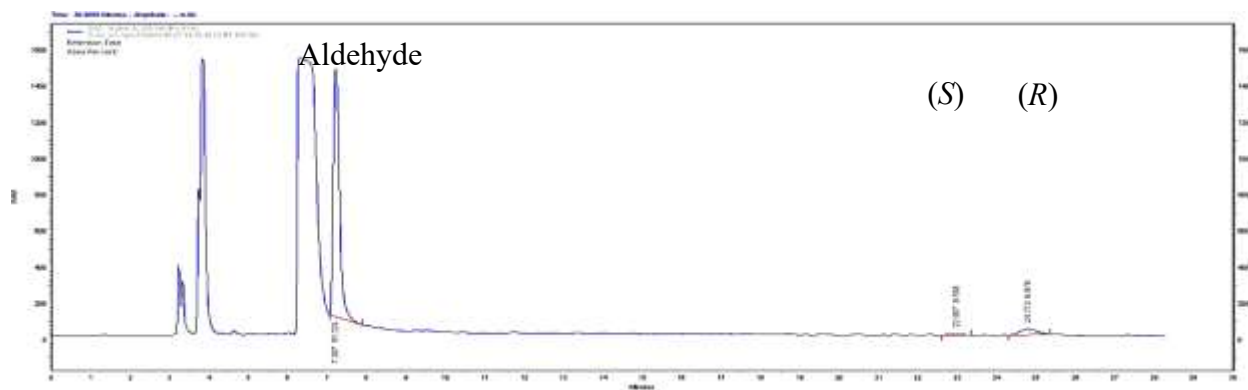


**Figure S71:** HPLC chromatogram of wild type *AtHNL* showing enantioselective synthesis of (*R*)-**2b** at 3 h using **1b** as the substrate.

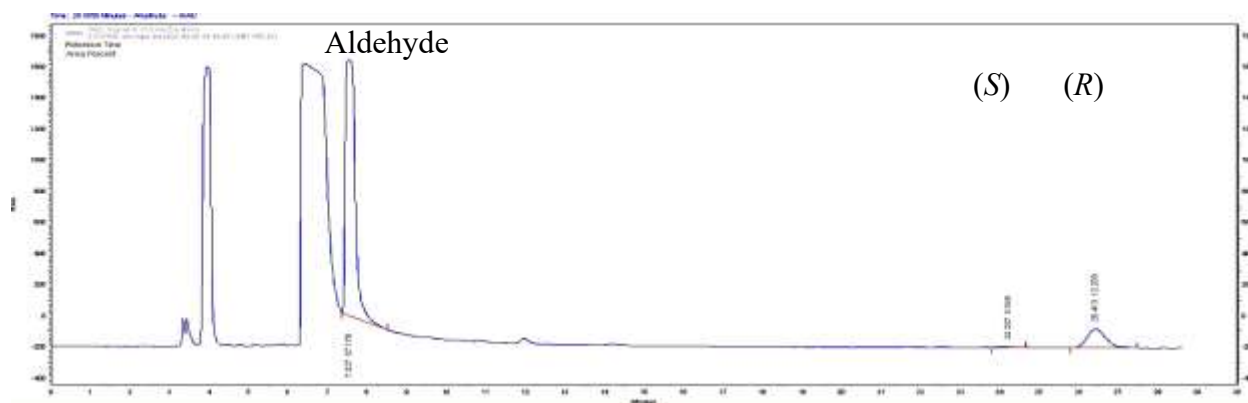


**Figure S72:** HPLC chromatogram of the F179W variant showing enantioselective synthesis of (*R*)-**2b** at 3 h using **1b** as the substrate.

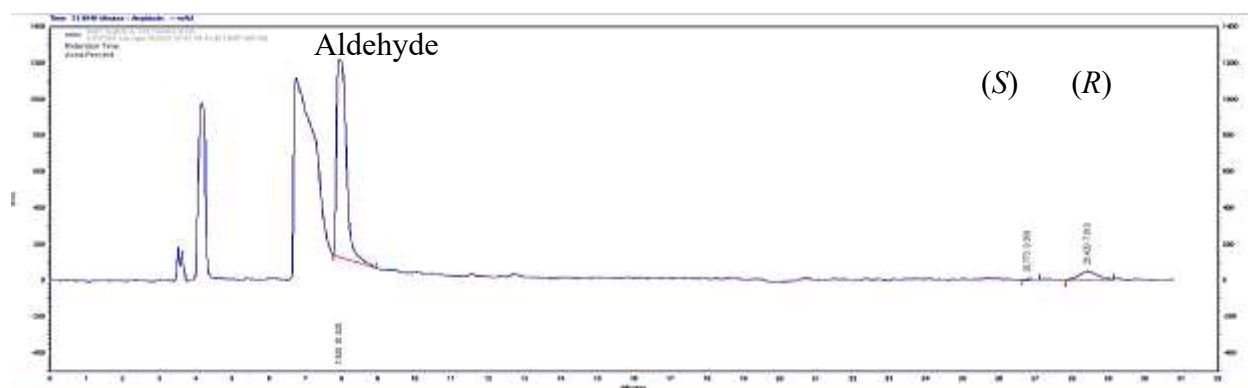


**Figure S73:** HPLC chromatogram of the F179N variant showing enantioselective synthesis of (*R*)-**2b** at 3 h using **1b** as the substrate.



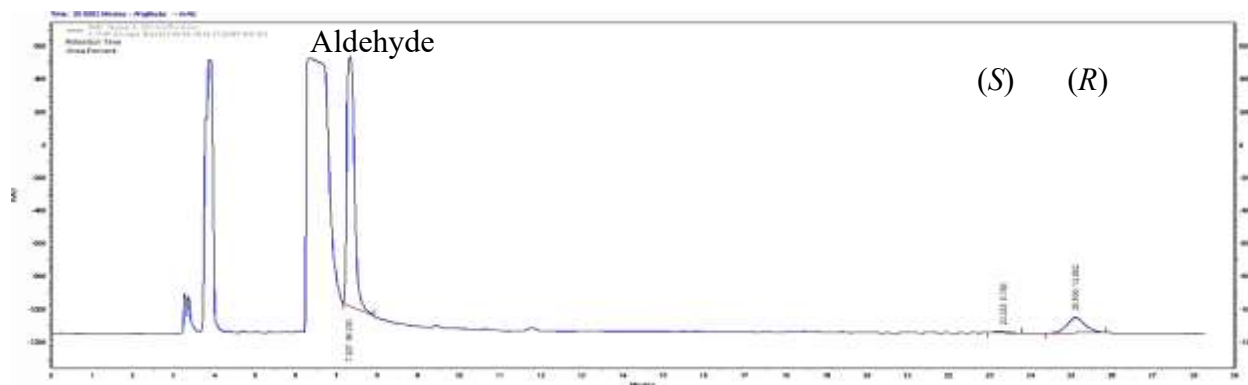


**Figure S74:** HPLC chromatogram of the Y14F variant showing enantioselective synthesis of (*R*)-(*R*)-**2b** at 3 h using **1b** as the substrate.

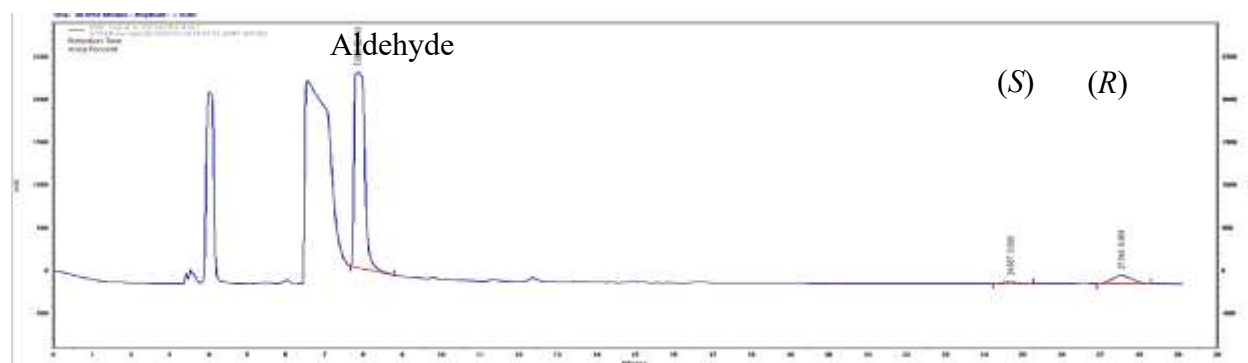


**Figure S75:** HPLC chromatogram of the Y14M variant showing enantioselective synthesis of (*R*)-**2b** at 3 h using **1b** as the substrate.

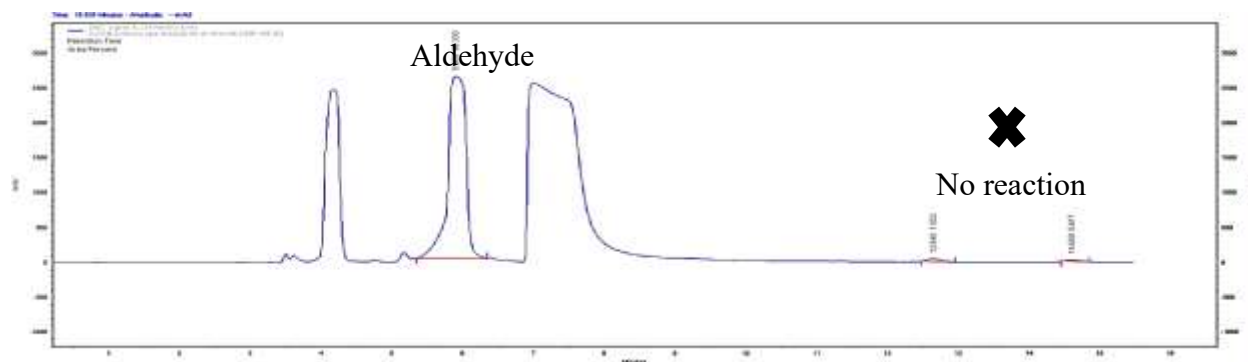


**Figure S76:** HPLC chromatogram of control reaction at 3 h where enzyme is replaced by 20 mM KPB and **1g** used as the substrate.

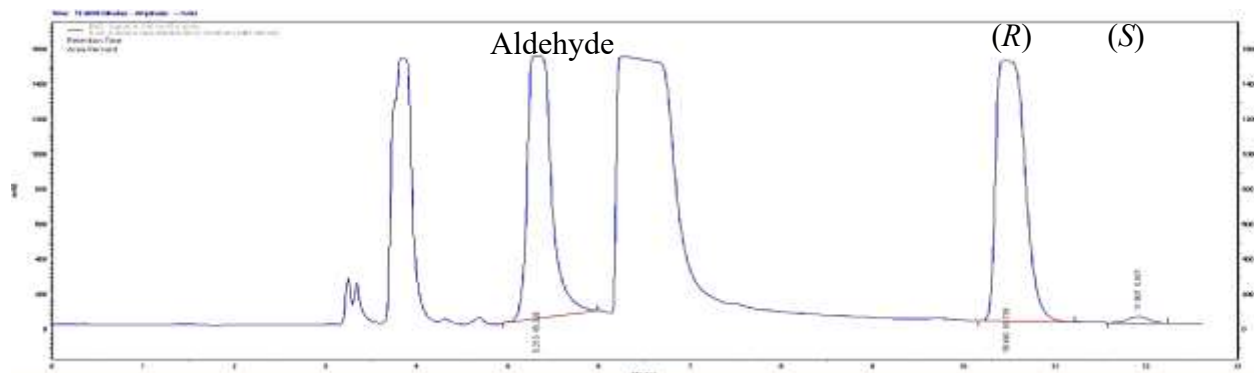


**Figure S77:** HPLC chromatogram of wild type *AtHNL* showing enantioselective synthesis of (*R*)-**2g** at 3 h using **1g** as the substrate.

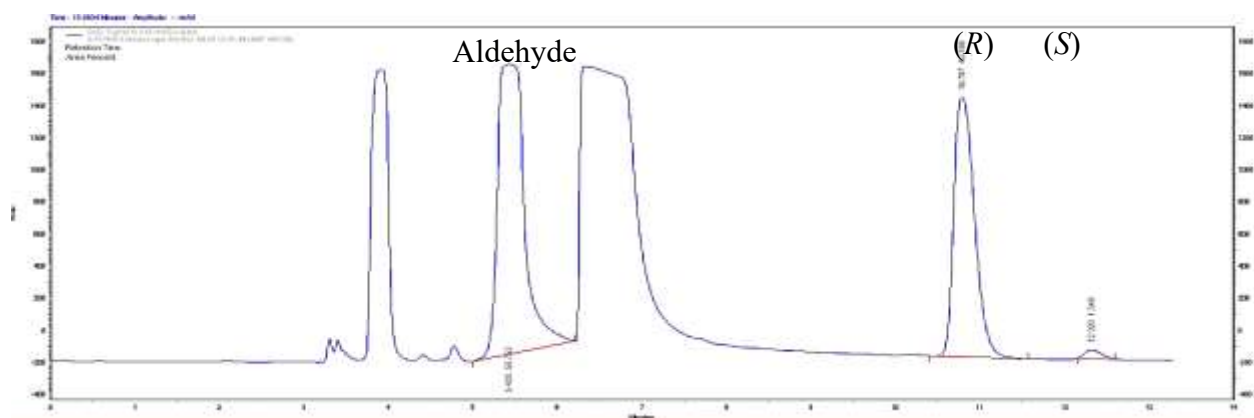


**Figure S78:** HPLC chromatogram of the F179W variant showing enantioselective synthesis of (*R*)-**2g** at 3 h using **1g** as the substrate.

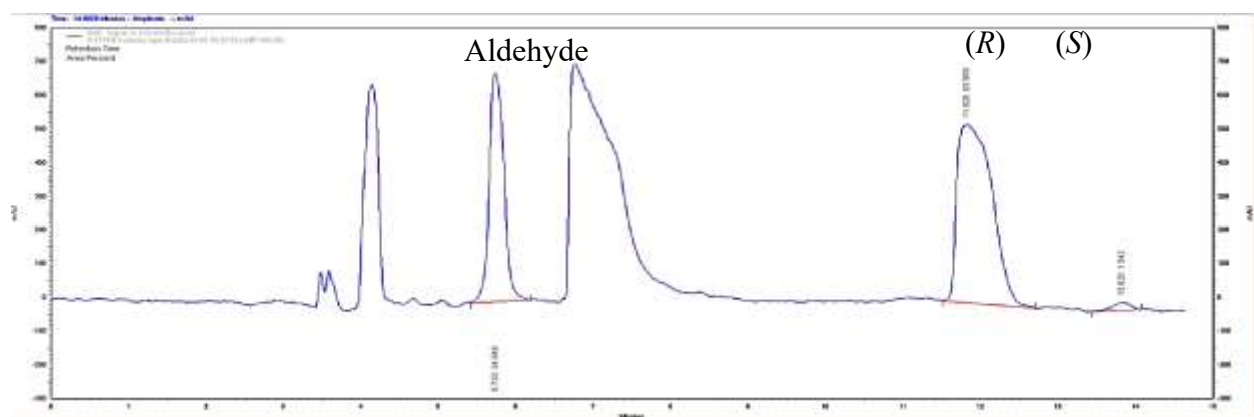


**Figure S79:** HPLC chromatogram of the F179N variant showing enantioselective synthesis of (*R*)-**2g** at 3 h using **1g** as the substrate.

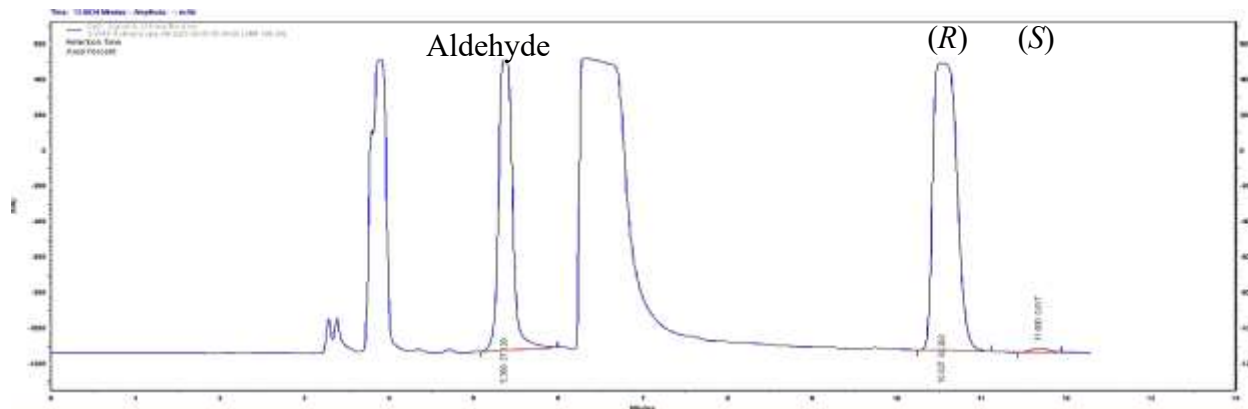


**Figure S80:** HPLC chromatogram of the Y14F variant showing enantioselective synthesis of (*R*)-**2g** at 3 h using **1g** as the substrate.

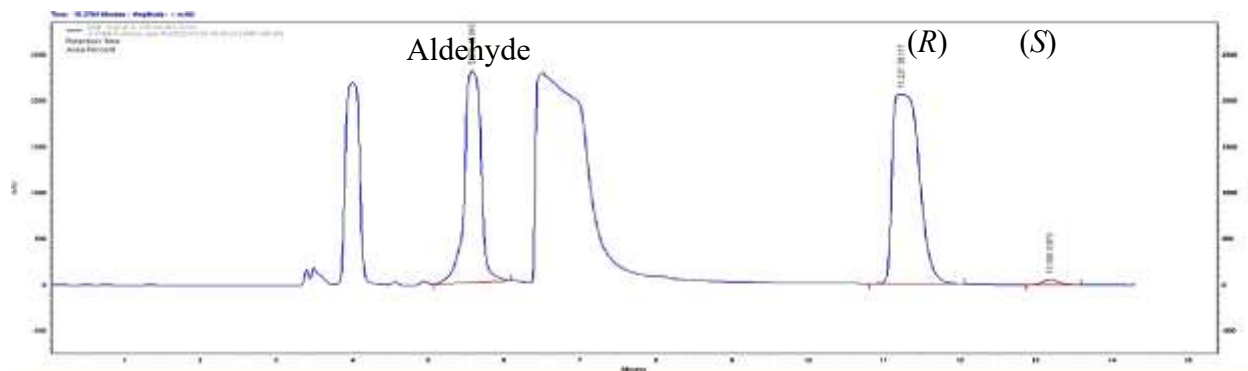


**Figure S81:** HPLC chromatogram of the Y14M variant showing enantioselective synthesis of (*R*)-**2g** at 3 h using **1g** as the substrate.

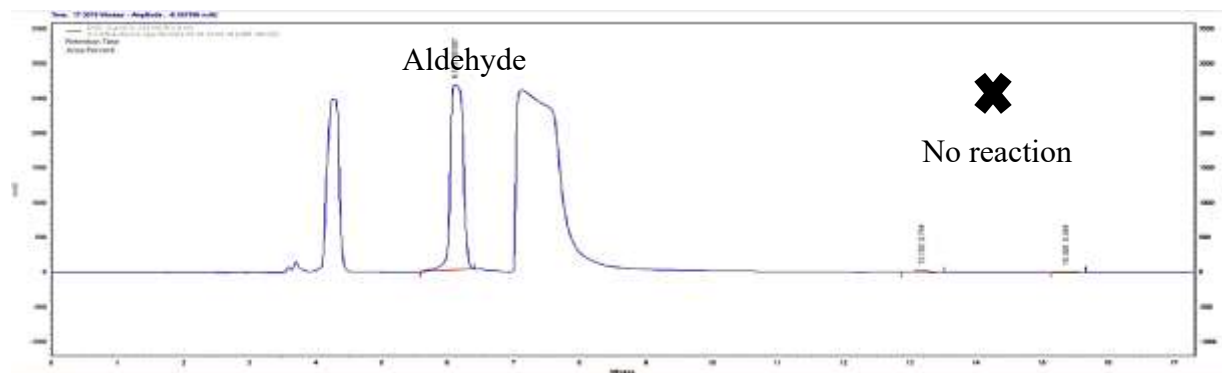


**Figure S82:** HPLC chromatogram of control reaction at 3 h where enzyme is replaced by 20 mM KPb and **2d** used as the substrate.

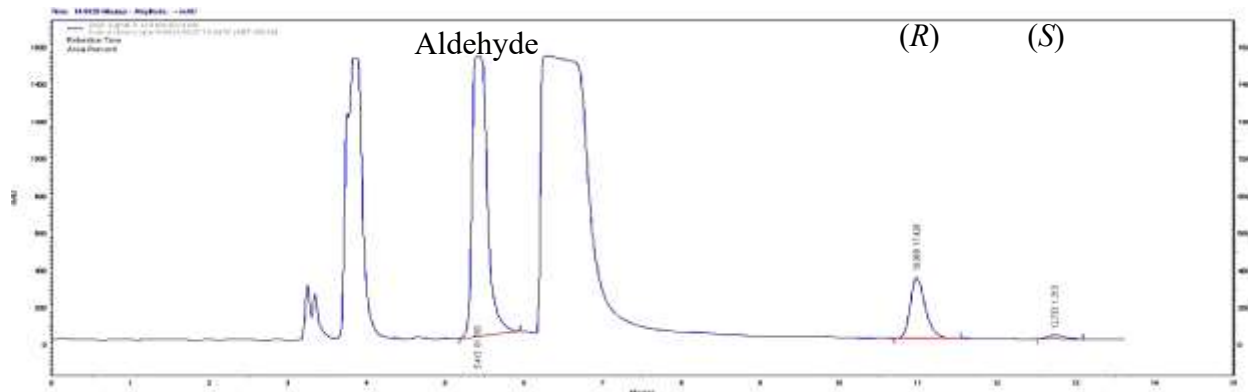


**Figure S83:** HPLC chromatogram of wild type *AtHNL* showing enantioselective synthesis of (*R*)-**2d** at 3 h using **1d** as the substrate.

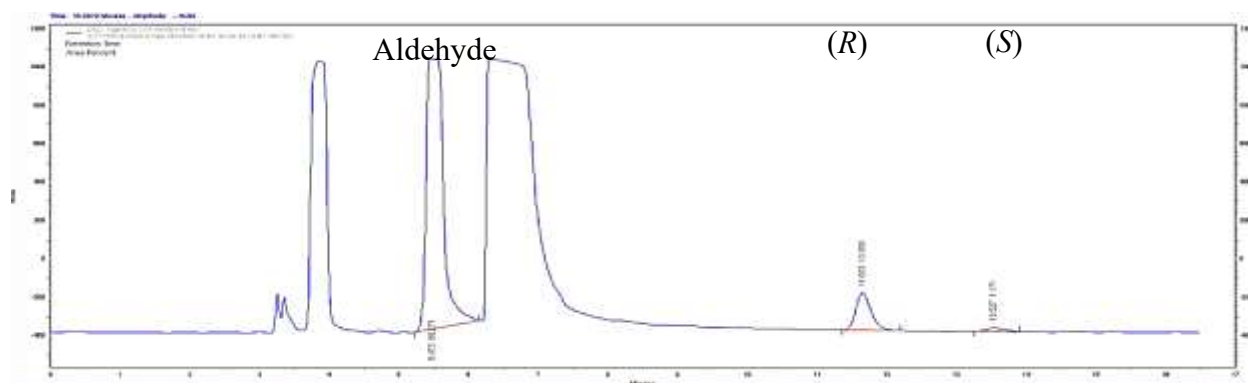


**Figure S84:** HPLC chromatogram of the F179W variant showing enantioselective synthesis of (*R*)-**2d** at 3 h using **1d** as the substrate.

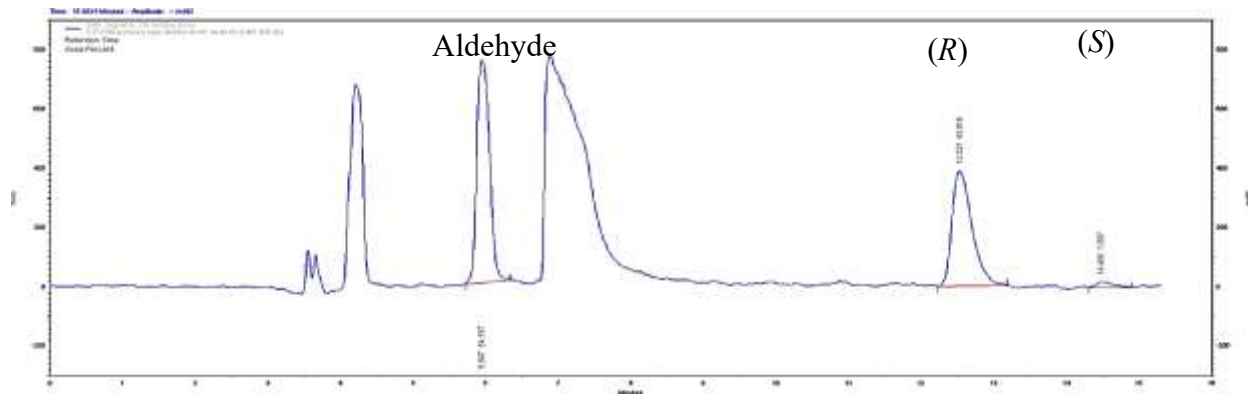


**Figure S85:** HPLC chromatogram of the F179N variant showing enantioselective synthesis of (*R*)-**2d** at 3 h using **1d** as the substrate.

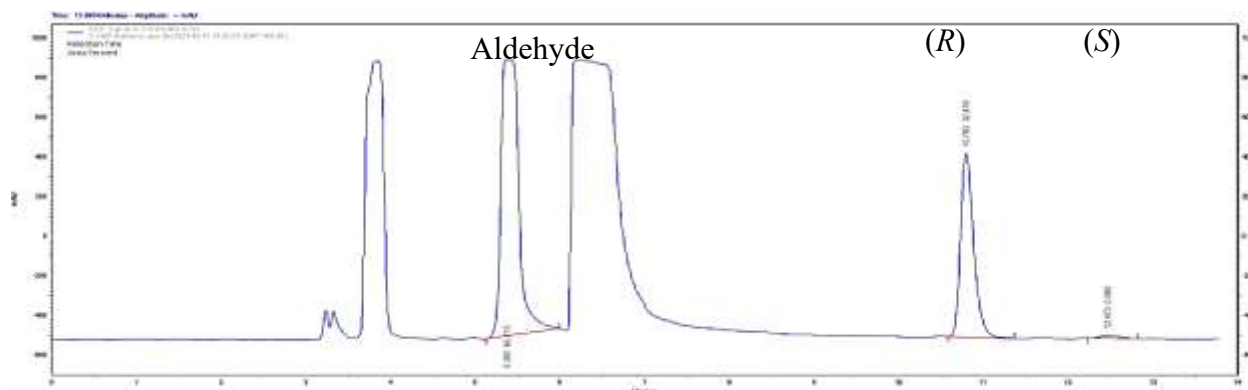


**Figure S86:** HPLC chromatogram of the Y14F variant showing enantioselective synthesis of (*R*)-**2d** at 3 h using **1d** as the substrate.

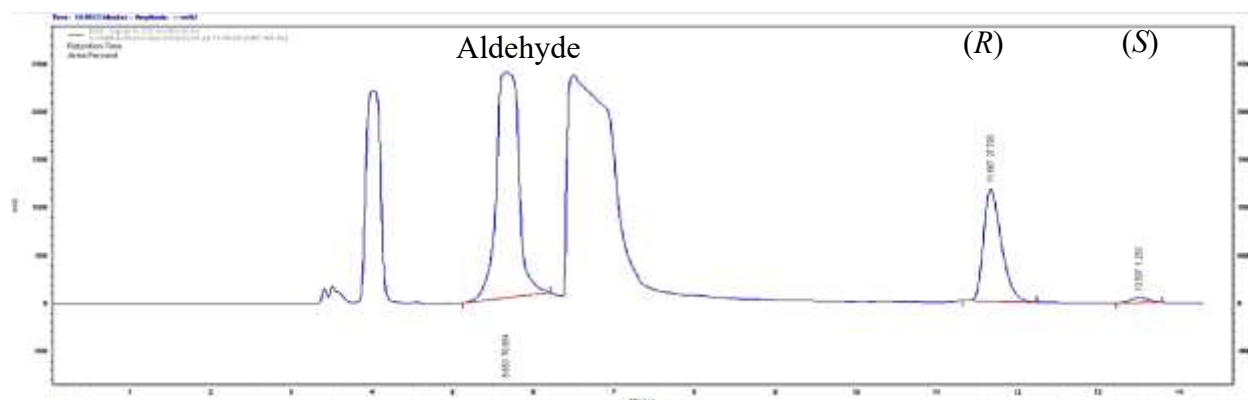


**Figure S87:** HPLC chromatogram of the Y14M variant showing enantioselective synthesis of (*R*)-**2d** at 3 h using **1d** as the substrate.

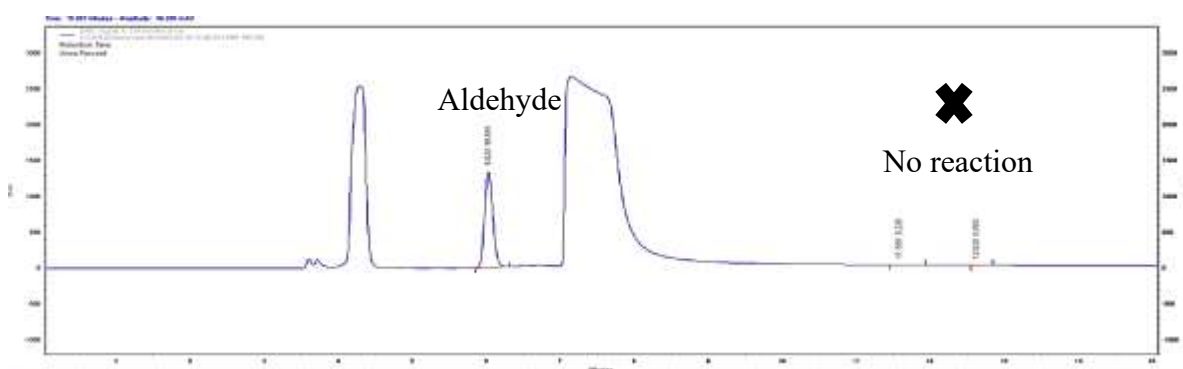


**Figure S88:** HPLC chromatogram of control reaction at 3 h where enzyme is replaced by 20 mM KPb and **2c** used as the substrate.

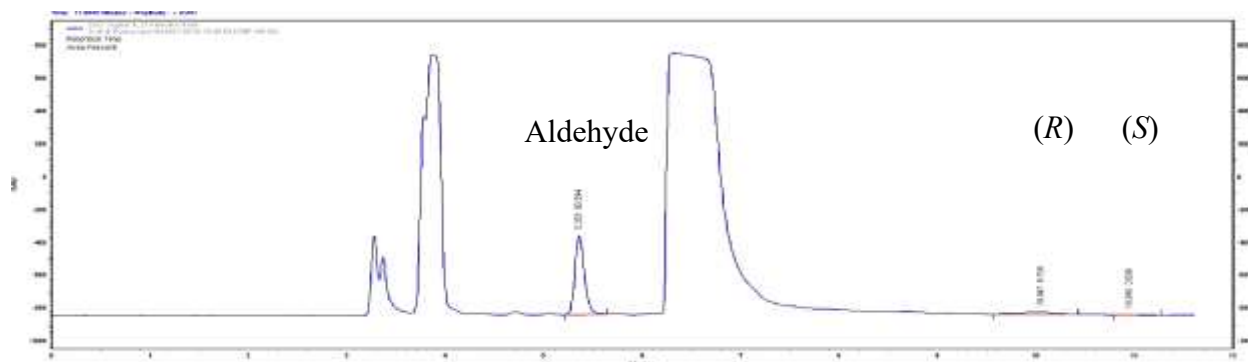


**Figure S89:** HPLC chromatogram of wild type *AtHNL* showing enantioselective synthesis of (*R*)-**2c** at 3 h using **1c** as the substrate.

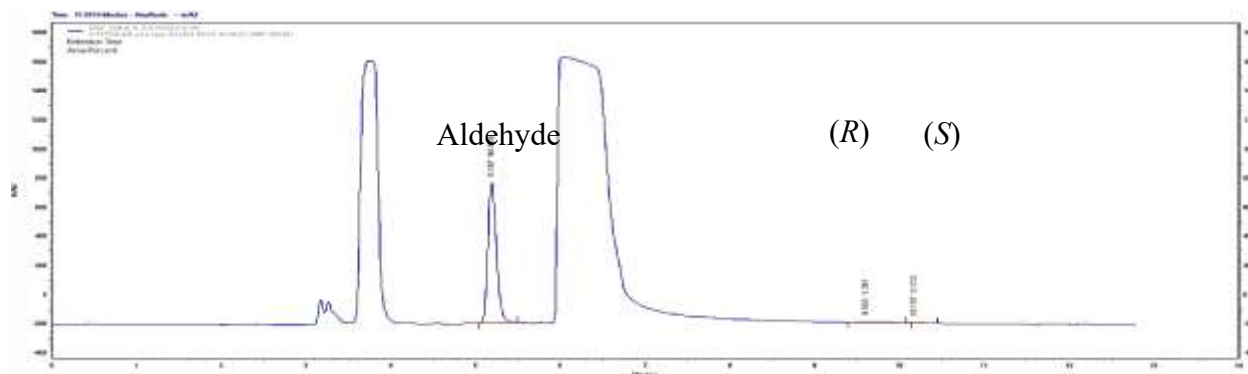


**Figure S90:** HPLC chromatogram of the F179W variant showing enantioselective synthesis of (*R*)-**2c** at 3 h using **1c** as the substrate.

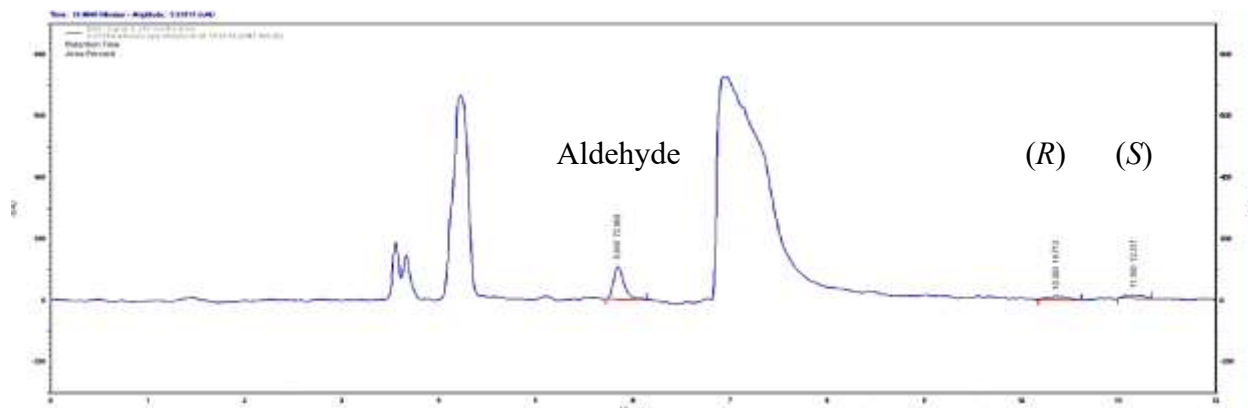


**Figure S91:** HPLC chromatogram of the F179N variant showing enantioselective synthesis of (*R*)-**2c** at 3 h using **1c** as the substrate.

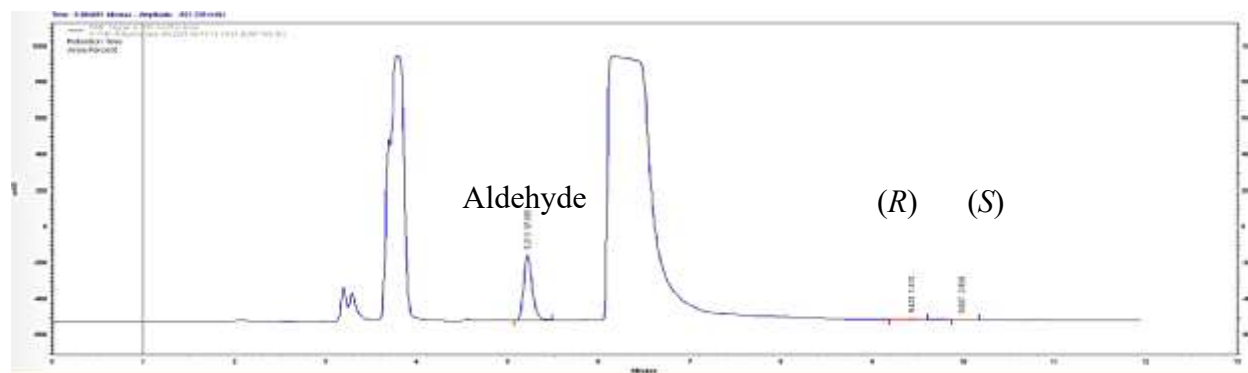


**Figure S92:** HPLC chromatogram of the Y14F variant showing enantioselective synthesis of (*R*)-**2c** at 3 h using **1c** as the substrate.

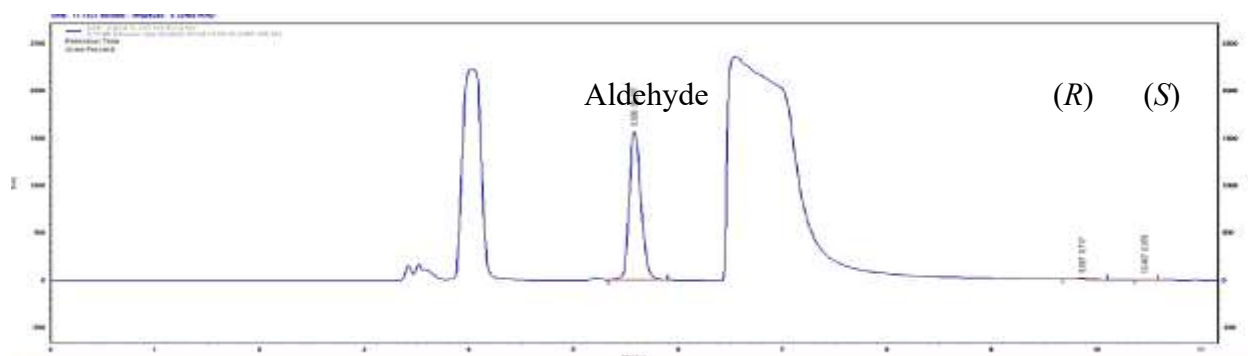


**Figure S93:** HPLC chromatogram of the Y14M variant showing enantioselective synthesis of (*R*)-**2c** at 3 h using **1c** as the substrate.

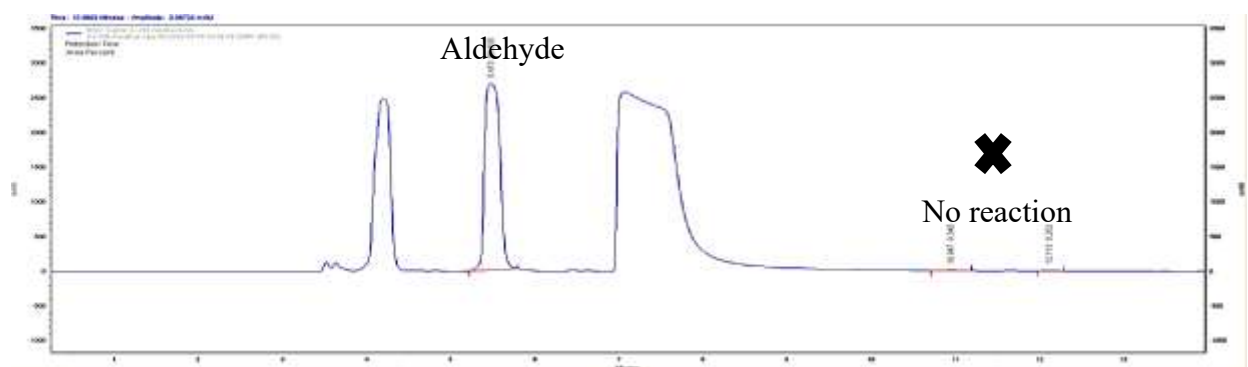


**Figure S94:** HPLC chromatogram of control reaction at 3 h where enzyme is replaced by 20 mM KPb and **2h** used as the substrate.

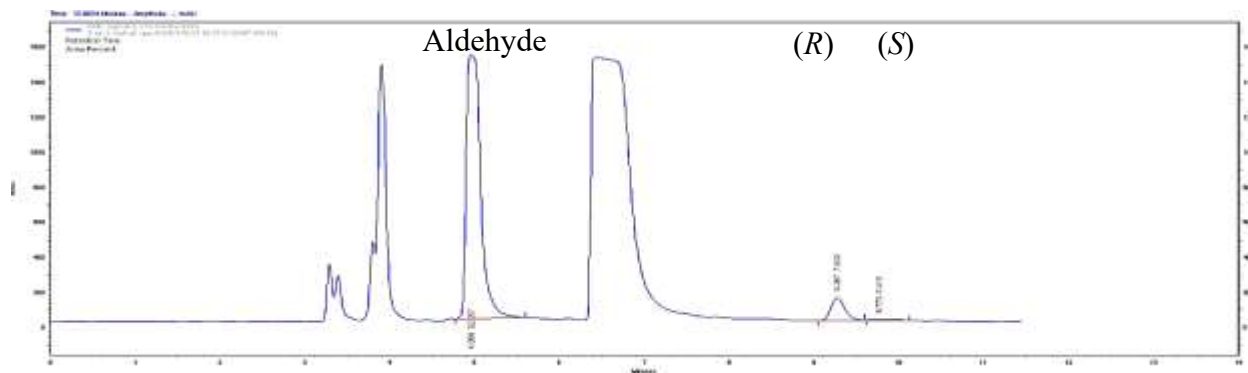


**Figure S95:** HPLC chromatogram of wild type *AtHNL* showing enantioselective synthesis of (*R*)-**2h** at 3 h using **1h** as the substrate.

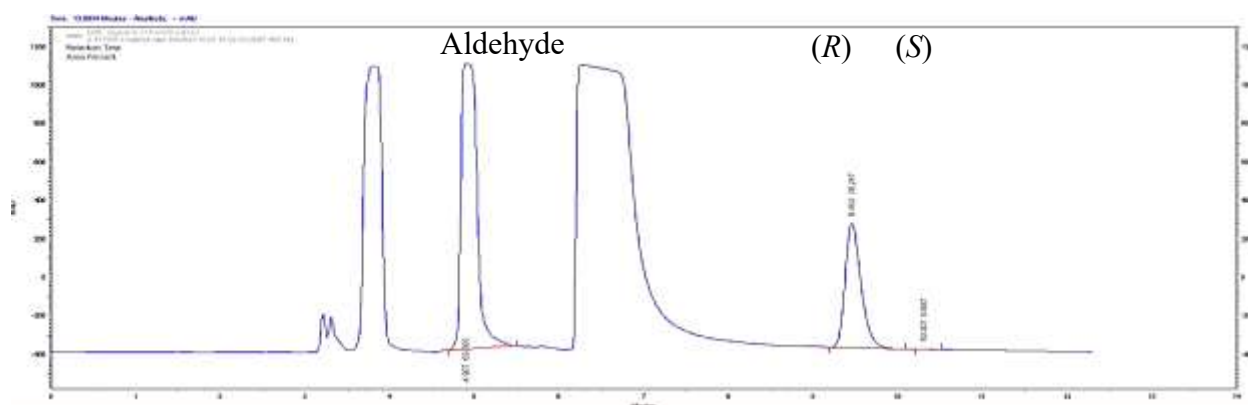


**Figure S96:** HPLC chromatogram of the F179W variant showing enantioselective synthesis of (*R*)-**2h** at 3 h using **1h** as the substrate.

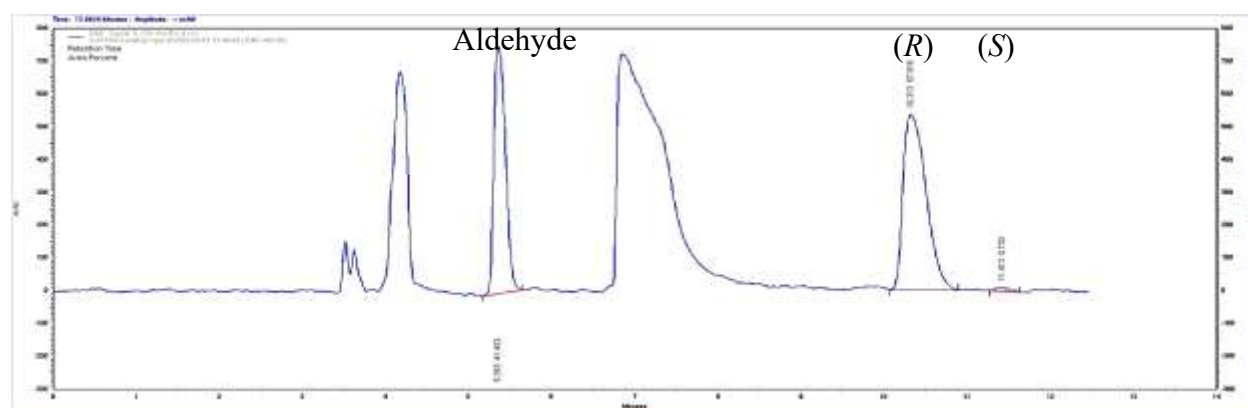


**Figure S97:** HPLC chromatogram of the F179N variant showing enantioselective synthesis of (*R*)-**2h** at 3 h using **1h** as the substrate.



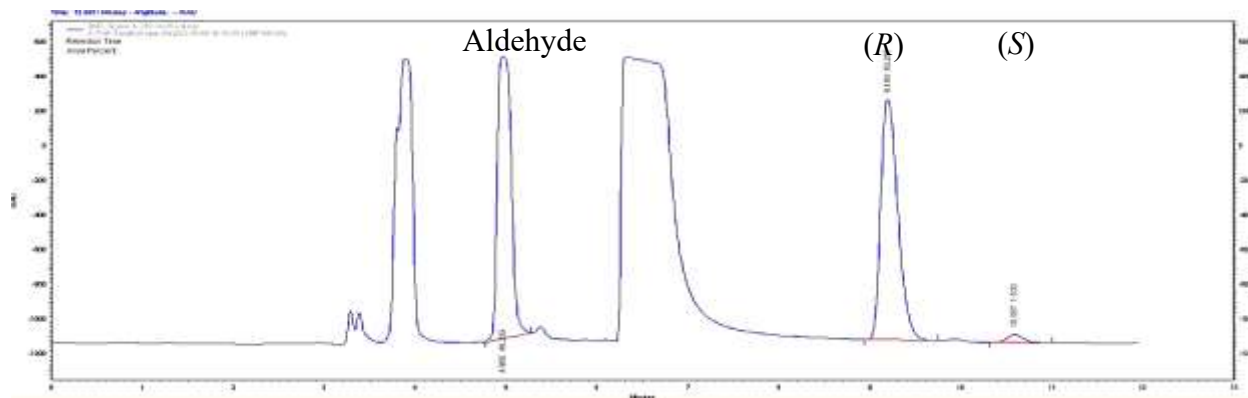


**Figure S98:** HPLC chromatogram of the Y14F variant showing enantioselective synthesis of (*R*)-**2h** at 3 h using **1h** as the substrate.

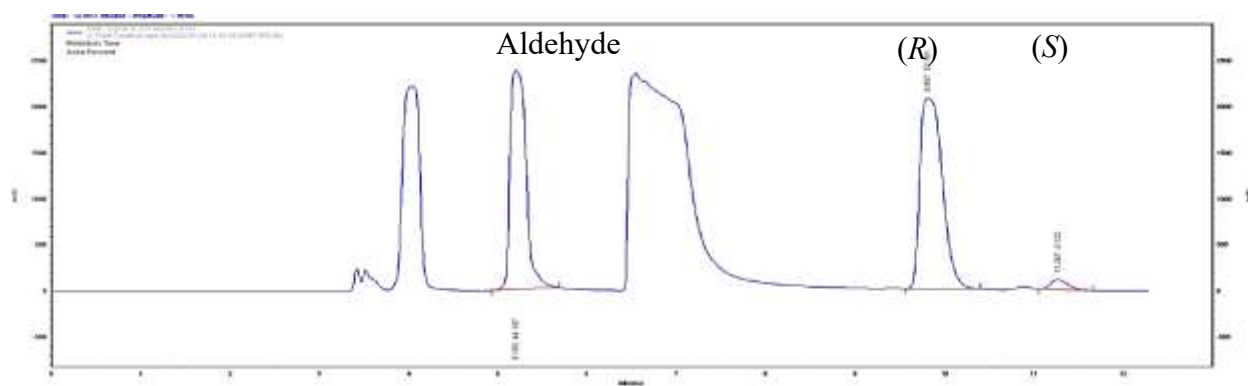


**Figure S99:** HPLC chromatogram of the Y14M variant showing enantioselective synthesis of (*R*)-**2h** at 3 h using **1h** as the substrate.

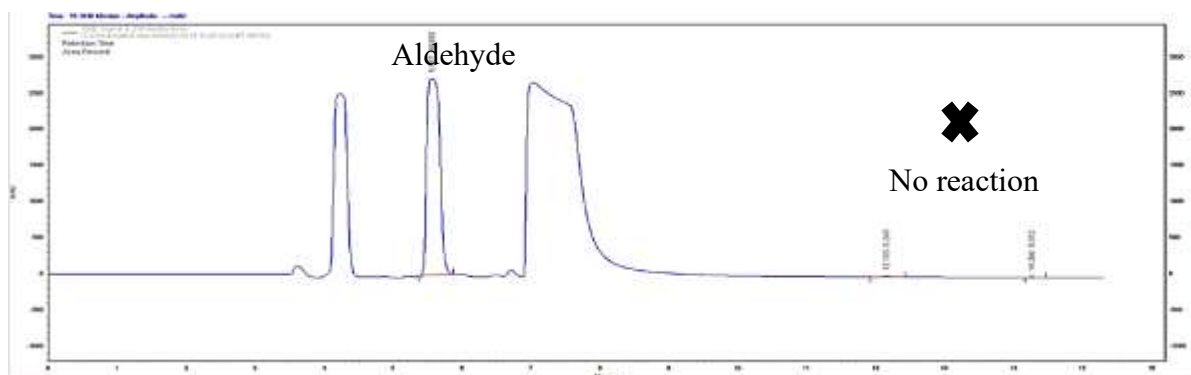


**Figure S100:** HPLC chromatogram of control reaction at 3 h where enzyme is replaced by 20 mM KPb and **1i** used as the substrate.

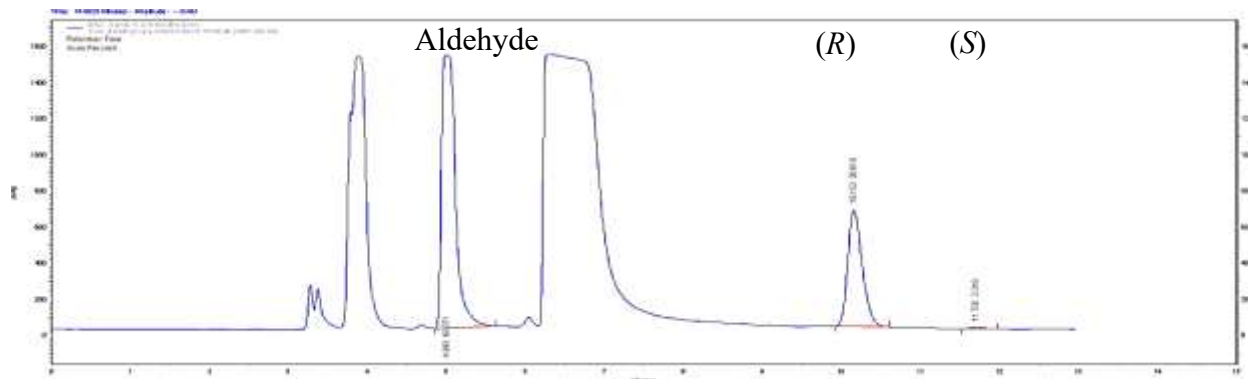


**Figure S101:** HPLC chromatogram of wild type *AtHNL* showing enantioselective synthesis of (*R*)-**2i** at 3 h using **1i** as the substrate.

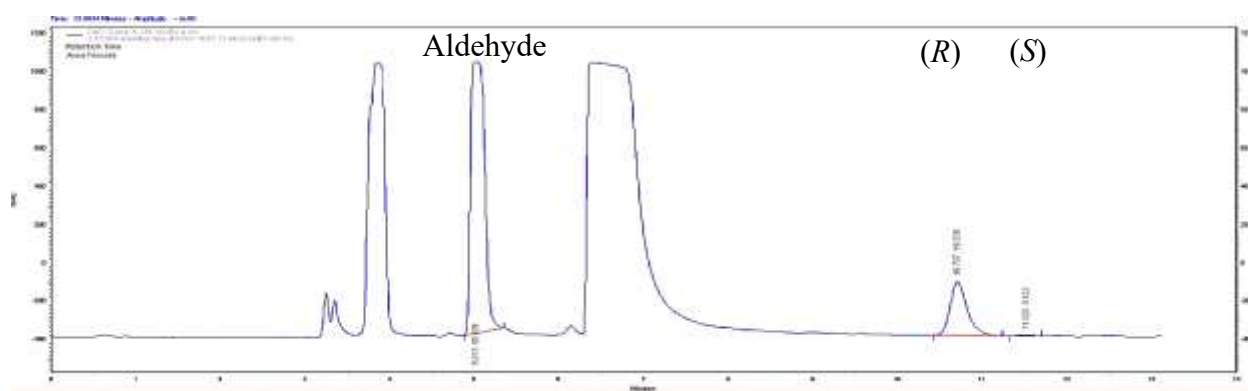


**Figure S102:** HPLC chromatogram of the F179W variant showing enantioselective synthesis of (*R*)-**2i** at 3 h using **1i** as the substrate.

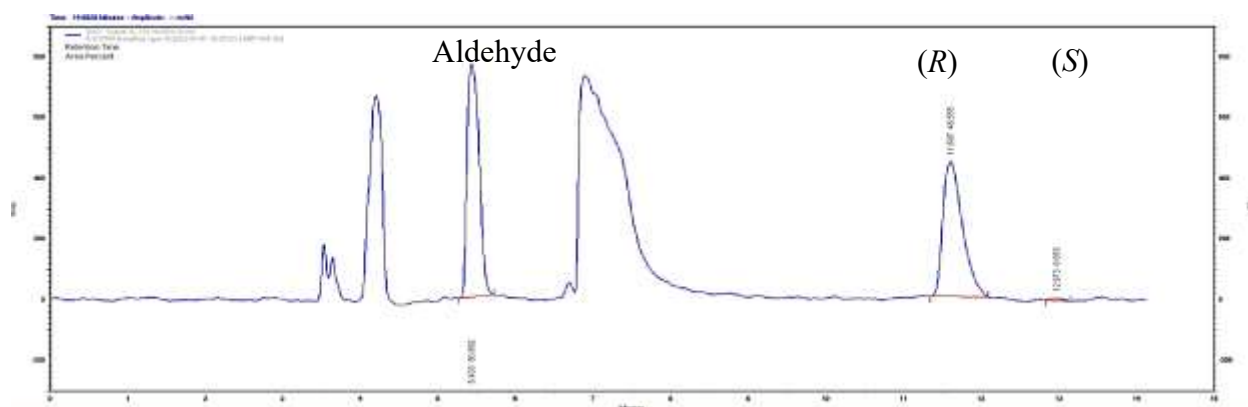


**Figure S103:** HPLC chromatogram of the F179N variant showing enantioselective synthesis of (*R*)-**2i** at 3 h using **1i** as the substrate.

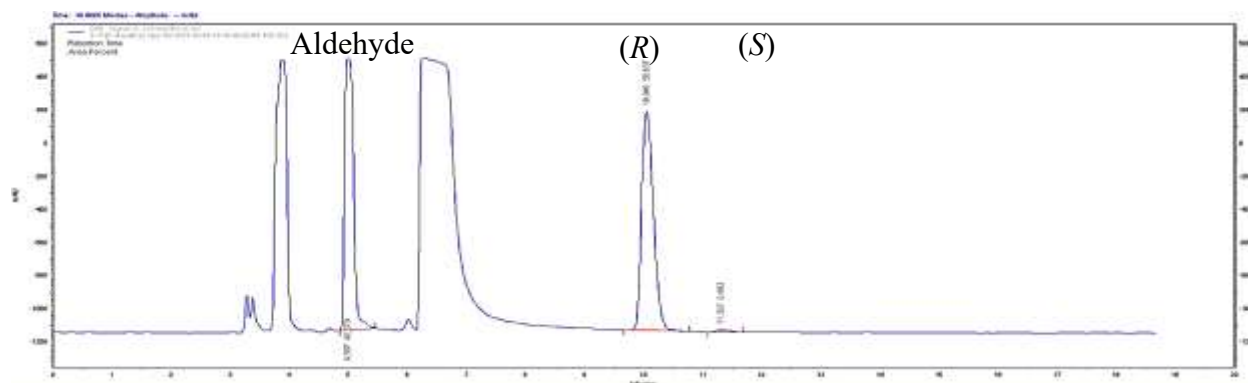


**Figure S104:** HPLC chromatogram of the Y14F variant showing enantioselective synthesis of (*R*)-**2i** at 3 h using **1i** as the substrate.

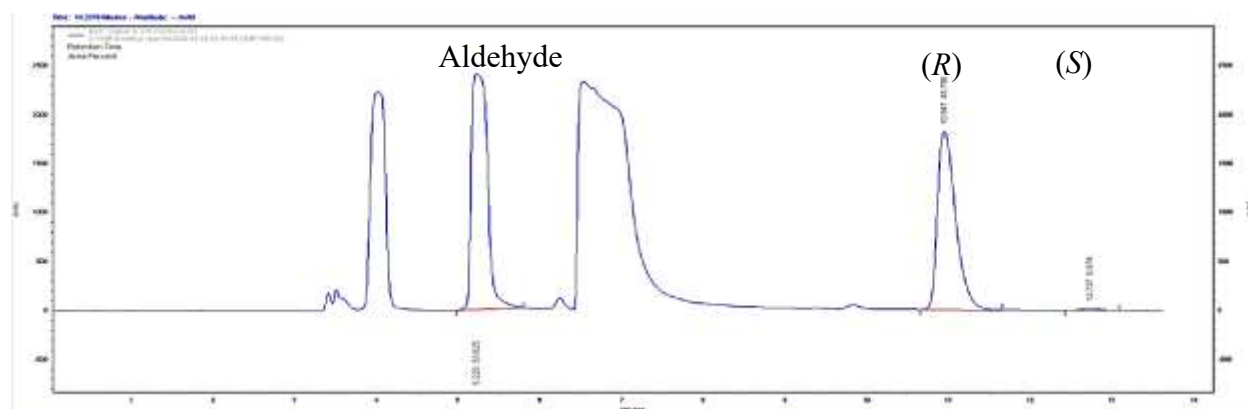


**Figure S105:** HPLC chromatogram of the Y14M variant showing enantioselective synthesis of (*R*)-**2i** at 3 h using **1i** as the substrate.

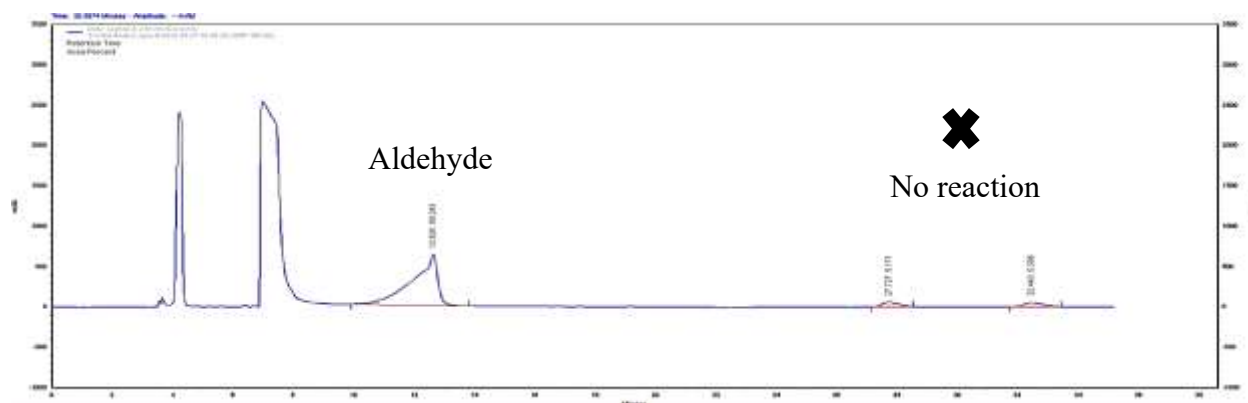


**Figure S106:** HPLC chromatogram of control reaction at 3 h where enzyme is replaced by 20 mM KPb and **1e** used as the substrate.

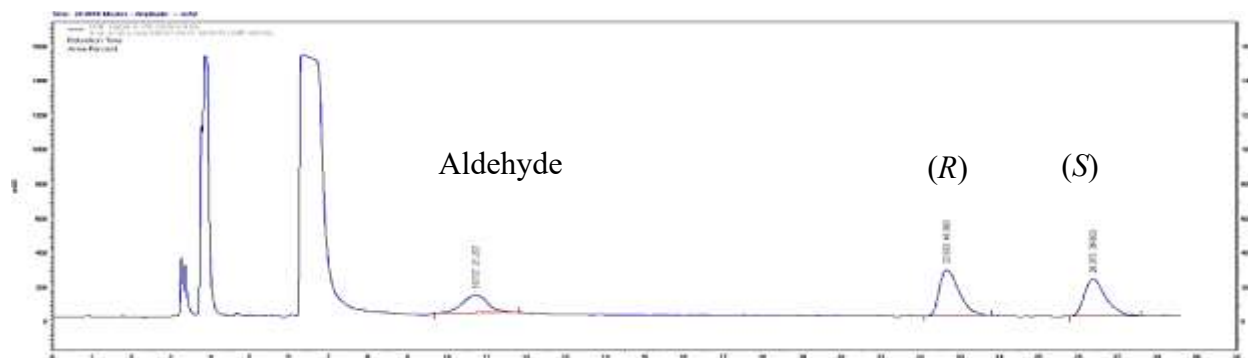


**Figure S107:** HPLC chromatogram of wild type AtHNL showing enantioselective synthesis of (R)-2e at 3 h using 1e as the substrate.

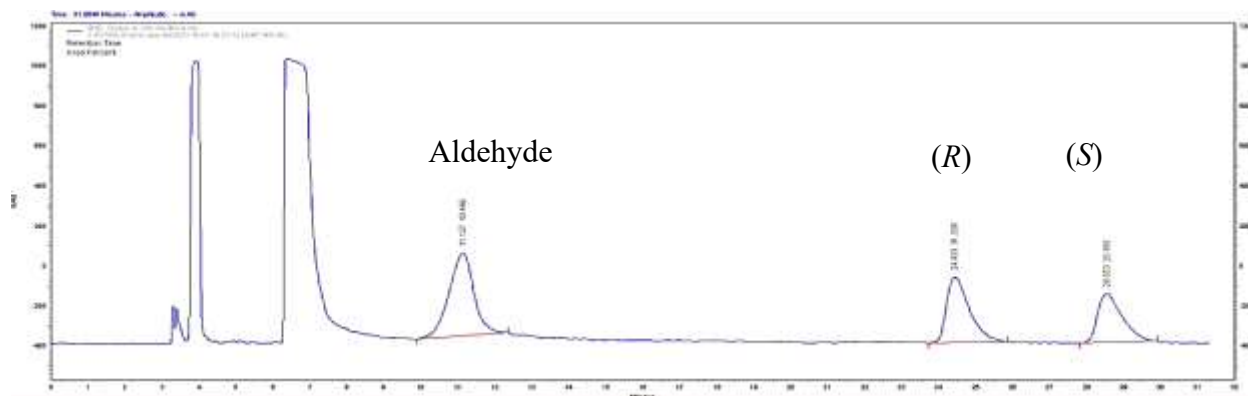


**Figure S108:** HPLC chromatogram of the F179W variant showing enantioselective synthesis of (R)-2e at 3 h using 1e as the substrate.

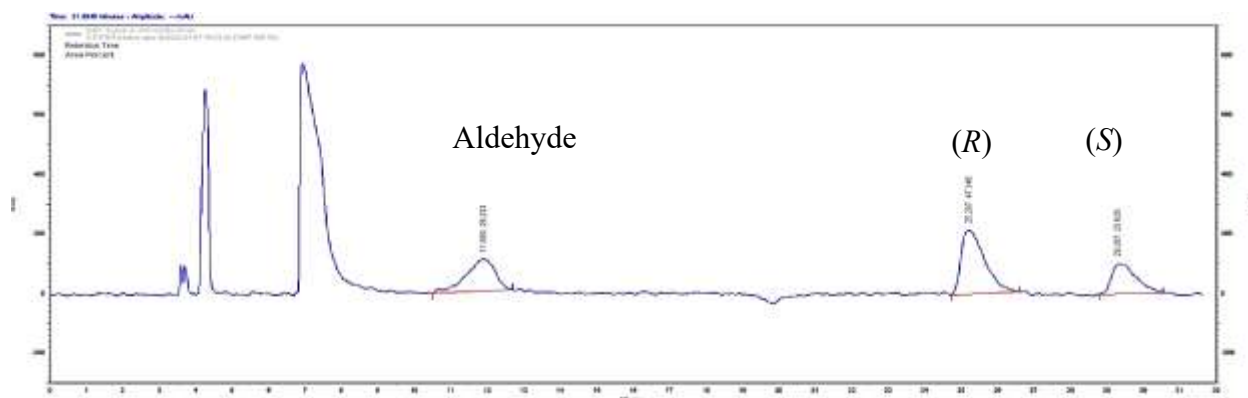


**Figure S109:** HPLC chromatogram of the F179N variant showing enantioselective synthesis of (R)-2e at 3 h using 1e as the substrate.

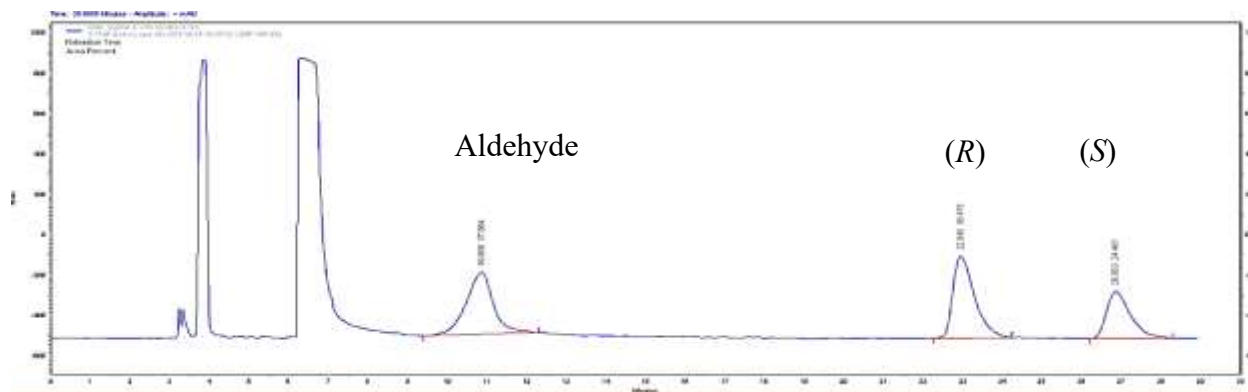


**Figure S110:** HPLC chromatogram of the Y14F variant showing enantioselective synthesis of (*R*)-**2e** at 3 h using **1e** as the substrate.

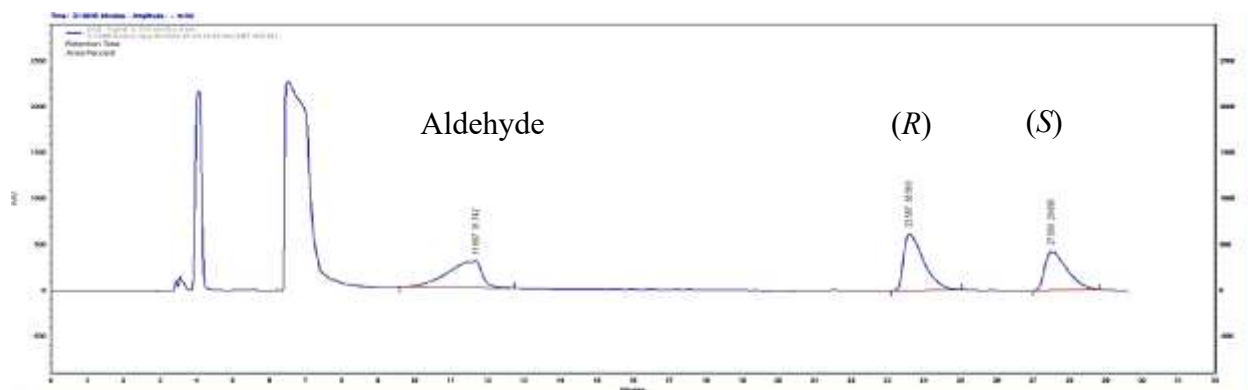


**Figure S111:** HPLC chromatogram of the Y14M variant showing enantioselective synthesis of (*R*)-**2e** at 3 h using **1e** as the substrate.

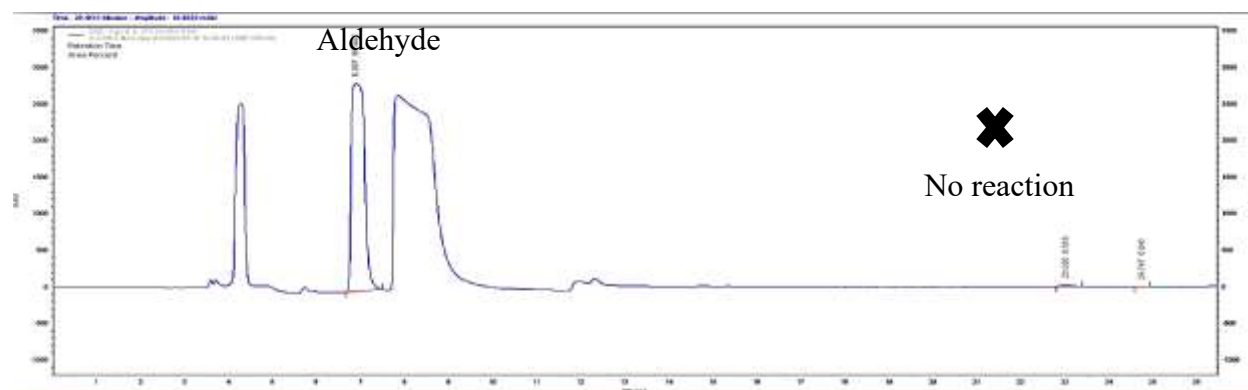


**Figure S112:** HPLC chromatogram of control reaction at 3 h where enzyme is replaced by 20 mM KPB and **1j** used as the substrate.

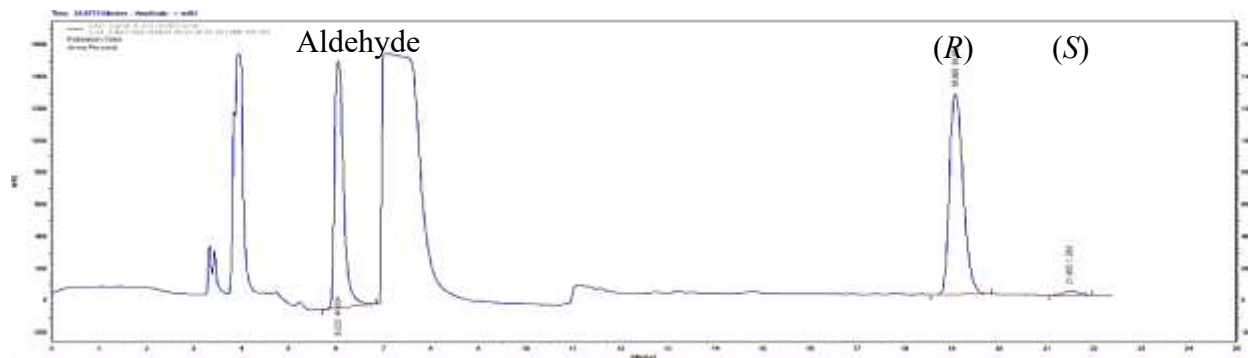


**Figure S113:** HPLC chromatogram of wild type *AtHNL* showing enantioselective synthesis of (*R*)-**2j** at 3 h using **1j** as the substrate.

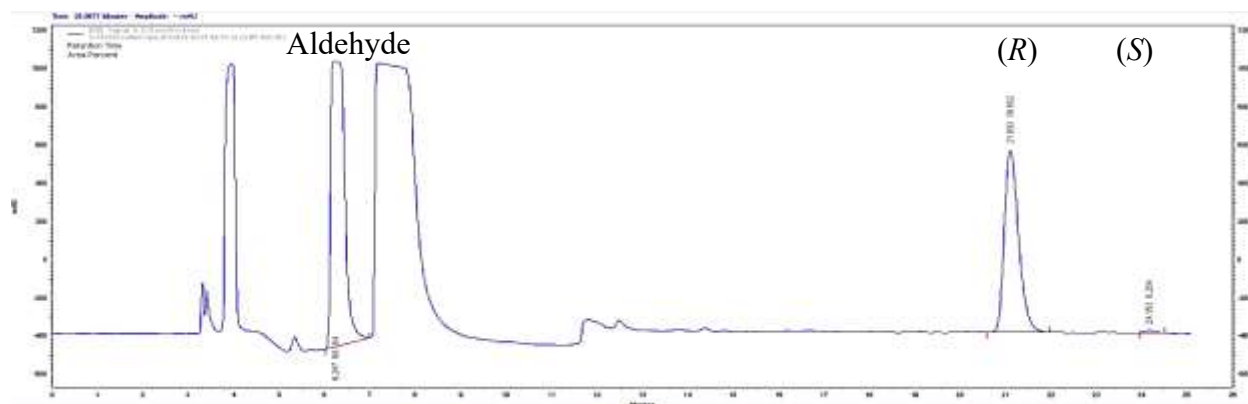


**Figure S114:** HPLC chromatogram of the F179W variant showing enantioselective synthesis of (*R*)-**2j** at 3 h using **1j** as the substrate.

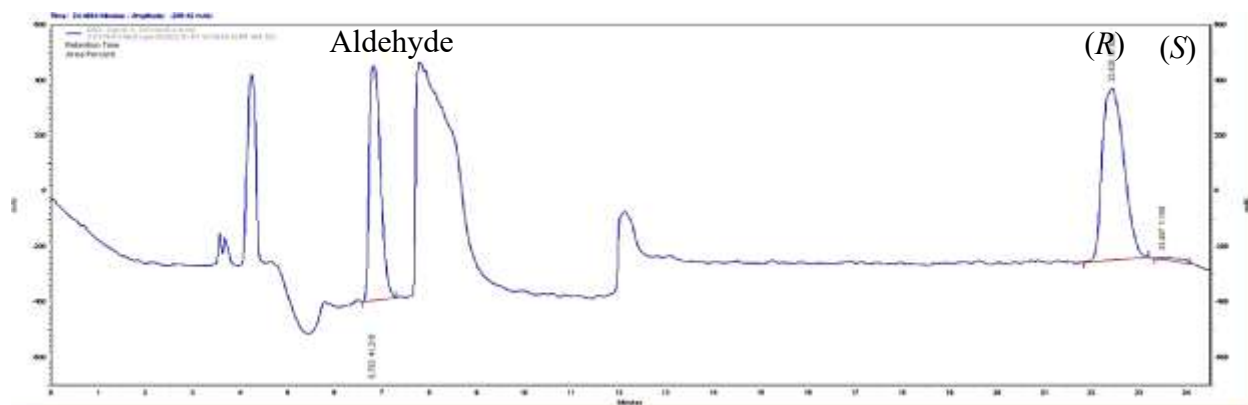


**Figure S115:** HPLC chromatogram of the F179N variant showing enantioselective synthesis of (*R*)-**2j** at 3 h using **1j** as the substrate.

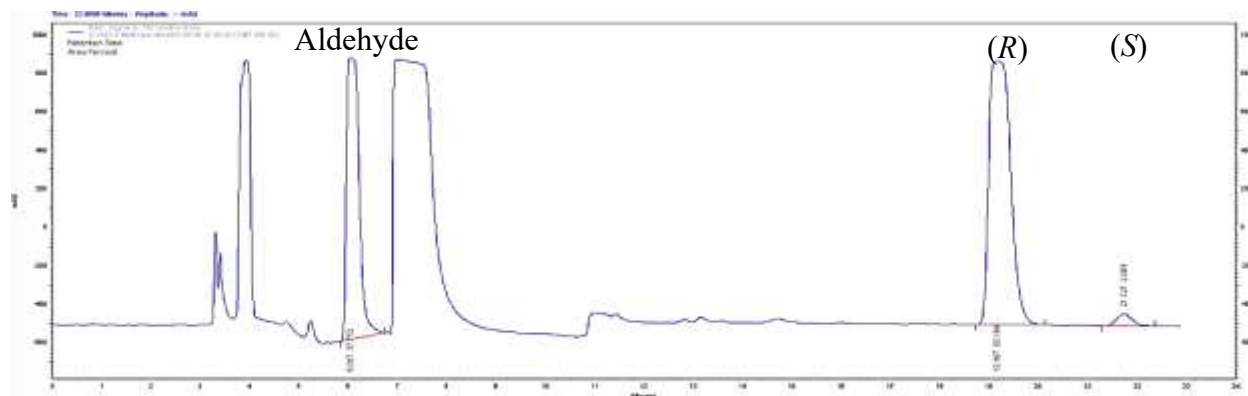


**Figure S116:** HPLC chromatogram of the Y14F variant showing enantioselective synthesis of (*R*)-**2j** at 3 h using **1j** as the substrate.

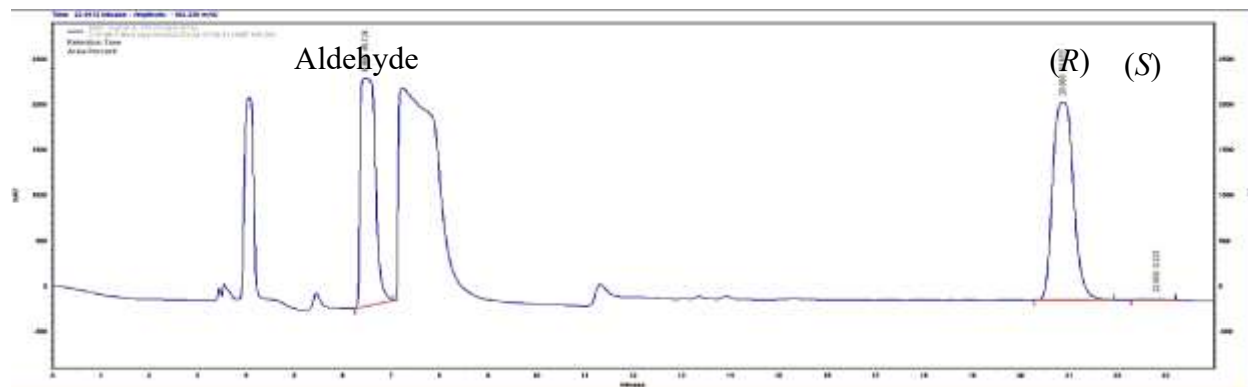


**Figure S117:** HPLC chromatogram of the Y14M variant showing enantioselective synthesis of (*R*)-**2j** at 3 h using **1j** as the substrate.

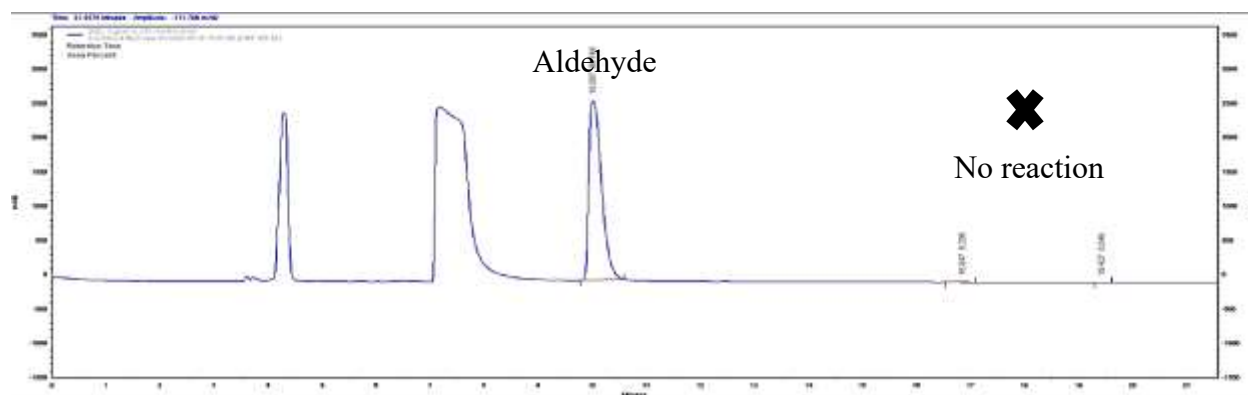


**Figure S118:** HPLC chromatogram of control reaction at 3 h where enzyme is replaced by 20 mM KPB and **1f** used as the substrate.

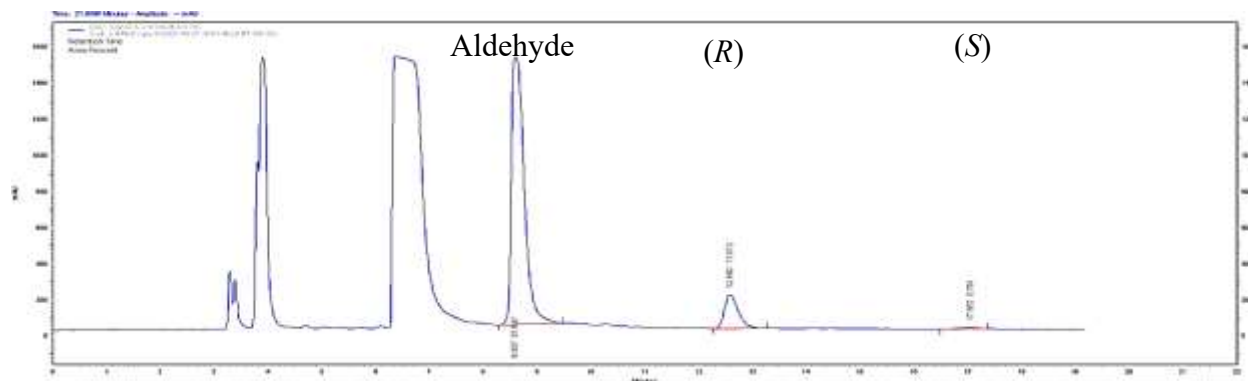


**Figure S119:** HPLC chromatogram of wild type *AtHNL* showing enantioselective synthesis of (*R*)-**2f** at 3 h using **1f** as the substrate.

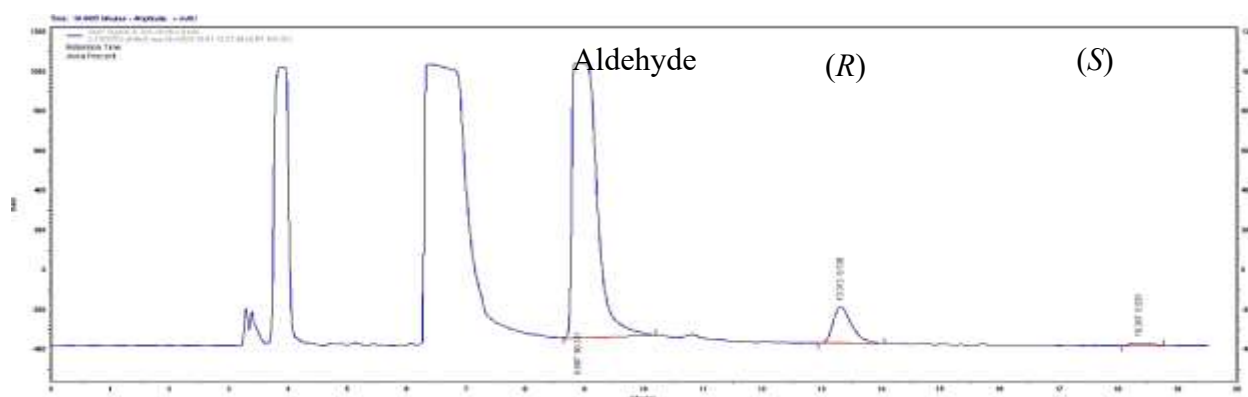


**Figure S120:** HPLC chromatogram of the F179W variant showing enantioselective synthesis of (*R*)-**2f** at 3 h using **1f** as the substrate.

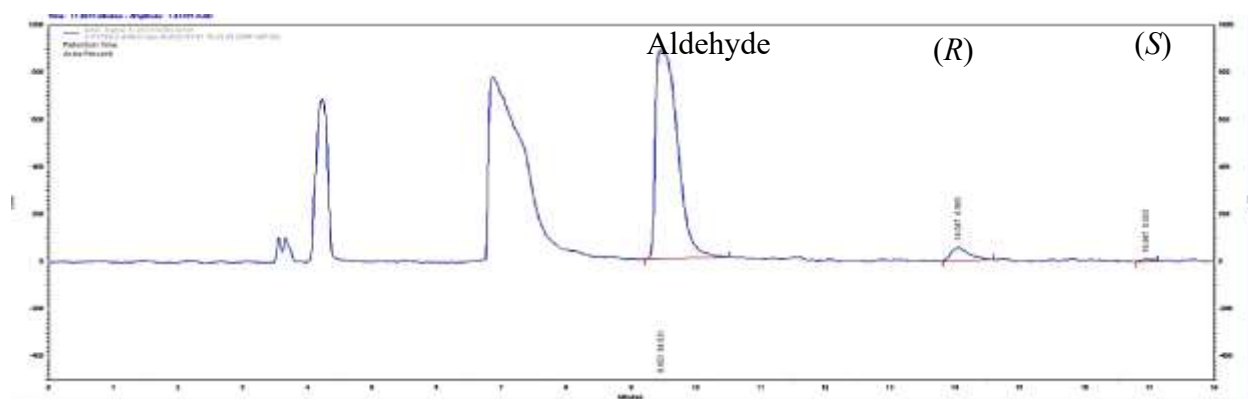


**Figure S121:** HPLC chromatogram of the F179N variant showing enantioselective synthesis of (*R*)-**2f** at 3 h using **1f** as the substrate.



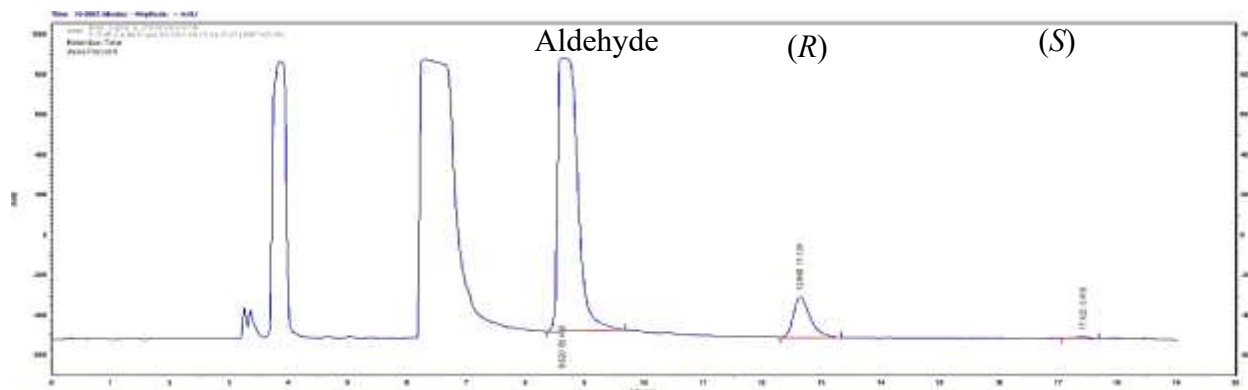


**Figure S122:** HPLC chromatogram of the Y14F variant showing enantioselective synthesis of (*R*)-**2f** at 3 h using **1f** as the substrate.

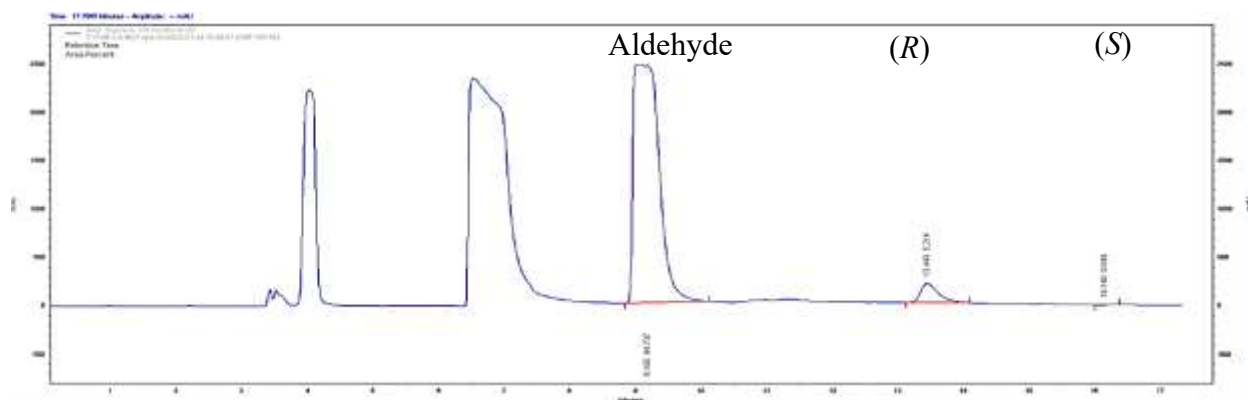


**Figure S123:** HPLC chromatogram of the Y14M variant showing enantioselective synthesis of (*R*)-**2f** at 3 h using **1f** as the substrate.

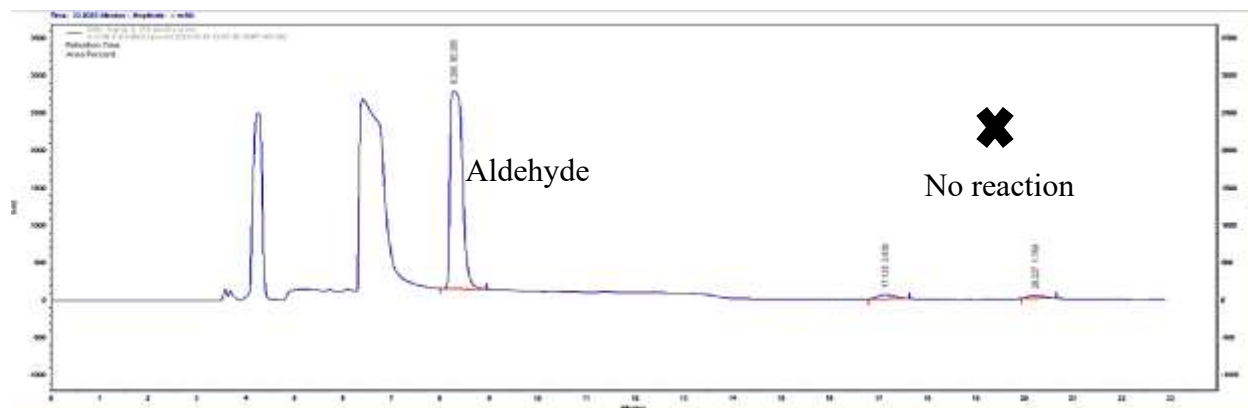


**Figure S124:** HPLC chromatogram of control reaction at 3 h where enzyme is replaced by 20 mM KPB and **1k** used as the substrate.

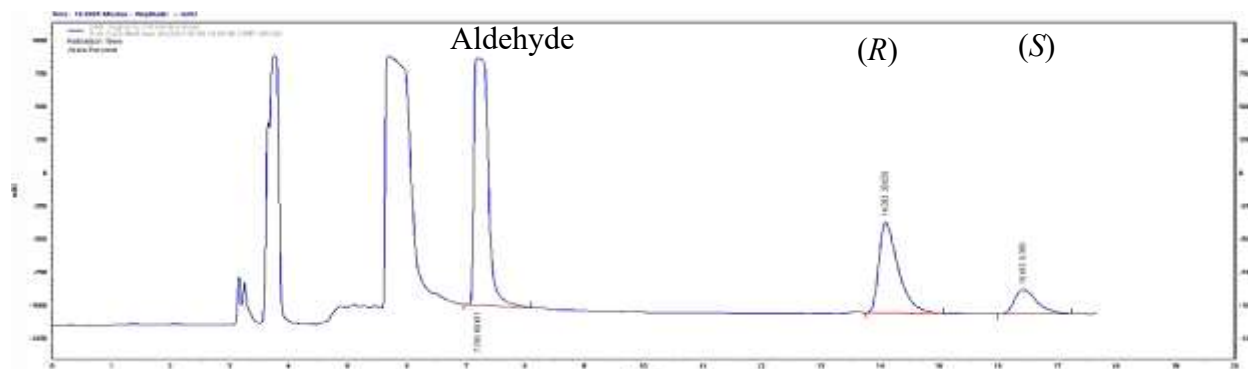


**Figure S125:** HPLC chromatogram of wild type *AtHNL* showing enantioselective synthesis of (*R*)-**2k** at 3 h using **1k** as the substrate.

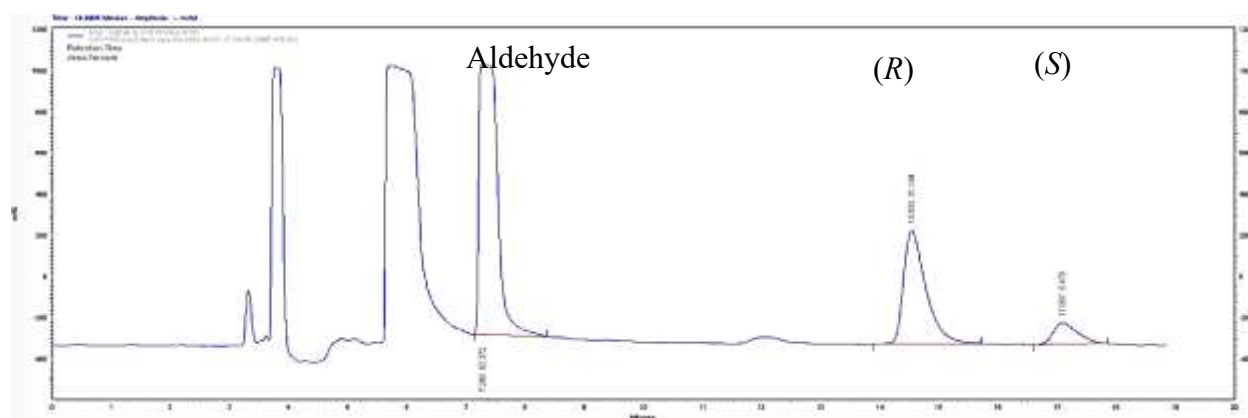


**Figure S126:** HPLC chromatogram of the F179W variant showing enantioselective synthesis of (*R*)-**2k** at 3 h using **1k** as the substrate.

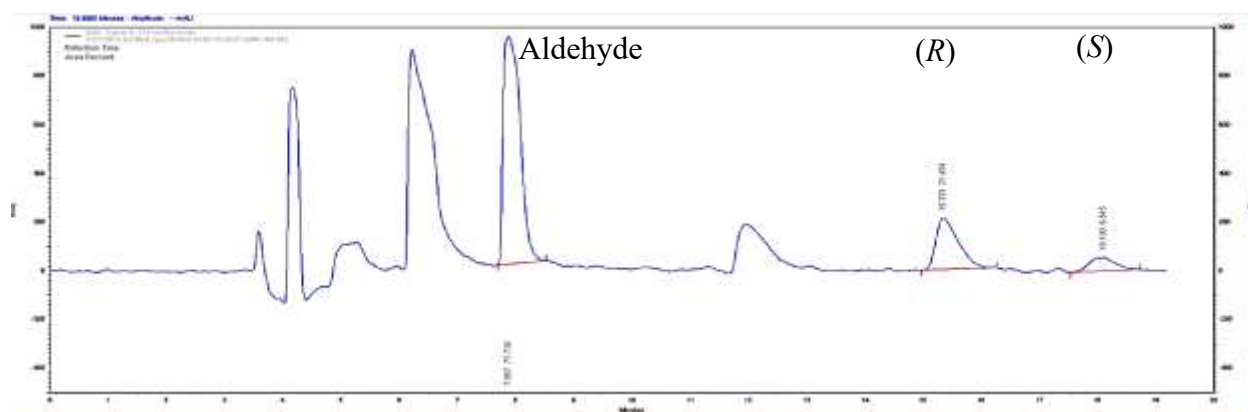


**Figure S127:** HPLC chromatogram of the F179N variant showing enantioselective synthesis of (*R*)-**2k** at 3 h using **1k** as the substrate.

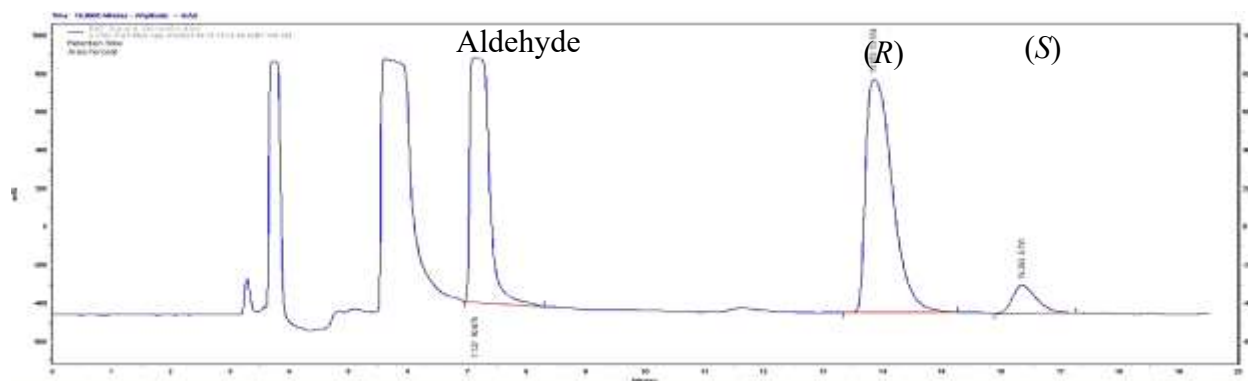


**Figure S128:** HPLC chromatogram of the Y14F variant showing enantioselective synthesis of (*R*)-**2k** at 3 h using **1k** as the substrate.

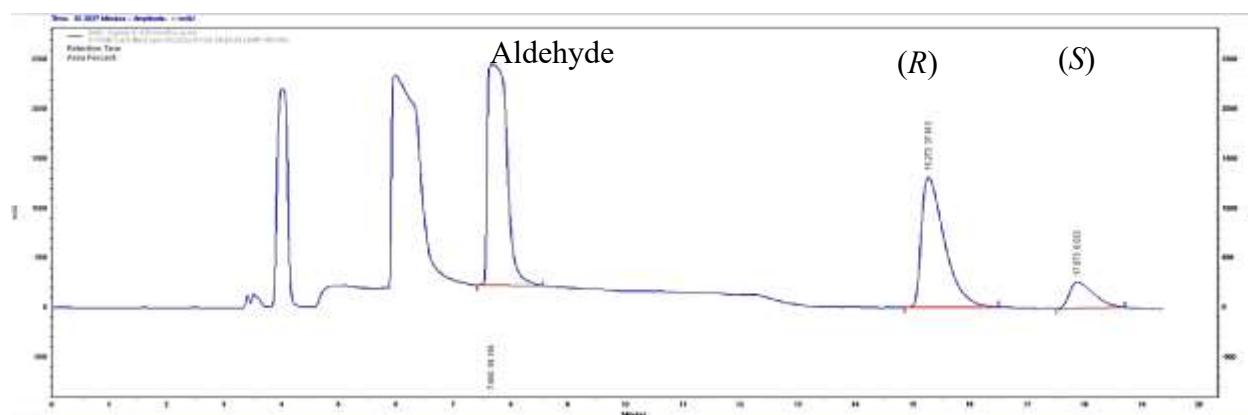


**Figure S129:** HPLC chromatogram of the Y14M variant showing enantioselective synthesis of (*R*)-**2k** at 3 h using **1k** as the substrate.

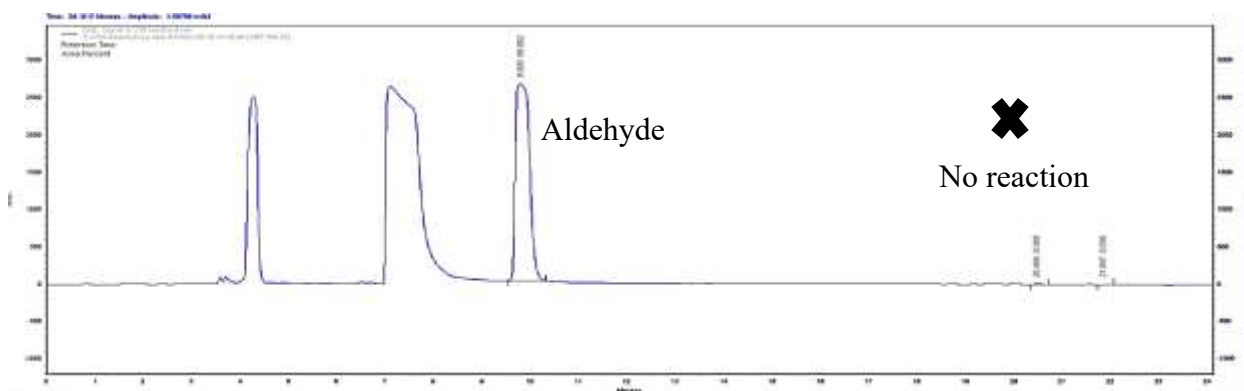


**Figure S130:** HPLC chromatogram of control reaction at 3 h where enzyme is replaced by 20 mM KPB and **1l** used as the substrate.

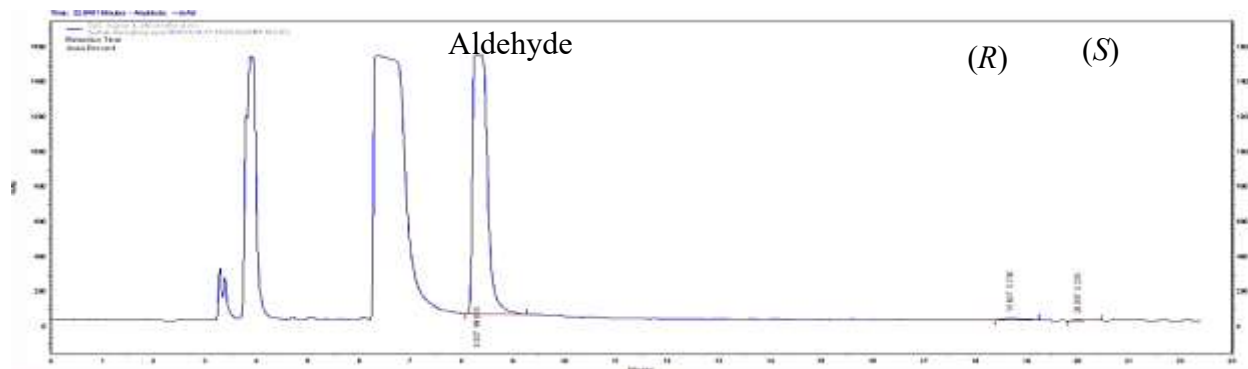


**Figure S131:** HPLC chromatogram of wild type *AtHNL* showing enantioselective synthesis of (*R*)-**2I** at 3 h using **1I** as the substrate.

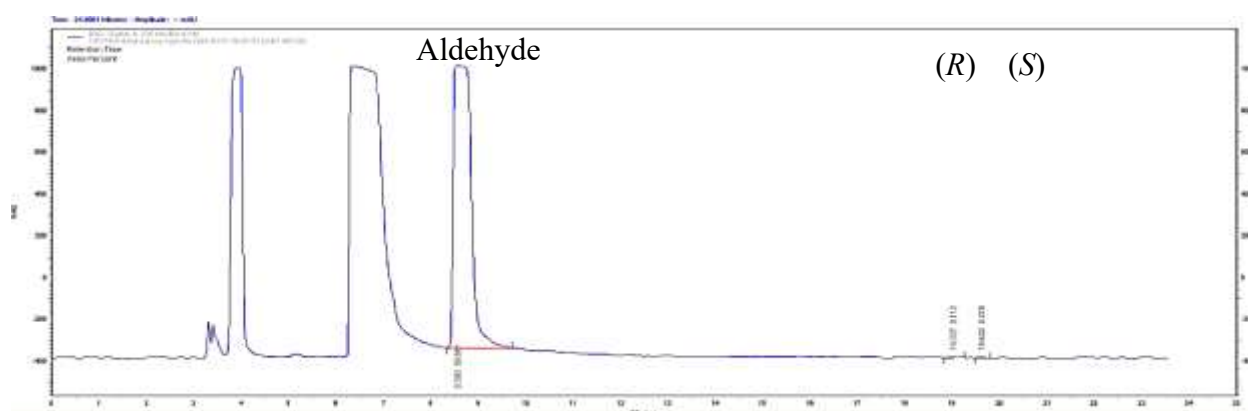


**Figure S132:** HPLC chromatogram of the F179W variant showing enantioselective synthesis of (*R*)-**2I** at 3 h using **1I** as the substrate.

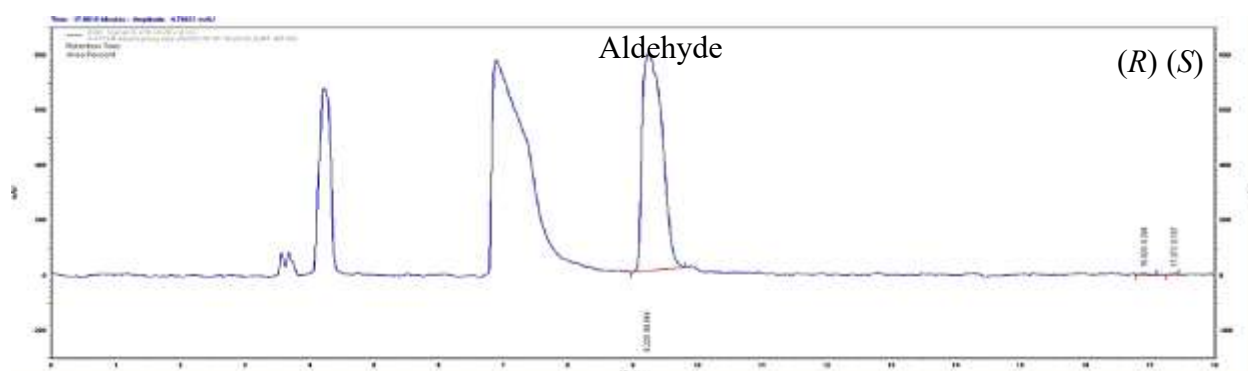


**Figure S133:** HPLC chromatogram of the F179N variant showing enantioselective synthesis of (*R*)-**2I** at 3 h using **1I** as the substrate.

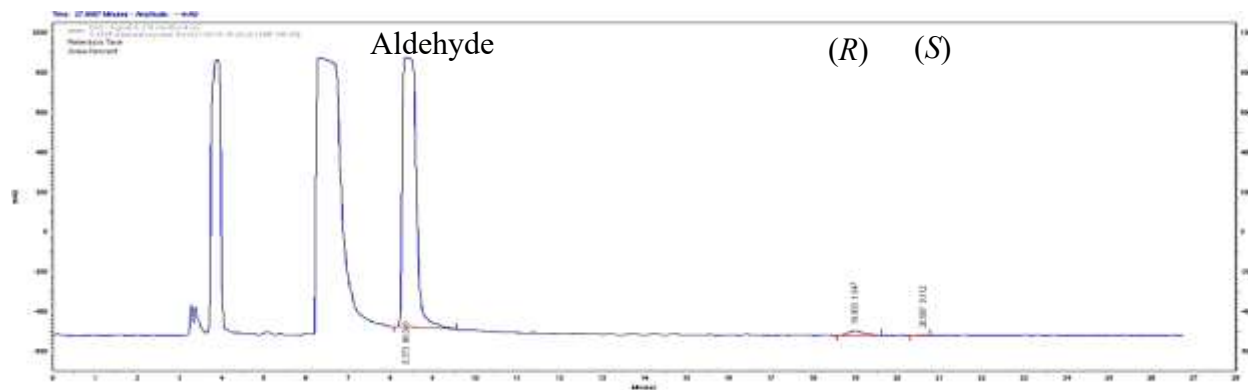


**Figure S134:** HPLC chromatogram of the Y14F variant showing enantioselective synthesis of (*R*)-**2I** at 3 h using **1I** as the substrate.

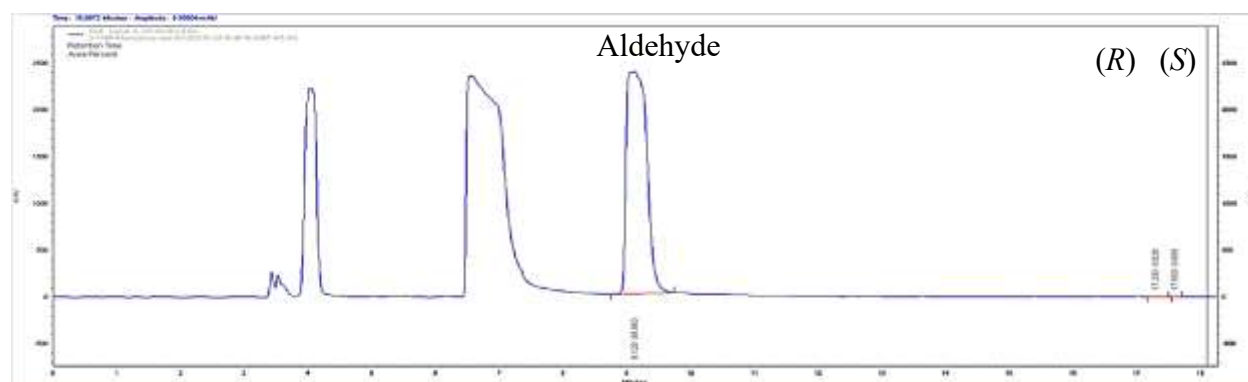


**Figure S135:** HPLC chromatogram of the Y14M variant showing enantioselective synthesis of (*R*)-**2I** at 3 h using **1I** as the substrate.

**Figure S136-S150:** AtHNL variants in enantioselective synthesis of  $\beta$ -nitroalcohols using higher amount of enzyme (125 U)

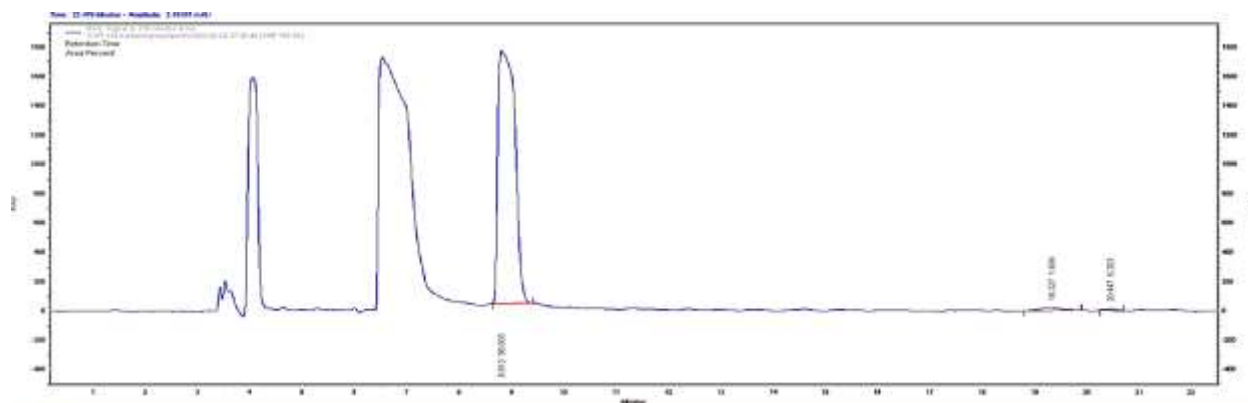


**Figure S136:** HPLC chromatogram of AtHNL WT (125 U) catalyzed synthesis of (*R*)-**2I** at 3 h.

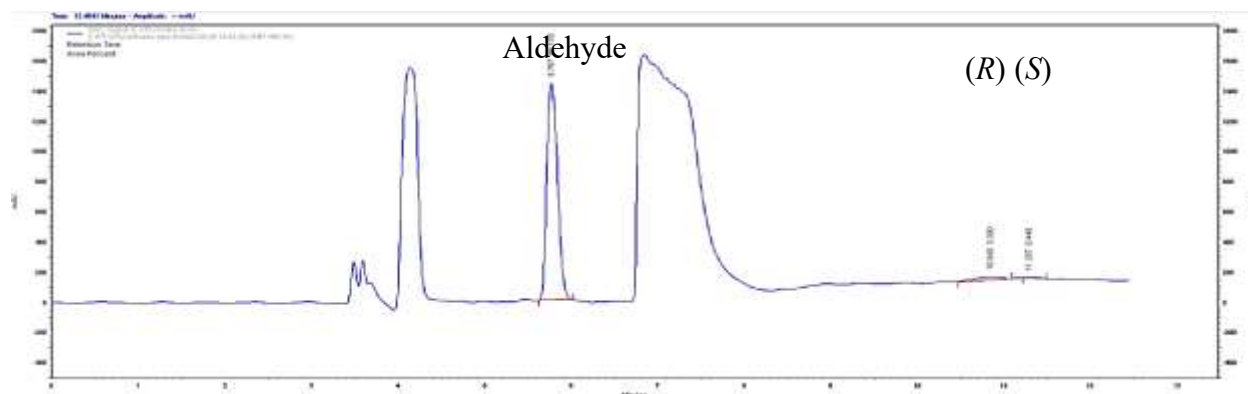


**Figure S137:** HPLC chromatogram of *AtHNL* WT (125 U) catalyzed synthesis of (*R*)-**2c** at 3 h.

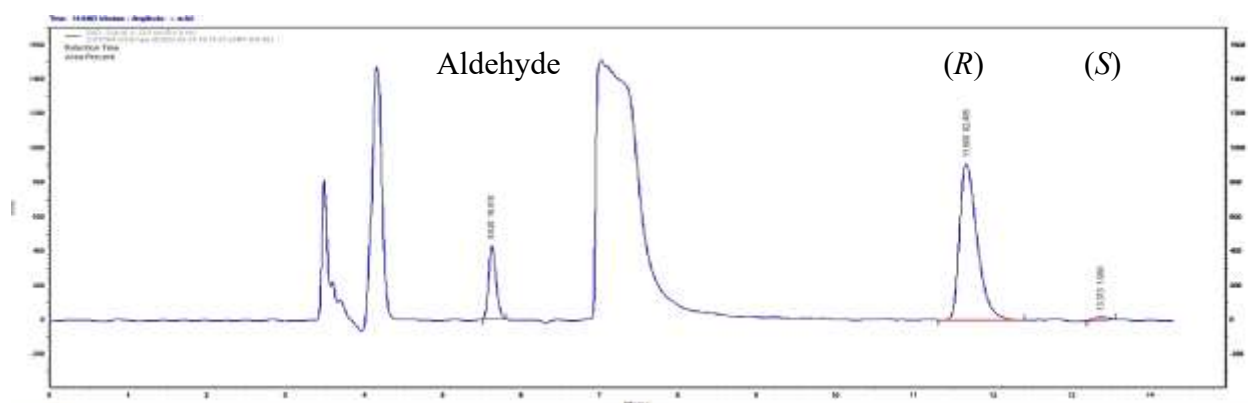


**Figure S138:** HPLC chromatogram of the F179N variant (125 U) catalyzed synthesis of (*R*)-**2a** at 3 h.

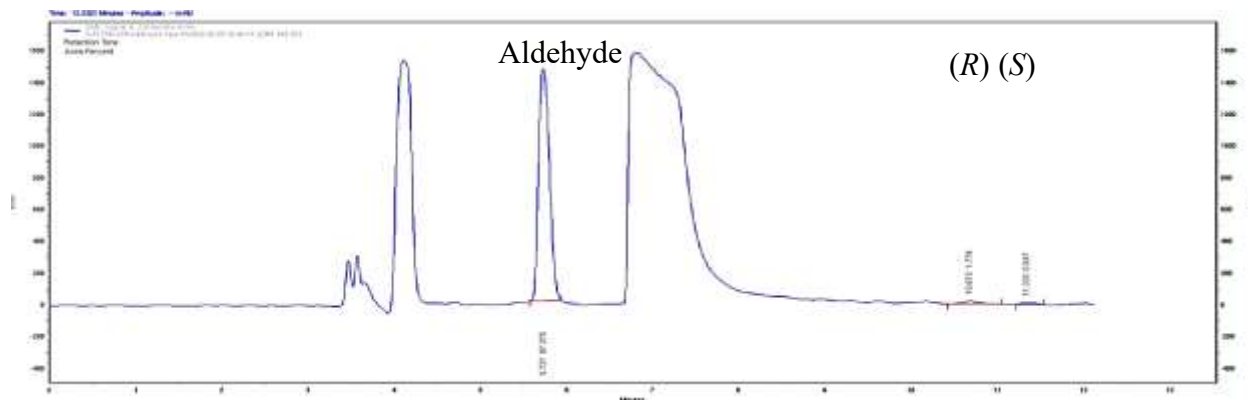


**Figure S139:** HPLC chromatogram of the F179N variant (125 U) catalyzed synthesis of (*R*)-**2c** at 3 h.

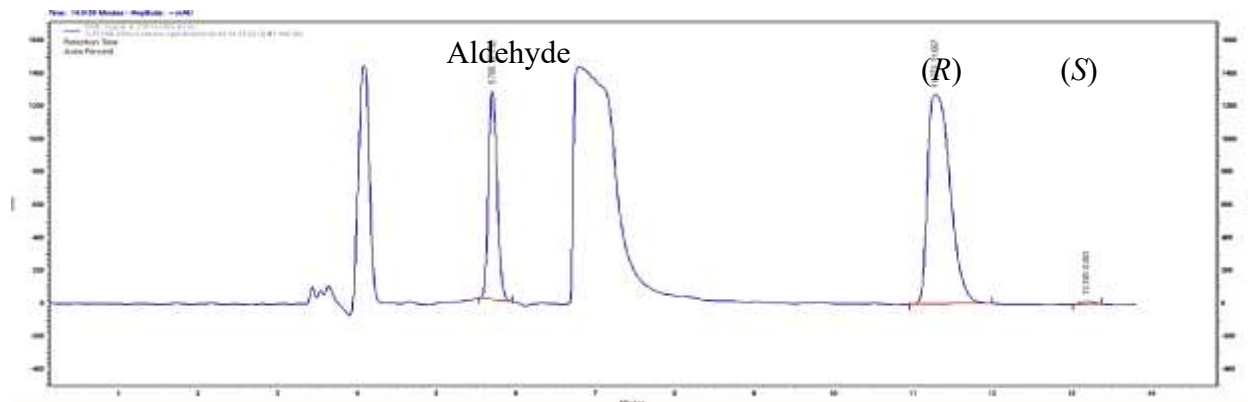


**Figure S140:** HPLC chromatogram of the F179N variant (125 U) catalyzed synthesis of (*R*)-**2g** at 3 h.

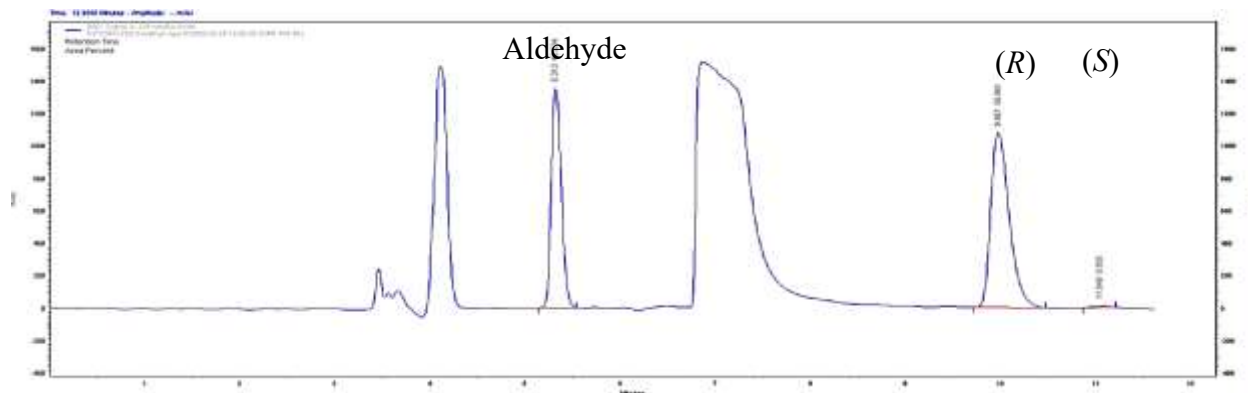


**Figure S141:** HPLC chromatogram of the F179N variant (125 U) catalyzed synthesis of (*R*)-**2h** at 3 h.

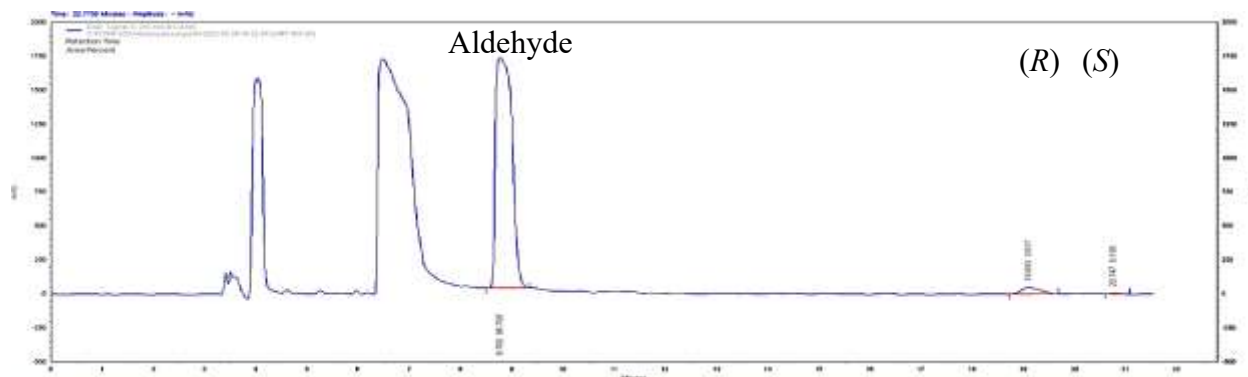


**Figure S142:** HPLC chromatogram of the F179N variant (125 U) catalyzed synthesis of (*R*)-**2i** at 3 h.

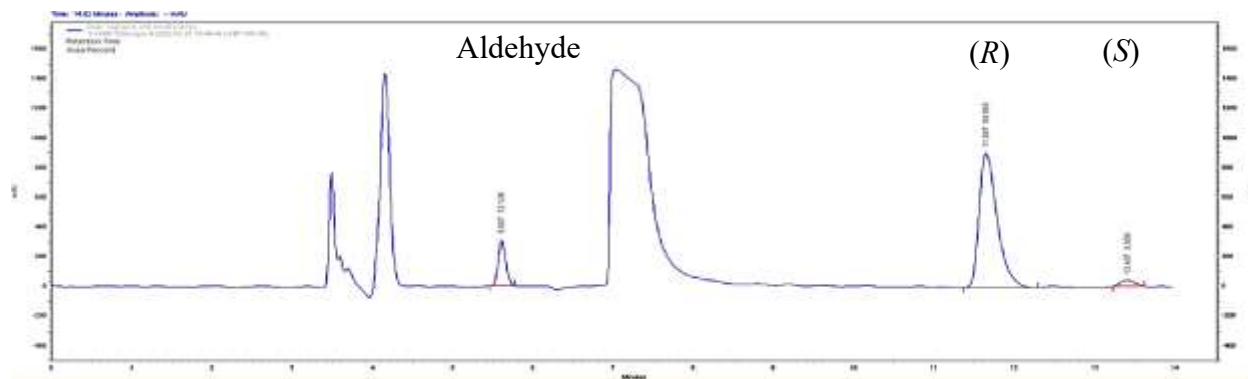


**Figure S143:** HPLC chromatogram of the Y14M variant (125 U) catalyzed synthesis of (*R*)-**2a** at 3 h.

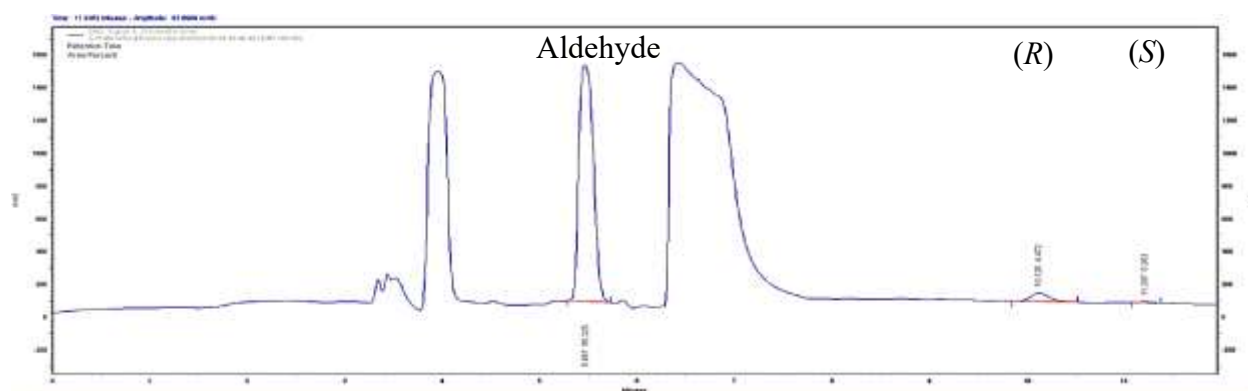


**Figure S144:** HPLC chromatogram of the Y14M variant (125 U) catalyzed synthesis of (*R*)-**2c** at 3 h.

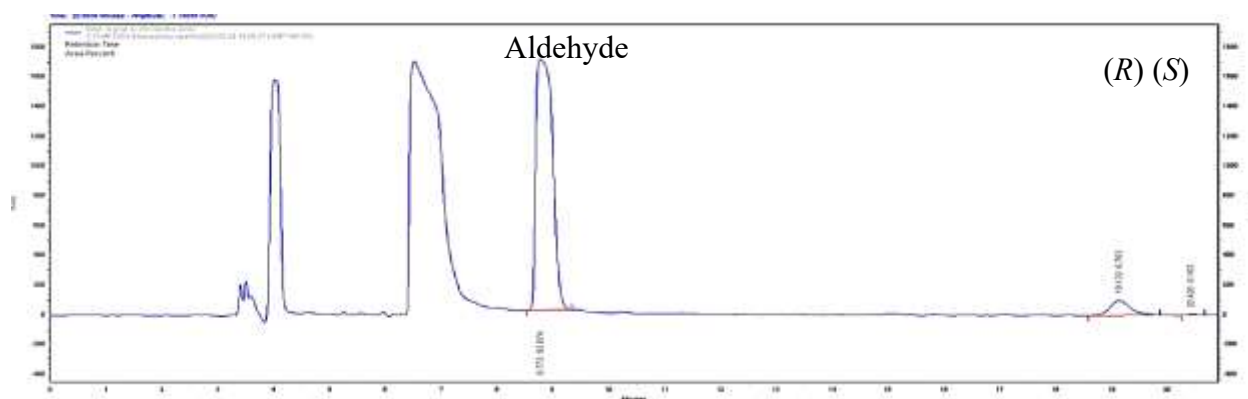


**Figure S145:** HPLC chromatogram of the Y14M variant (125 U) catalyzed synthesis of (*R*)-**2l** at 3 h.



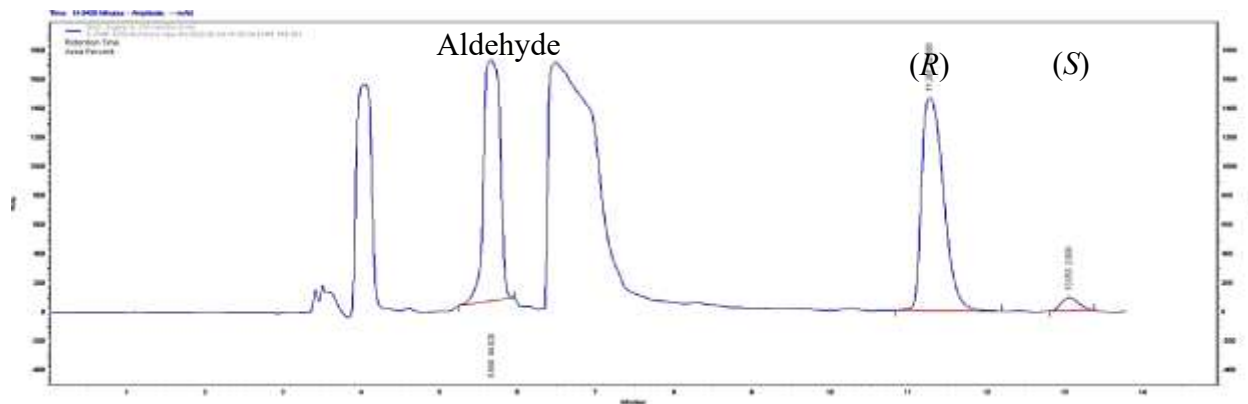


**Figure S146:** HPLC chromatogram of the Y14F variant (125 U) catalyzed synthesis of (*R*)-**2d** at 3 h.

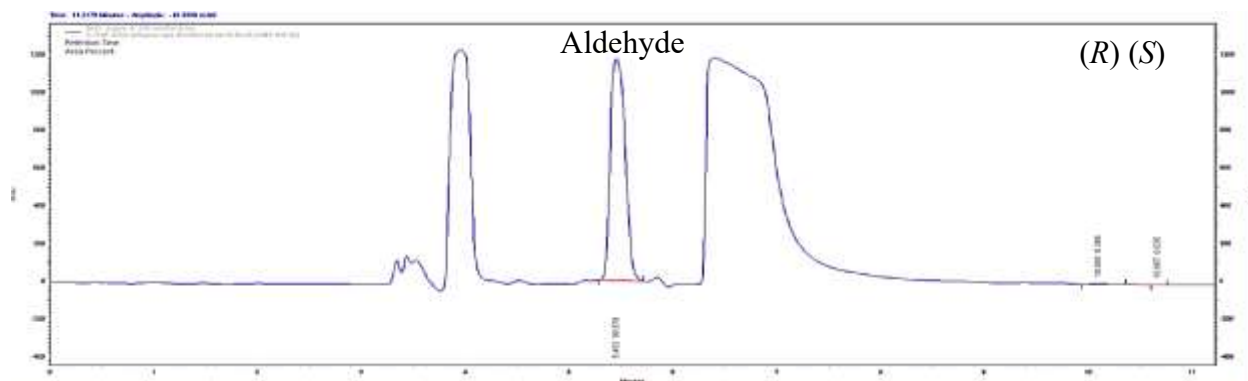


**Figure S147:** HPLC chromatogram of the Y14F variant (125 U) catalyzed synthesis of (*R*)-**2c** at 3 h.

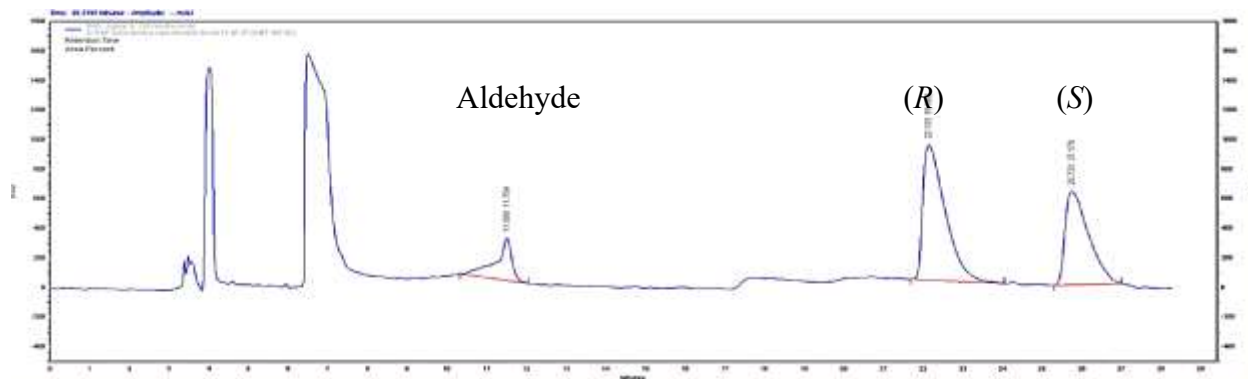


**Figure S148:** HPLC chromatogram of the Y14F variant (125 U) catalyzed synthesis of (*R*)-**2e** at 3 h.

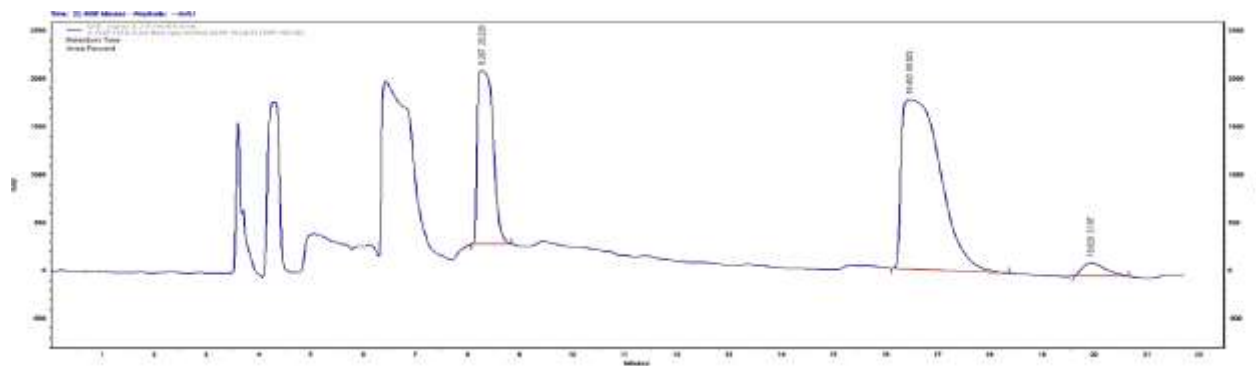


**Figure S149:** HPLC chromatogram of the Y14F variant (125 U) catalyzed synthesis of (*R*)-**2k** at 3 h.

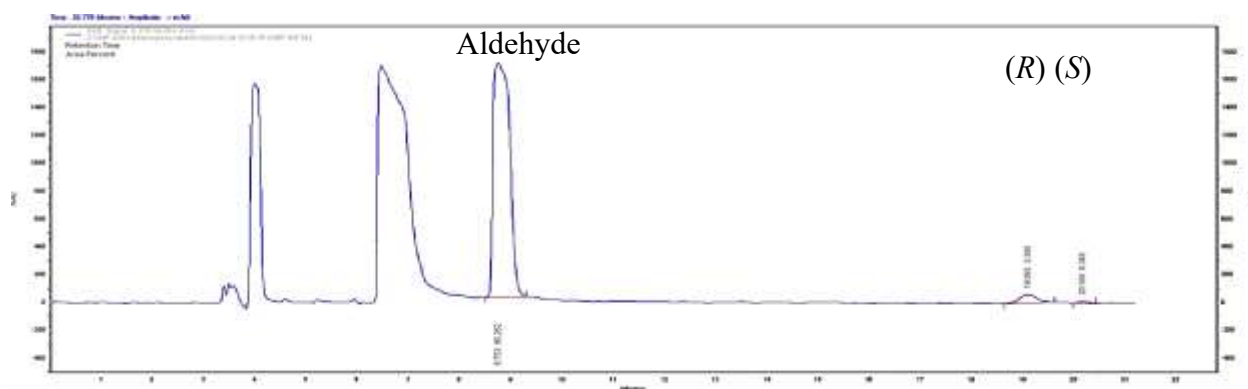


**Figure S150:** HPLC chromatogram of the Y14F variant (125 U) catalyzed synthesis of (*R*)-**2l** at 3 h.

**Figure S151-S168: AtHNL double variants in enantioselective synthesis of  $\beta$ -nitroalcohols**

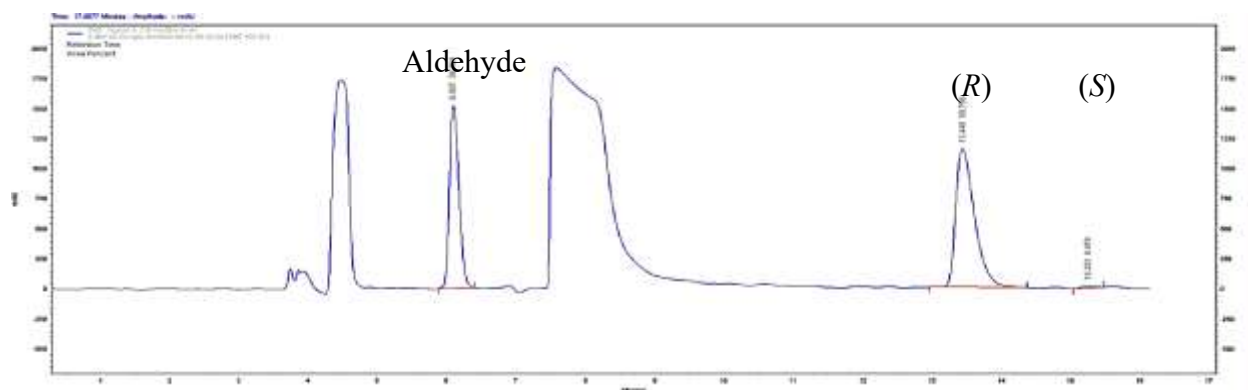


**Figure S151:** HPLC chromatogram of the Y14M-F179W catalyzed enantioselective synthesis of (*R*)-**2a** at 3 h.

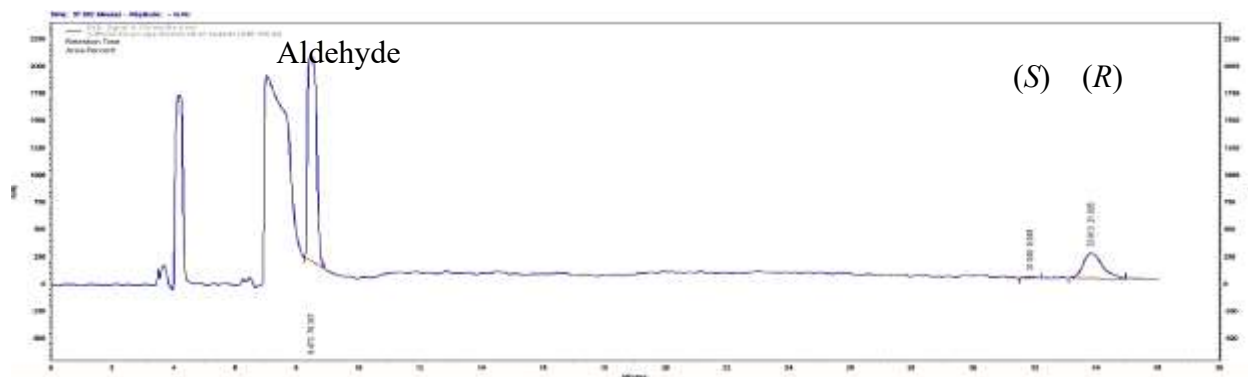


**Figure S152:** HPLC chromatogram of the Y14M-F179W catalyzed enantioselective synthesis of *(R)*-**2b** at 3 h.

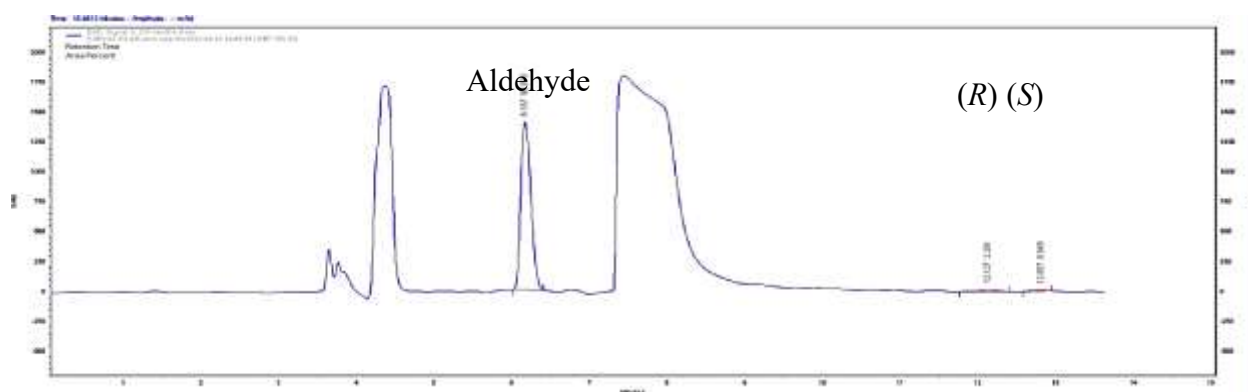


**Figure S153:** HPLC chromatogram of the Y14M-F179W catalyzed enantioselective synthesis of *(R)*-**2c** at 3 h.

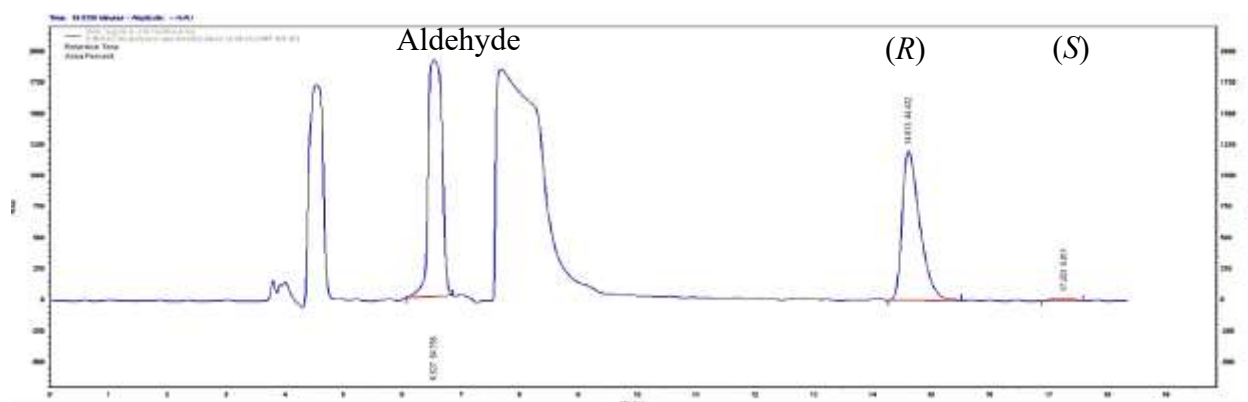


**Figure S154:** HPLC chromatogram of the Y14M-F179W catalyzed enantioselective synthesis of *(R)*-**2d** at 3 h.

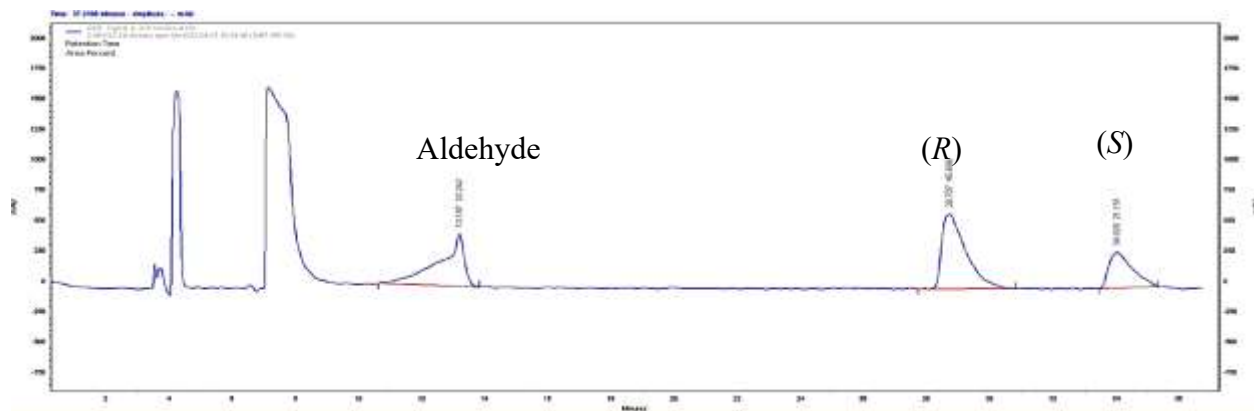


**Figure S155:** HPLC chromatogram of the Y14M-F179W catalyzed enantioselective synthesis of (*R*)-**2e** at 3 h.

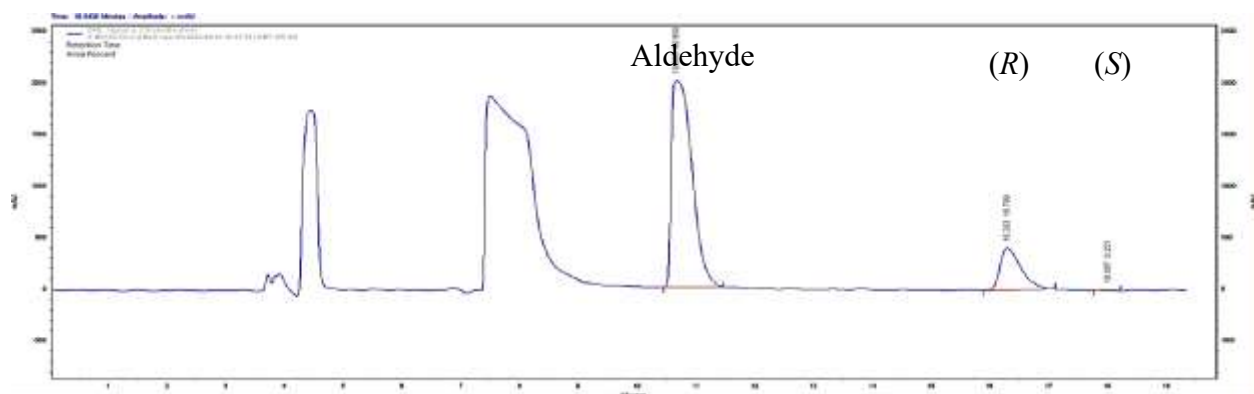


**Figure S156:** HPLC chromatogram of the Y14M-F179W catalyzed enantioselective synthesis of (*R*)-**2f** at 3 h.

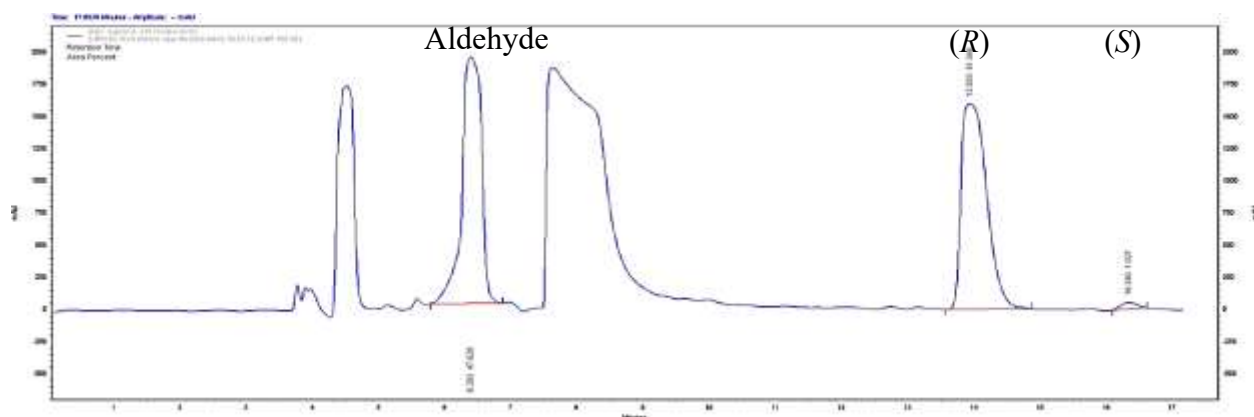


**Figure S157:** HPLC chromatogram of the Y14M-F179W catalyzed enantioselective synthesis of (*R*)-**2g** at 3 h.

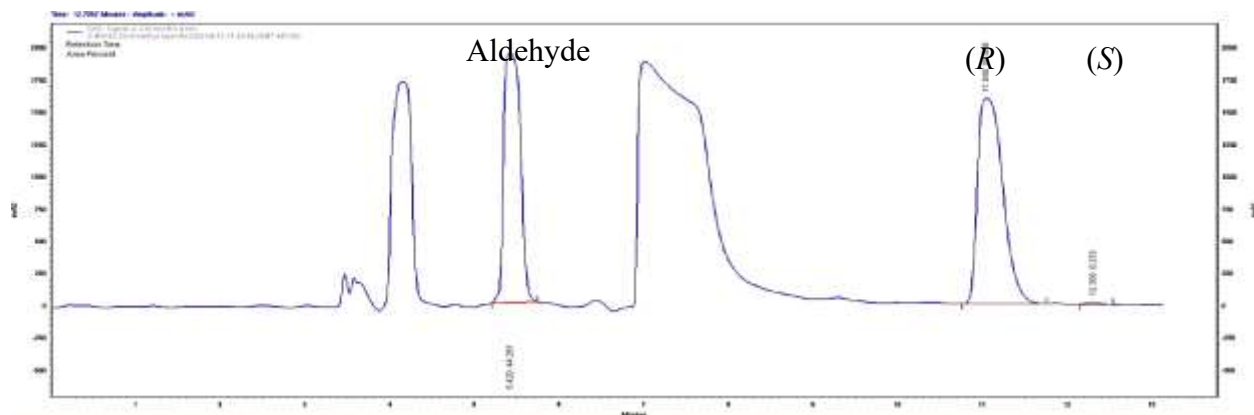


**Figure S158:** HPLC chromatogram of the Y14M-F179W catalyzed enantioselective synthesis of (*R*)-**2h** at 3 h.

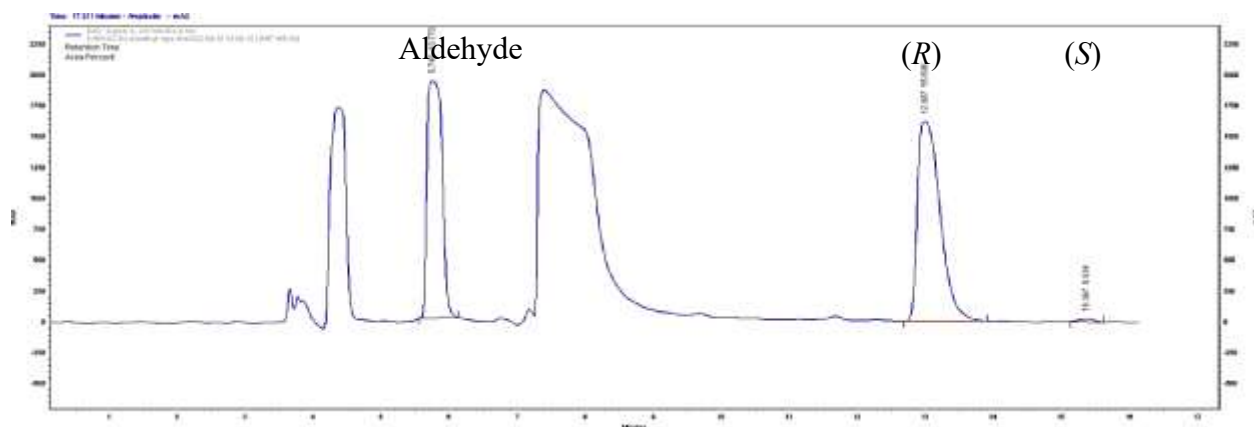


**Figure S159:** HPLC chromatogram of the Y14M-F179W catalyzed enantioselective synthesis of (*R*)-**2i** at 3 h.

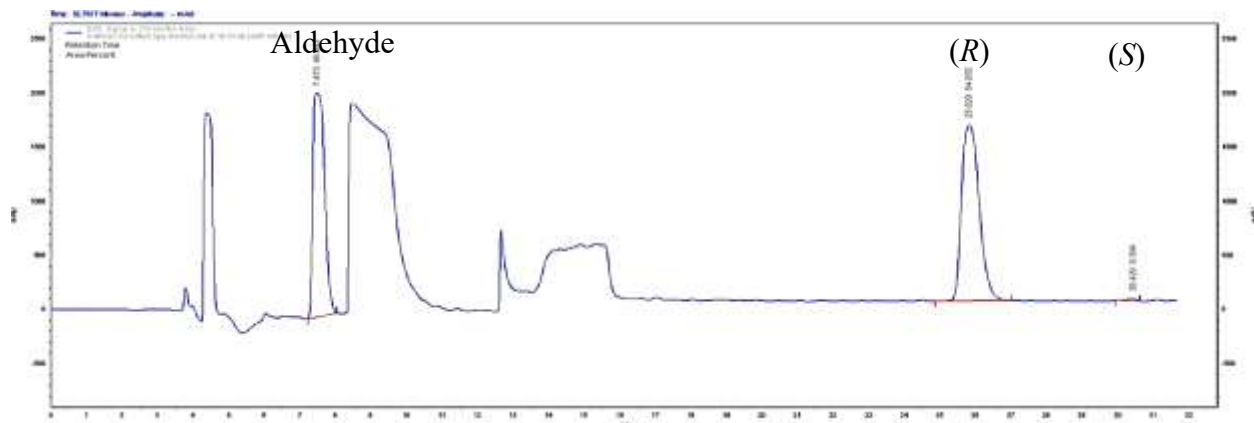


**Figure S160:** HPLC chromatogram of the Y14M-F179W catalyzed enantioselective synthesis of (*R*)-**2j** at 3 h.

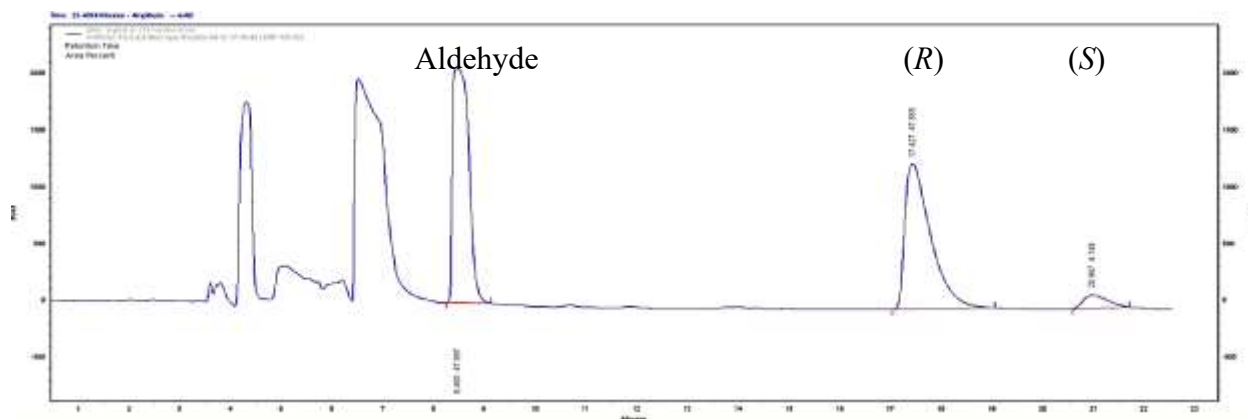


**Figure S161:** HPLC chromatogram of the Y14M-F179W catalyzed enantioselective synthesis of (*R*)-**2k** at 3 h.

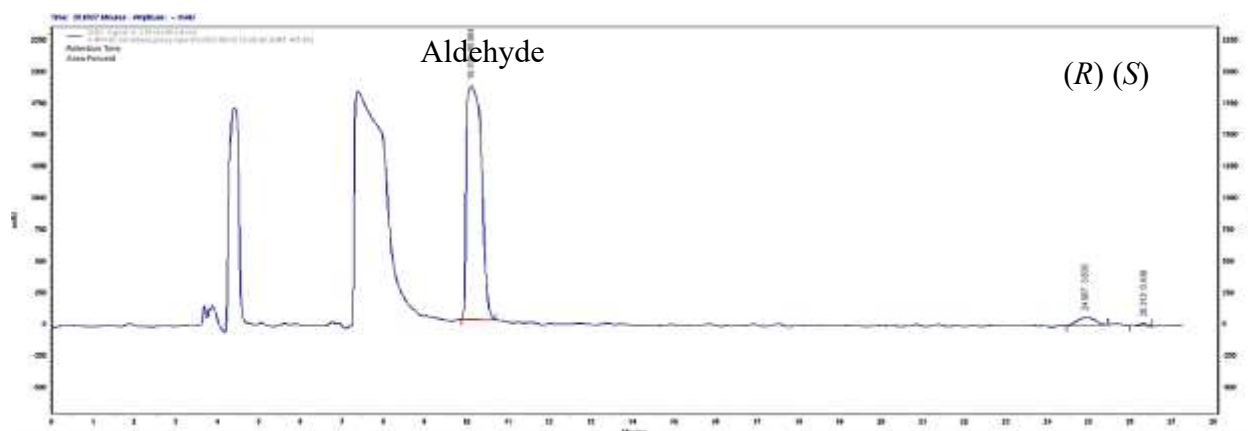


**Figure S162:** HPLC chromatogram of the Y14M-F179W catalyzed enantioselective synthesis of (*R*)-**2l** at 3 h.

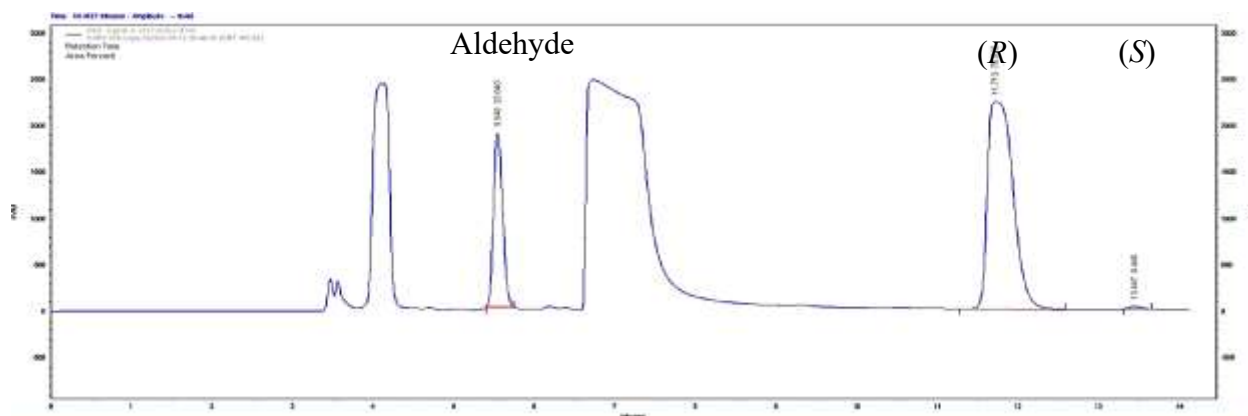


**Figure S163:** HPLC chromatogram of the Y14M-F179W (125 U) catalyzed enantioselective synthesis of (*R*)-**2a** at 3 h.

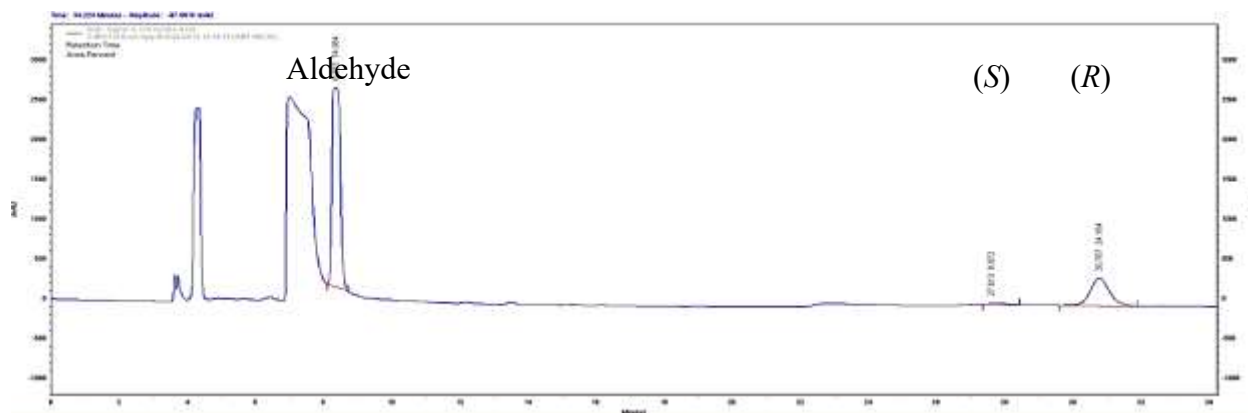


**Figure S164:** HPLC chromatogram of the Y14M-F179W (125 U) catalyzed enantioselective synthesis of (*R*)-**2b** at 3 h.

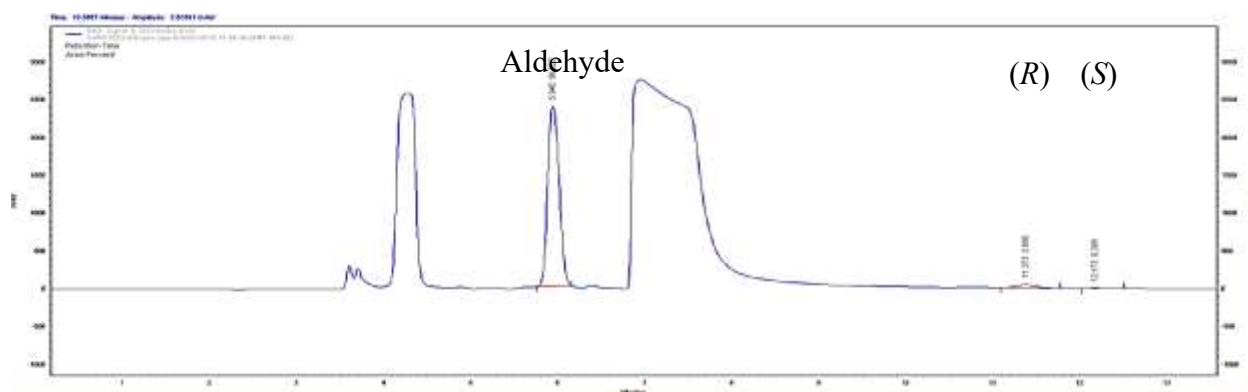


**Figure S165:** HPLC chromatogram of the Y14M-F179W (125 U) catalyzed enantioselective synthesis of (*R*)-**2c** at 3 h.

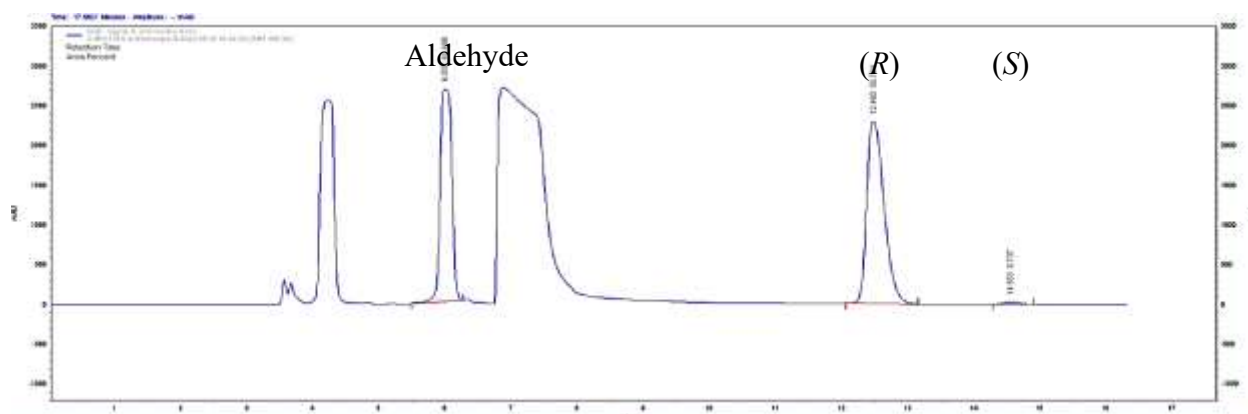


**Figure S166:** HPLC chromatogram of the Y14M-F179W (125 U) catalyzed enantioselective synthesis of (*R*)-**2d** at 3 h.

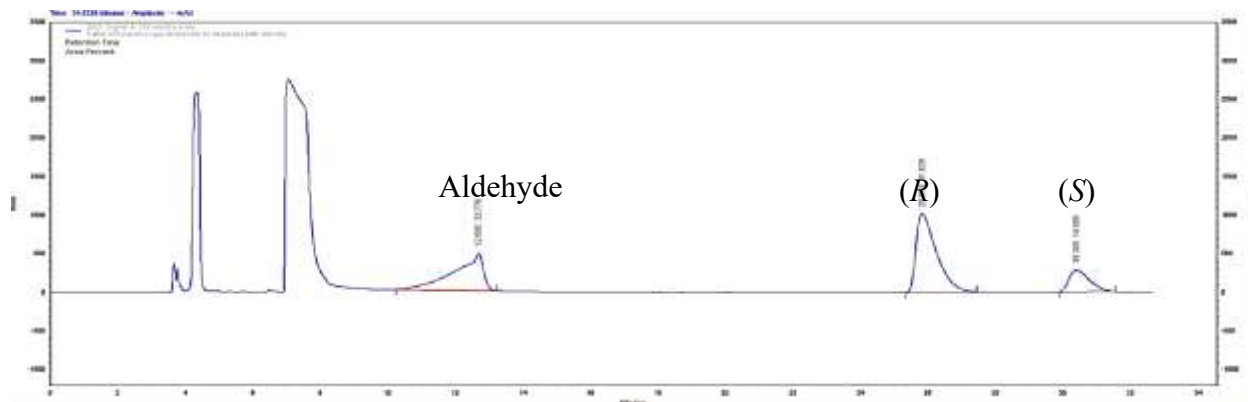


**Figure S167:** HPLC chromatogram of the Y14M-F179W (125 U) catalyzed enantioselective synthesis of (*R*)-**2e** at 3 h.

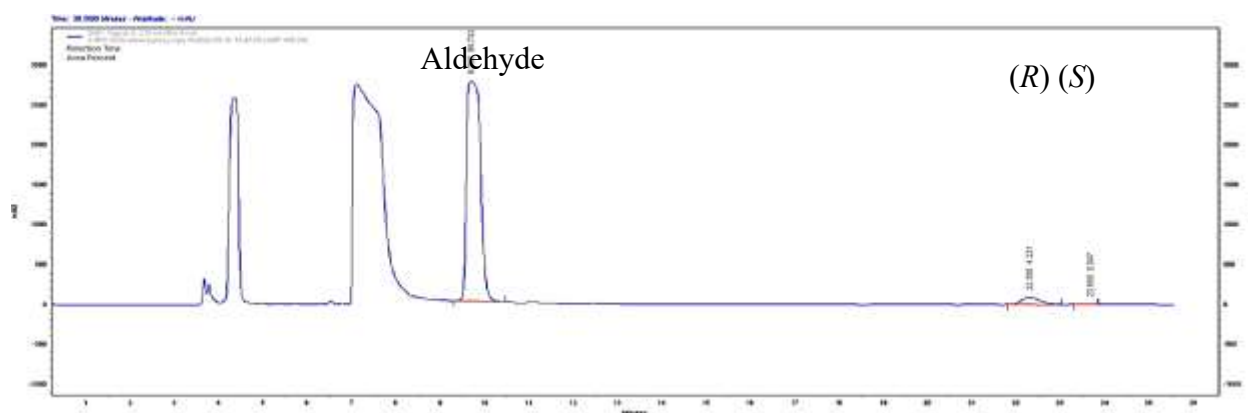


**Figure S168:** HPLC chromatogram of the Y14M-F179W (125 U) catalyzed enantioselective synthesis of (*R*)-**2k** at 3 h.

### Figure S169-177: *At*HNL variants in enantioselective synthesis of (*R*)-**2m**

#### *At*HNL variants in enantioselective synthesis of (*R*)-1-(4-methoxyphenyl)-2-nitroethanol

The purified variants Y14F, Y14M, F179W, F179N and Y14M-F179W (125 U) along with the wild type *At*HNL were employed in the synthesis of (*R*)-1-(4-methoxyphenyl)-2-nitroethanol where 20 mM of 4-methoxybenzaldehyde and 1.75 M of nitromethane were used as the substrates. In our study to synthesize (*R*)-1-(4-methoxyphenyl)-2-nitroethanol using promiscuous Henry reaction, wild type *At*HNL showed 47% conversion and 98% *ee*, while other single variants (F179N, F179W, Y14M and Y14F) showed 51-56% conversions with 96-99% *ee* in 3 h. The double variant, Y14M-F179W showed the highest, 70% conversion among others with >99% *ee* in the synthesis of (*R*)-1-(4-methoxyphenyl)-2-nitroethanol (Figure S169-177). Finally, the double variant Y14M-F179W was chosen for preparative scale synthesis.



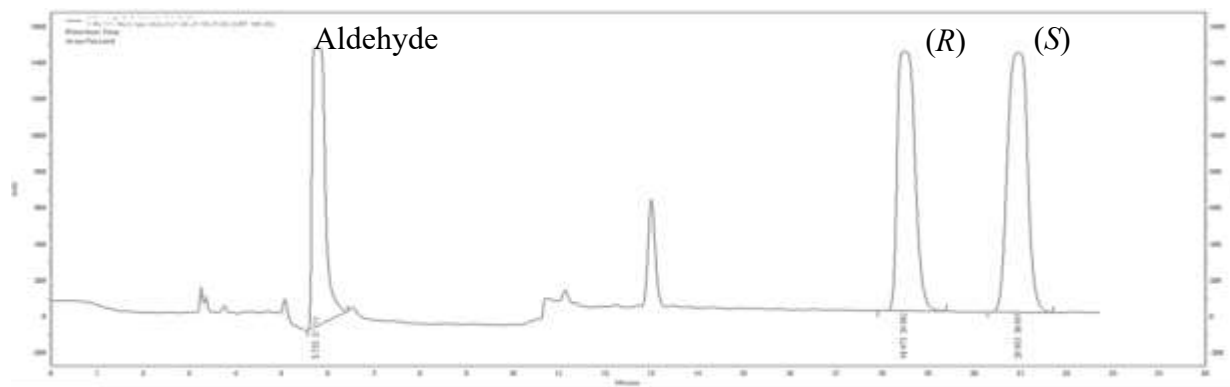


**Figure S169:** HPLC chromatogram of the standards: **1m** and racemic **2m**.

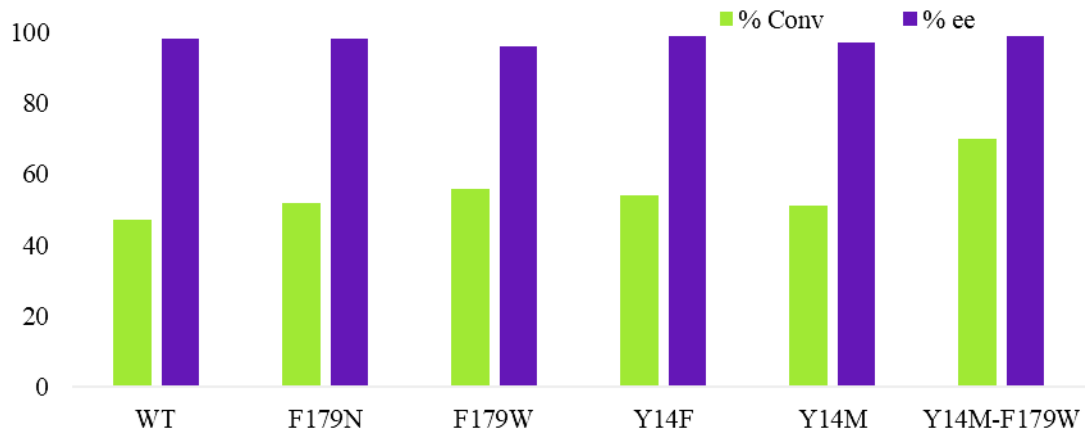


**Figure S170:** *AtHNL* variants catalysed enantioselective synthesis of (*R*)-**2m**. A 1 mL reaction carrying 500  $\mu$ L of *n*-butyl acetate, 125 units of purified enzyme, 1.75 M of nitromethane, 20 mM of **1m** and the rest volume of 20 mM KPB was shaken at 1,200 rpm for 3 h at 30°C. In the control, the enzyme was replaced by an equal volume of 20 mM KPB. The 3 h analysis data is considered for analysis.

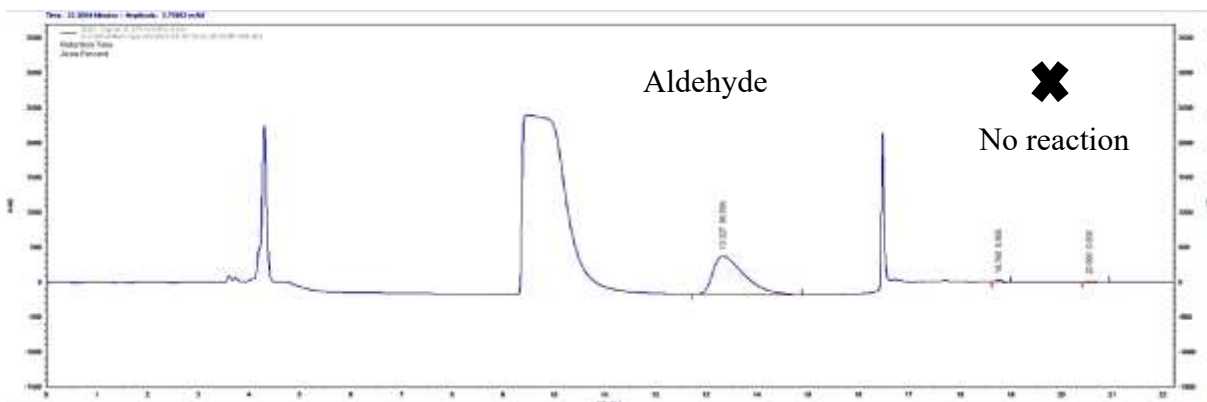


**Figure S171:** HPLC chromatogram of control reaction at 3 h where enzyme is replaced by 20 mM KPB and **1m** was used as the substrate.

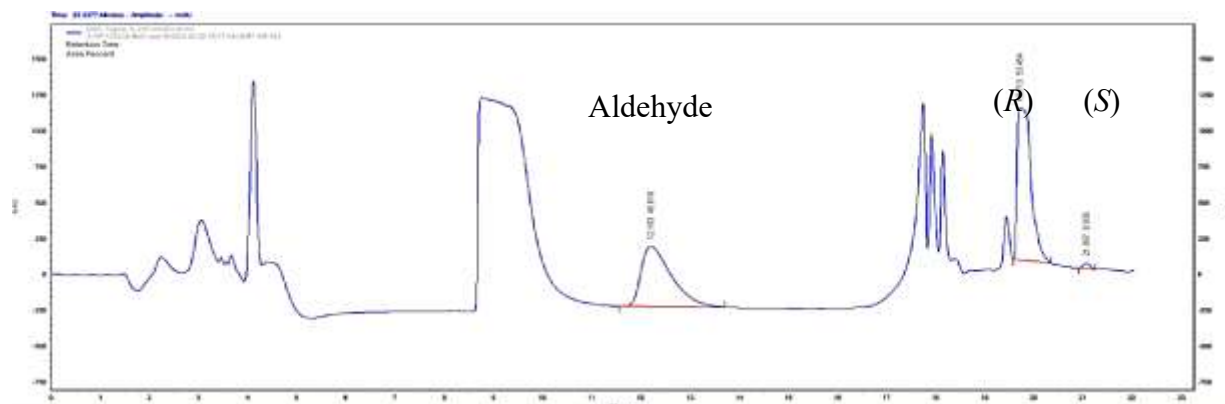


**Figure S172:** HPLC chromatogram of wild type *AtrHNL* (125 U) catalyzed nitroaldol reaction showing enantioselective synthesis of (*R*)-**2m** at 3 h.

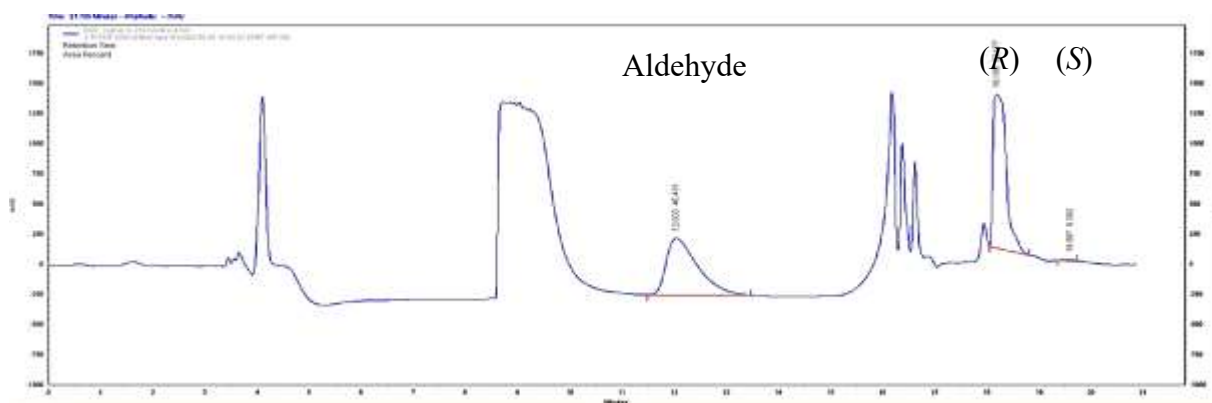


**Figure S173:** HPLC chromatogram of F179N (125 U) catalyzed nitroaldol reaction showing enantioselective synthesis of (*R*)-**2m** at 3 h.

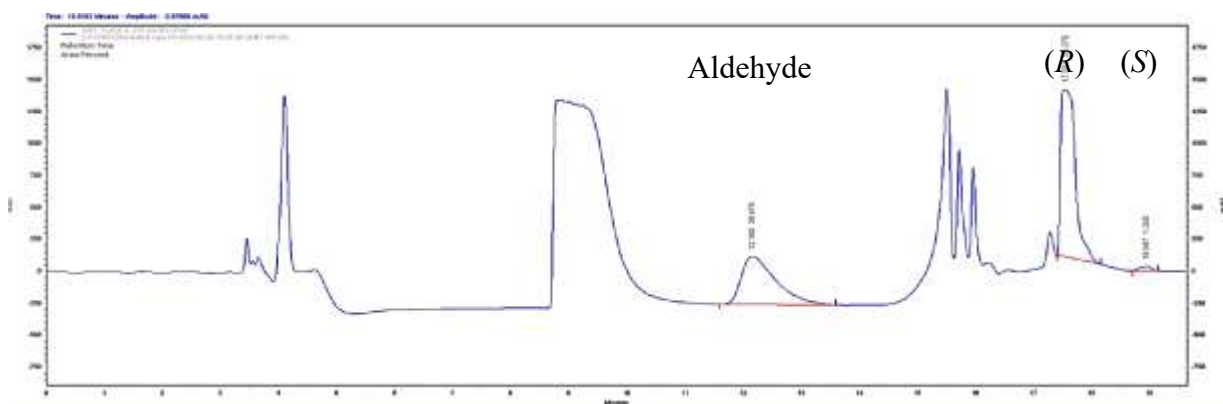


**Figure S174:** HPLC chromatogram of F179W (125 U) catalyzed nitroaldol reaction showing enantioselective synthesis of (*R*)-**2m** at 3 h.

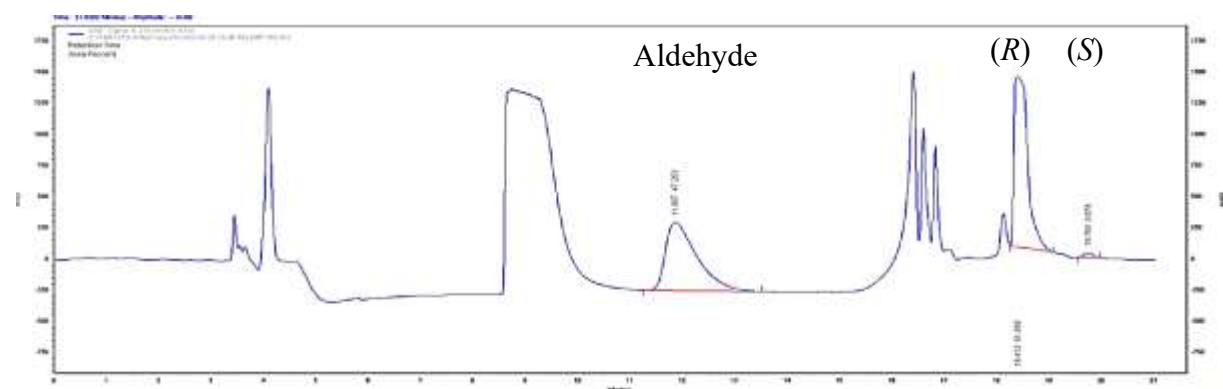


**Figure S175:** HPLC chromatogram of Y14M (125 U) catalyzed nitroaldol reaction showing enantioselective synthesis of (*R*)-**2m** at 3 h.

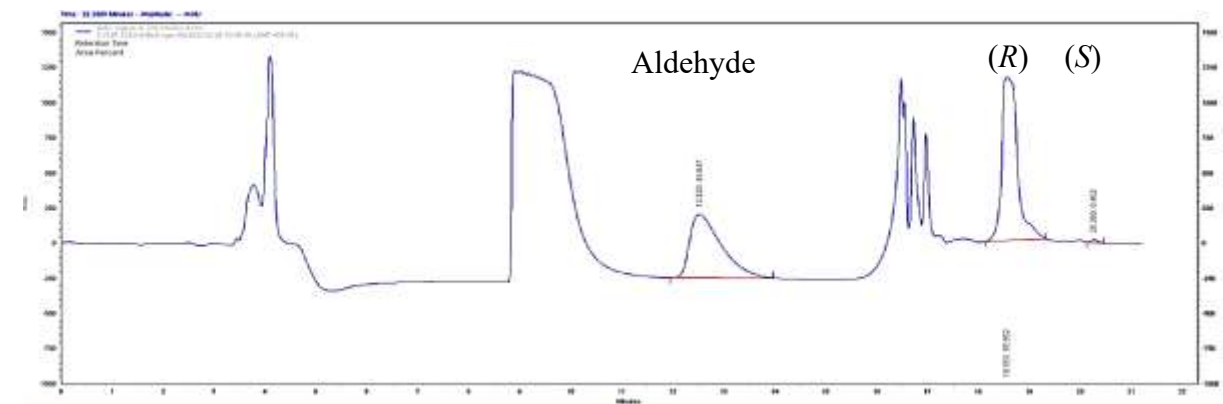


**Figure S176:** HPLC chromatogram of Y14F (125 U) catalyzed nitroaldol reaction showing enantioselective synthesis of (*R*)-**2m** at 3 h.

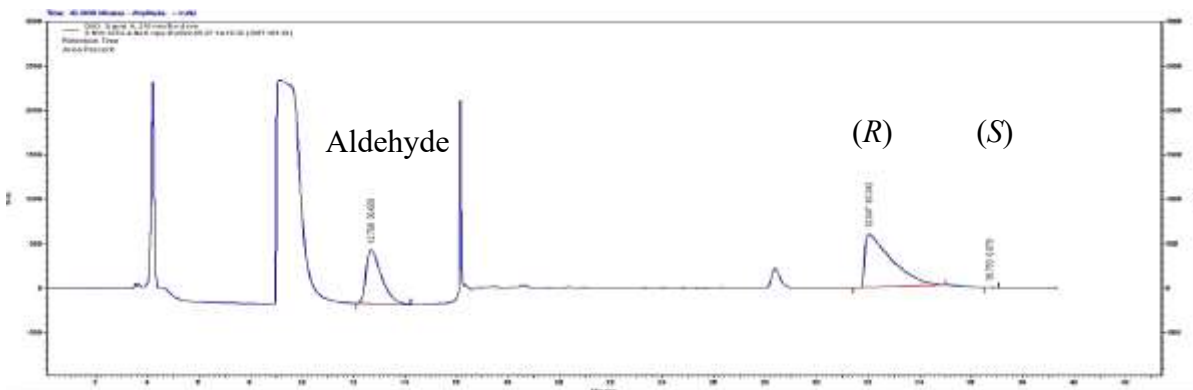


**Figure S177:** HPLC chromatogram of Y14M-F179W (125 U) catalyzed nitroaldol reaction showing enantioselective synthesis of (*R*)-**2m** at 3 h.

**Figure S178-182: Preparative scale synthesis of (*R*)-**2m** using Y14M-F179W crude cell lysate**

*Preparative scale synthesis of (*R*)-1-(4-methoxyphenyl)-2-nitroethanol using Y14M-F179W crude cell lysate*

The usage of crude cell lysates in biocatalysis is often preferred, especially for preparative as well as industrial scale synthesis. This is because use of crude cell lysates in biocatalysis is economical than the purified enzymes. Initially, *At*HNL-Y14M-F179W crude cell lysate (200 U) was employed to catalyze preparative scale synthesis of (*R*)-1-(4-methoxyphenyl)-2-nitroethanol, that resulted in 70% conversion and 99% *ee* (Figure S178). Further, the biotransformation was carried out with 1000 U of crude cell lysate (Figure S179), before using higher scale of enzyme. Subsequently, ten mini preparative scale reactions each containing 1000 U of Y14M-F179W cell lysate were carried out and the final product after column purification was found to have 99% *ee*, and 65.4% isolated yield (Figure S180) which was confirmed by <sup>1</sup>H and <sup>13</sup>C NMR (Figure S181-S182).

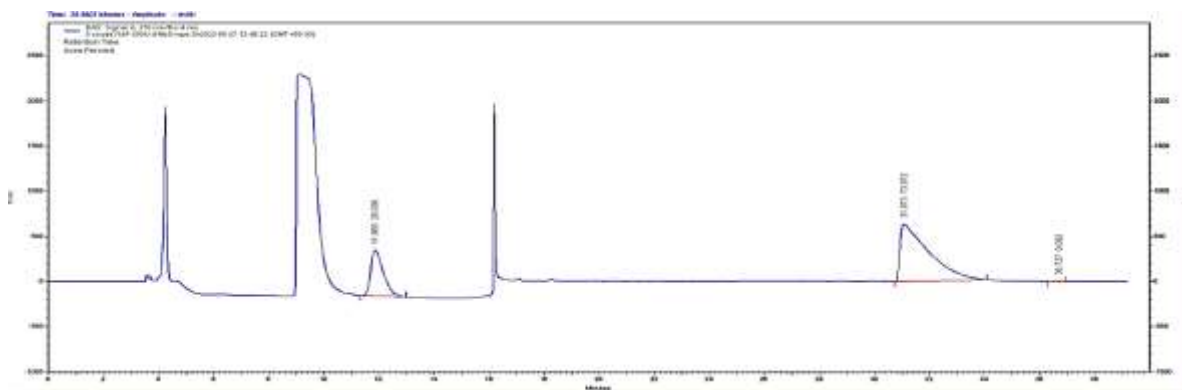


**Figure S178:** HPLC chromatogram of Y14M-F179W cell lysate (200 U) catalyzed nitroaldol reaction showing enantioselective synthesis of (*R*)-**2m** at 2 h.

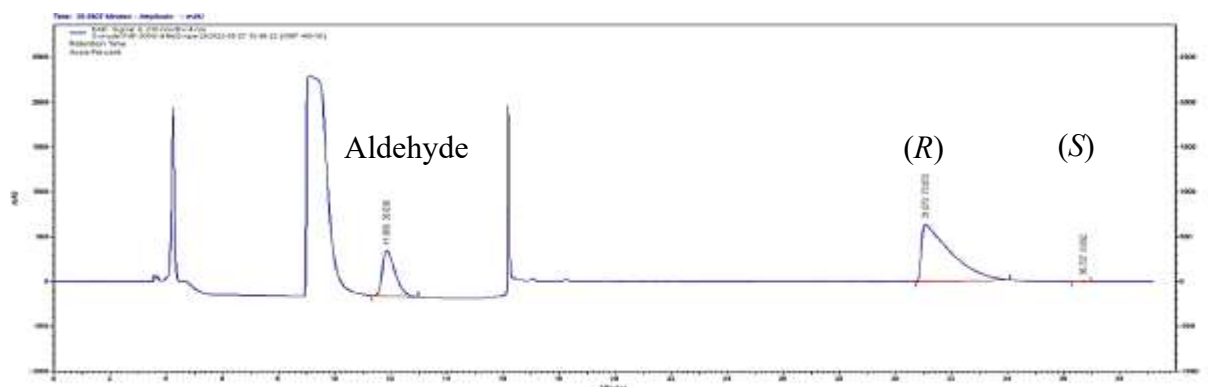


**Figure S179:** HPLC chromatogram of Y14M-F179W cell lysate (1000 U) catalyzed nitroaldol reaction showing enantioselective synthesis of (*R*)-**2m** at 2 h.

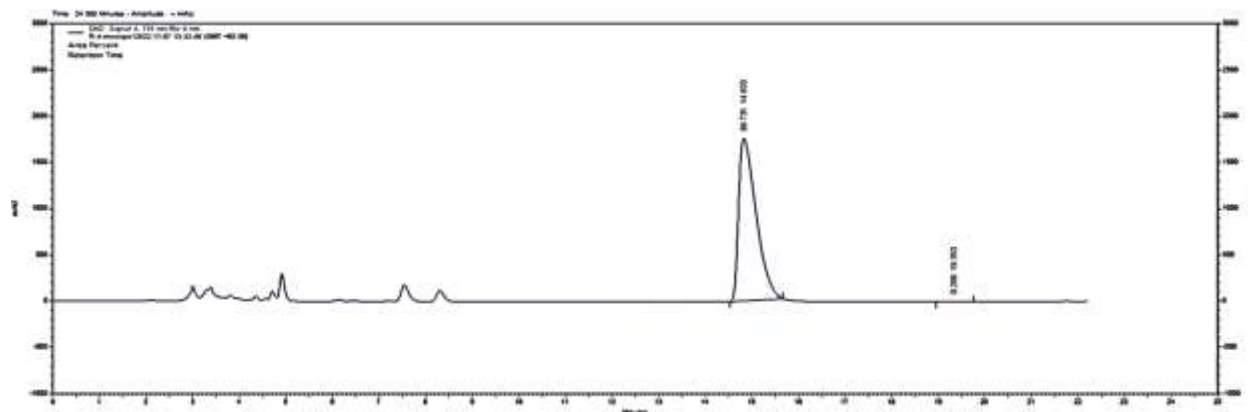


**Figure S180:** HPLC chromatogram of Y14M-F179W cell lysate catalyzed preparative scale enantioselective synthesis of (*R*)-**2m** at 2 h after column purification, >99 % *ee*.

**NMR characterization of Y14M-F179W catalyzed synthesis of (*R*)-1-(4-methoxyphenyl)-2-nitroethanol**

$^1\text{H}$  NMR (500 MHz,  $\text{CDCl}_3$ )  $\delta$  7.29 (d,  $J = 8.6$  Hz, 2H), 6.90 (d,  $J = 8.7$  Hz, 2H), 5.37 (dd,  $J = 9.7$ , 3.2 Hz, 1H), 4.57 (dd,  $J = 13.1$ , 9.7 Hz, 1H), 4.45 (dd,  $J = 13.1$ , 3.2 Hz, 1H), 3.80 (s, 3H).  $^{13}\text{C}$  NMR (126 MHz,  $\text{CDCl}_3$ )  $\delta$  160.06, 130.40, 127.39, 114.46, 81.35, 70.74, 55.44

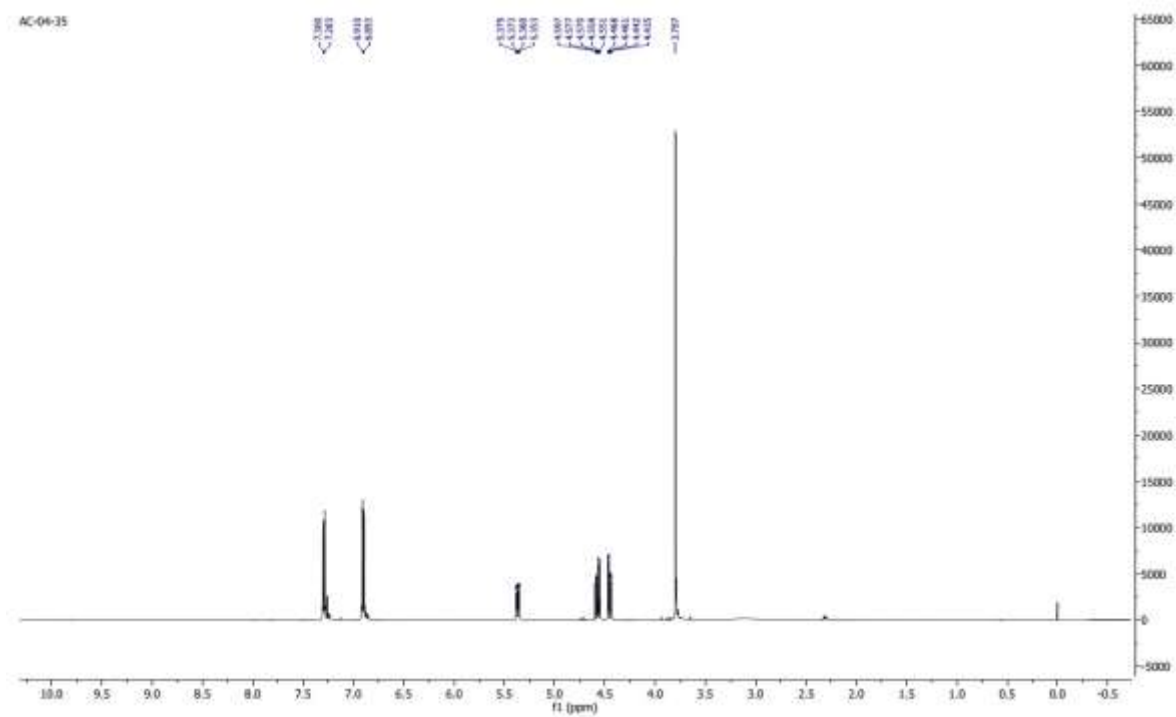


**Figure S181:**  $^1\text{H}$  NMR chromatogram of (*R*)-1-(4-methoxyphenyl)-2-nitroethanol (**2m**).

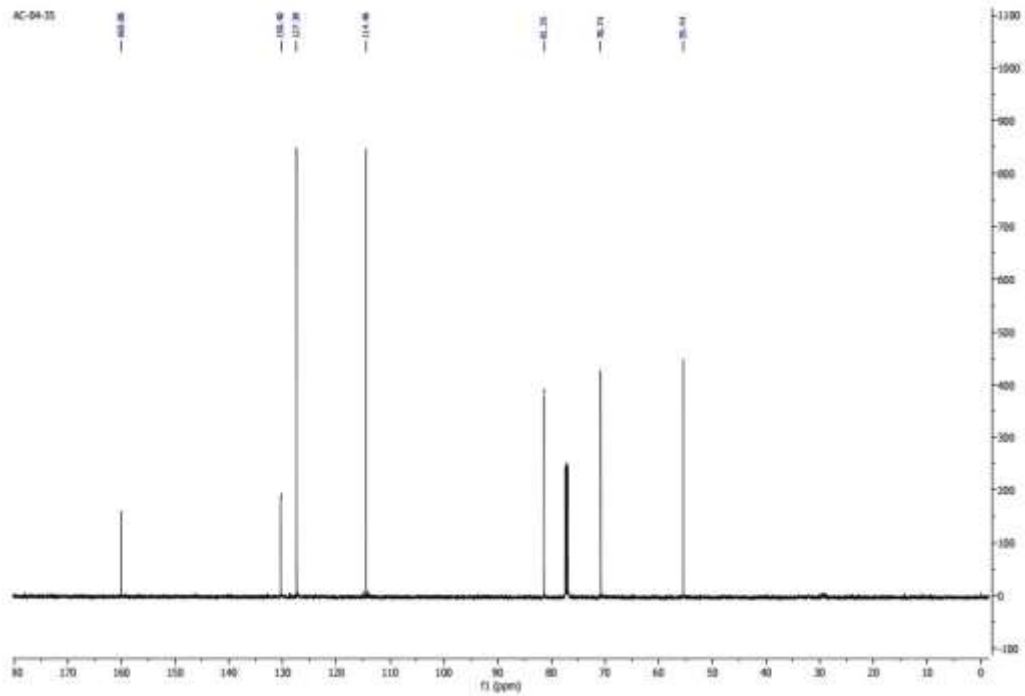


**Figure S182:**  $^{13}\text{C}$  NMR chromatogram of (*R*)-1-(4-methoxyphenyl)-2-nitroethanol (**2m**).

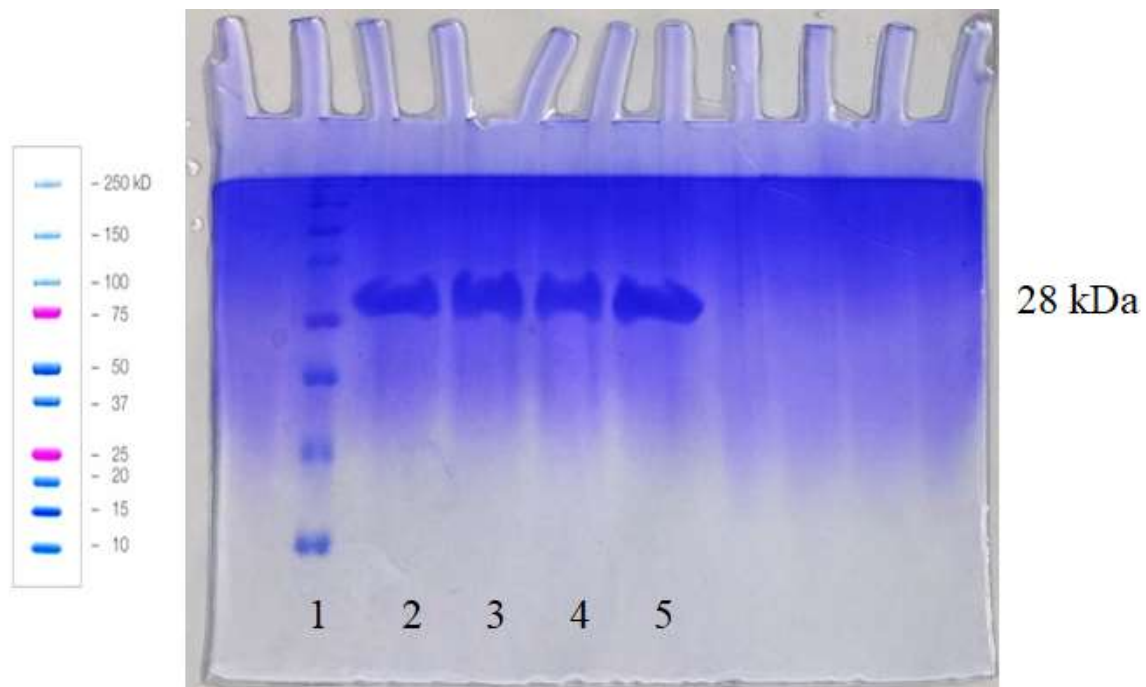


**Figure S183:** SDS-PAGE of *AtHNL* double variants. Lanes 1: Protein marker, 2: Y14F-F179N, 3: Y14F-F179W, 4: Y14M- F179N, 5: Y14M- F179W.

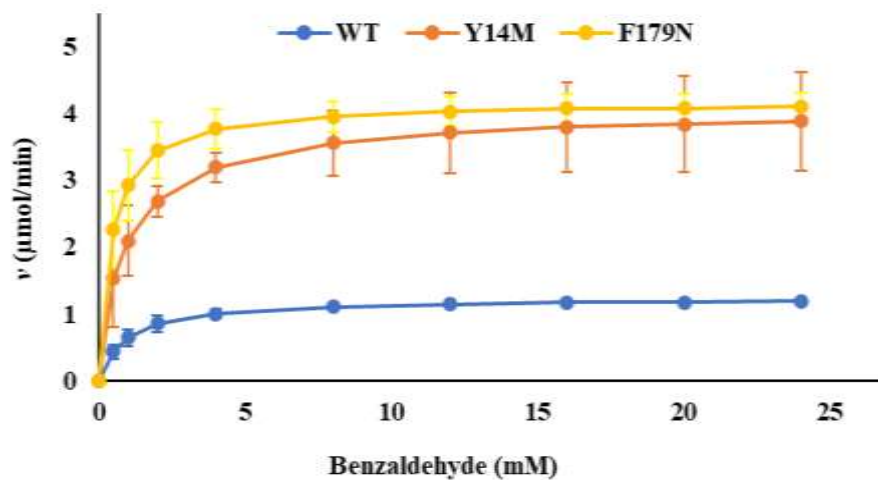


**Figure S184:** Michaelis-Menten curves of wild type *AtHNL*, Y14M and F179N in NPE (**2a**) synthesis by nitroaldol reaction.

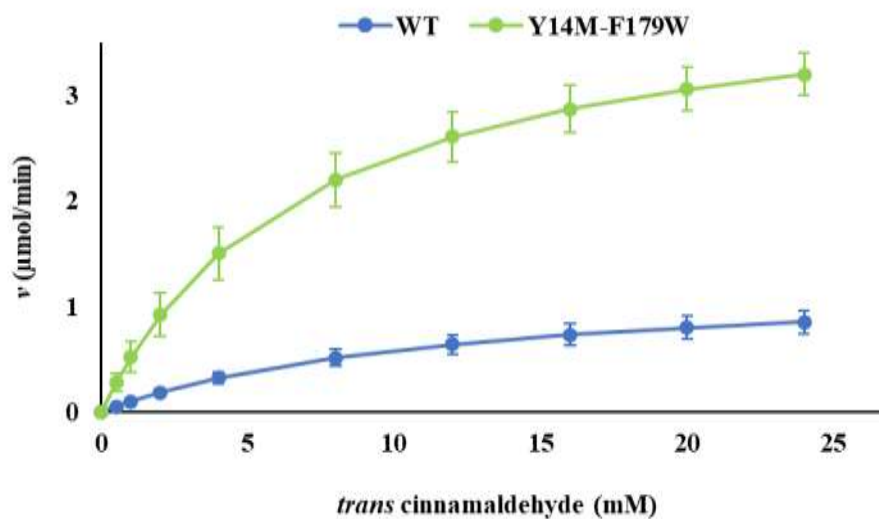


**Figure S185:** Michaelis-Menten curves for the wild type *AtHNL* and Y14M-F179W the synthesis of **2b** by nitroaldol reaction.



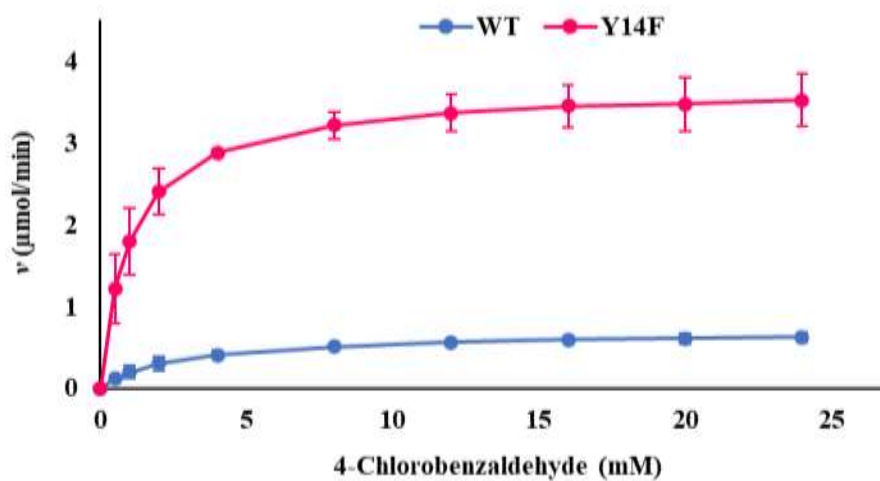


**Figure S186:** Michaelis-Menten curves for the wild type *AtHNL* and Y14F the synthesis of **2d** by nitroaldol reaction.

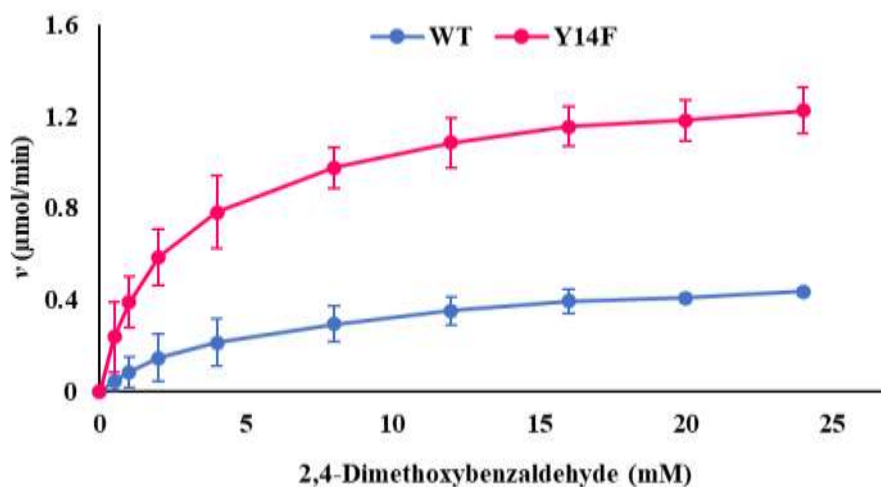


**Figure S187:** Michaelis-Menten curves for the wild type *AtHNL* and Y14F in the synthesis of **2f** by nitroaldol reaction.

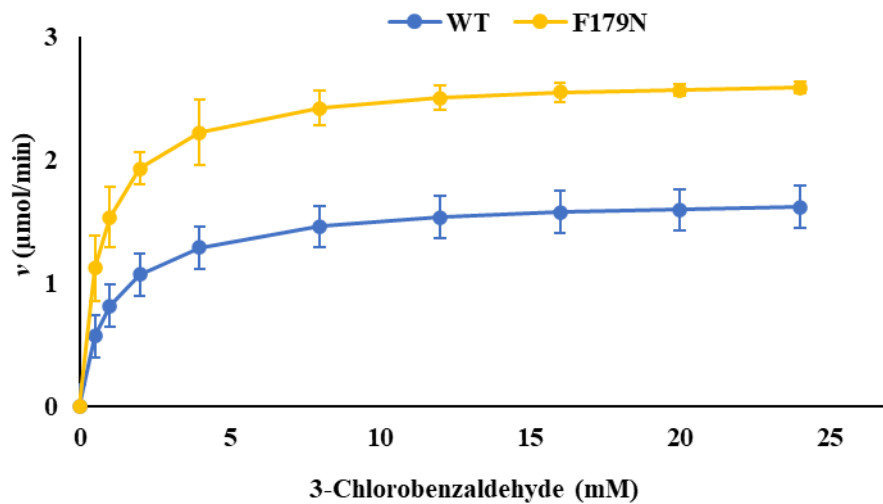


**Figure S188:** Michaelis-Menten curves for the wild type *AtHNL* and F179N in the synthesis of **2g** by nitroaldol reaction.

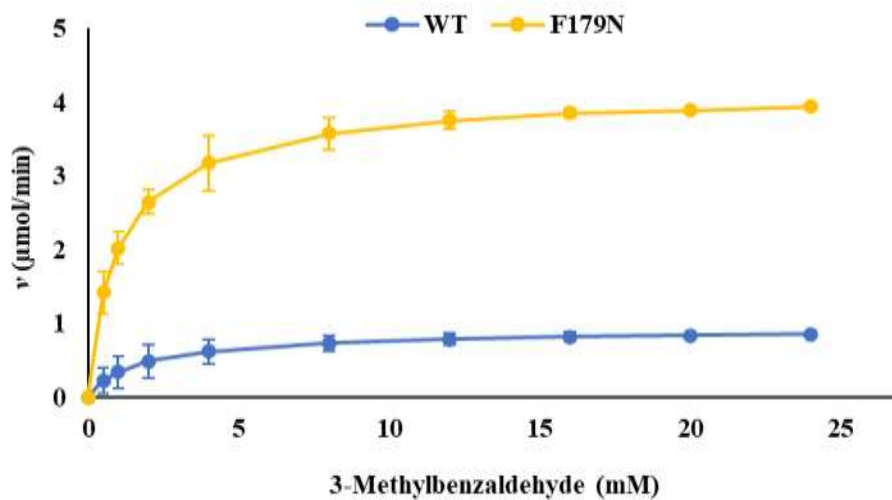


**Figure S189:** Michaelis-Menten curves for the wild type *AtHNL* and F179N in the synthesis of **2h** by nitroaldol reaction.

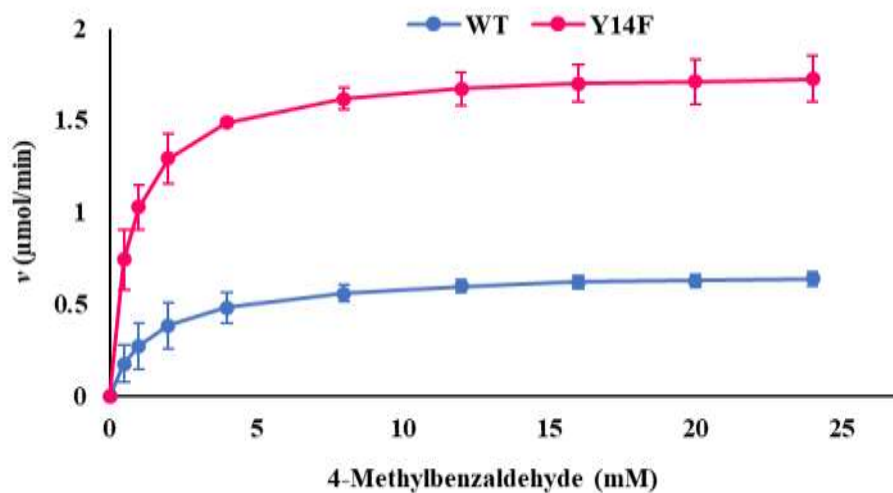


**Figure S190:** Michaelis-Menten curves for the wild type *A7HNL* and Y14F in the synthesis of **2i** by nitroaldol reaction.

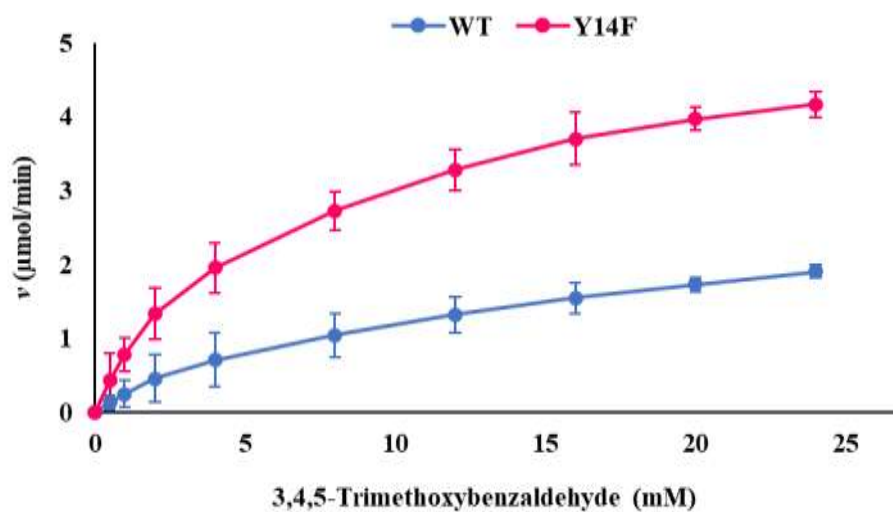


**Figure S191:** Michaelis-Menten curves for the wild type *A7HNL* and Y14F in the synthesis of **2k** by nitroaldol reaction.

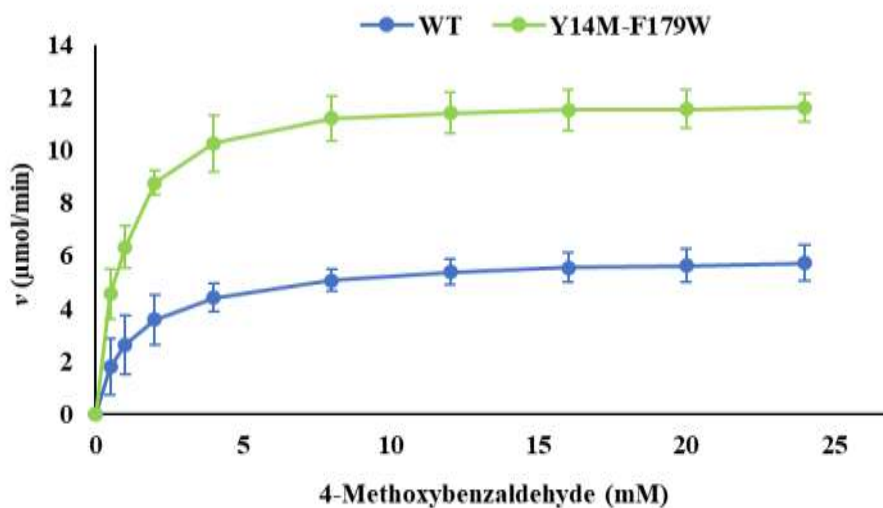


**Figure S192:** Michaelis-Menten curves for the wild type *A/HNL* and Y14M-F179W in the synthesis of **2m** by nitroaldol reaction.

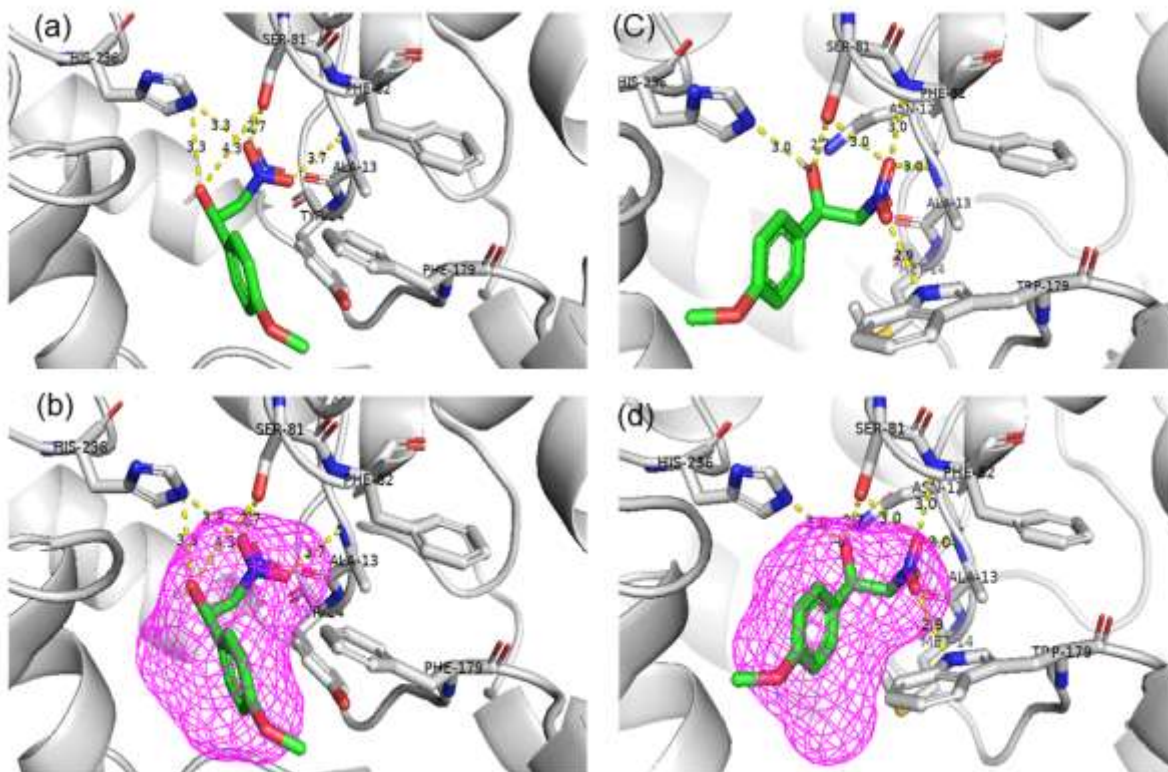


**Figure S193:** Molecular docking of **2m** with (a) WT and (c) Y14M-F179W depicts the H-bonding network. The product cavities are shown in (b) and (d)

#### 4. Supporting tables

**Table S1:** List of primers employed in the above work. Italicized nucleotides are the site of mutation.

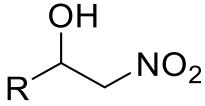
Name	Sequence
Y14F- FP	G TTCATAATGCG <i>TTT</i> CACGGTGC GTG
Y14F - RP	CACGCACCGTG <i>AA</i> ACGCATTATGAAC
F179N-FP	GTCAAGGCAGC <i>AACT</i> TTACCGAGGAT
F179N-RP	ATCCTCGGTAAAG <i>TTG</i> CTGCCTTGAC
F179W - FP	GTCAAGGCAGC <i>TGG</i> TTTACCGAGGAT
F179W - RP	ATCCTCGGTAAAC <i>C</i> AGCTGCCTTGAC

**Table S2:** Enantioselective synthesis of (*R*)-2-nitrophenyl ethanol catalysed by F179 and Y14 saturation library variants.

S. No	Variants	1 h		2 h		3 h	
		% conv	% <i>ee</i>	% conv	% <i>ee</i>	% conv	% <i>ee</i>
1	WT	17.45	97.5	23.31	96.32	24.45	96.24
2	F179A	3.09	98.77	8.97	98.10	13.01	98.11
3	F179H	6.3	98.3	11.01	97.29	12.09	95.9
4	F179S	5.5	94.32	7.94	95.1	8.19	96.39
5	F179C	2.68	96.97	3.78	97.74	3.78	97.96
6	F179P	0.15	7.04	0.25	3.33	0.60	2.86
7	F179R	0.39	1.64	0.96	6.94	1.00	3.83
8	F179N	6.26	97.34	8.47	96.87	10.13	94.39
9	F179Q	4.91	94.43	2.14	67.89	0.34	86.25
10	F179G	1.57	79.06	2.72	78.23	3.11	77.44
11	F179I	0.50	10.64	1.00	32.62	1.84	5.10
12	F179E	0.25	4.35	0.78	0.81	1.27	7.56
13	F179L	6.52	98.62	7.32	97.49	7.82	96.72
14	F179M	0.34	97.52	0.72	94.64	0.99	96.99

15	F179T	2.56	77.35	4.19	83.59	6.1	81.21
16	F179V	1.85	96.89	4.18	96.95	3.79	97.18
17	F179K	4.82	95.30	7.22	95.74	9.19	94.1
18	F179Y	0.85	83.8	1.3	84.42	2.16	91.3
19	F179W	16.58	97.1	17.37	96.20	17.9	91.11
20	F179D	0.25	5.17	0.59	1.45	1.13	3.98
21	Y14A	28.61	87.91	33.2	89.37	34.61	86.79
22	Y14C	29.84	95.32	32.53	93.96	34.05	91.95
23	Y14Q	22.01	88.35	3.33	-0.13	3.05	-38.35
24	Y14H	0.30	28.21	0.73	36.56	1.55	53.65
25	Y14N	0.77	4.11	0.98	9.84	1.3	2.8
26	Y14P	0.8	25	1.36	33.13	1.95	2.40
27	Y14S	0.23	11.86	0.65	28.14	1.06	37.5
28	Y14D	7.42	88.20	1.55	33.90	1.64	30.99
29	Y14F	30.65	97.00	32.89	94.68	33.95	92.60
30	Y14M	22.90	96.04	28.16	94.26	30.38	91.23
31	Y14V	11.79	77.89	18.58	76.92	24.83	70.50
32	Y14W	10.31	88.53	13.21	85.88	15.01	82.92
33	Y14L	22.81	93.54	23.01	87.43	23.47	83.84
34	Y14E	5.31	70.44	6.2	64.88	6.86	62.7
35	Y14T	14.57	87.82	15.1	88.17	15.4	86.09
36	Y14K	5.46	97.50	10.72	96.57	10.63	95.62
37	Y14G	8.52	94.16	12.94	92.18	13.02	73.73
38	Y14I	0.52	-5.82	0.08	28.57	0.01	100
39	Y14R	0.19	88.41	0.13	95.74	0.01	-100

**Table S3:** HPLC conditions and retention times of aldehydes and racemic  $\beta$ -nitroalcohols  
 (All the samples analyzed in an HPLC (Agilent) using Chiralpak® IB chiral column using 1 mL/min flow rate).

	HPLC conditions		Retention time	Retention time
	<i>n</i> -hexane: 2-propanol (v/v)		of aldehyde (min)	of ( <i>R</i> ) and ( <i>S</i> )-BNAs (min)
Ph	↑ 90:10 ↓		4.7	10.9, 12.4
<i>trans</i> -cinnamyl Ph			6.9	24.2, 22.8
3-chloro Ph			5.3	10.4, 11.8
4-chloro Ph			5.4	10.8, 12.5
4-fluoro Ph			5.2	9.7, 10.8
3-methyl Ph			4.9	9.1, 9.7
4-methyl Ph			4.9	9.9, 11.5
4-nitro Ph			10.4	22.1, 25.6
3-methoxy Ph			6.1	19.2, 21.7
2,4-dimethoxy Ph			97:3 for 6 minutes followed by 90:10	8.3
3,4,5-tri methoxy Ph	90:10	7.2	13.6, 15.7	
4-benzyloxy Ph	80:20 90:10	8.1	18.2, 20.4	

**Table S4:** *Az*HNL variants (62.5 U) catalysed enantioselective synthesis of (*R*)- $\beta$ -nitroalcohols.

Product	WT	F179H	F179N	F179L	F179W	Y14A	Y14M	Y14F	Y14C	Y14G	Y14L	Y14T
2a	61 <b>98</b>	53 <b>97</b>	76 <b>96</b>	44 <b>85</b>	47 <b>97</b>	57 <b>91</b>	75 <b>97</b>	68 <b>98</b>	49 <b>98</b>	39 <b>87</b>	69 <b>96</b>	39 <b>90</b>
2b	7 <b>82</b>	5 <b>24</b>	8 <b>91</b>	8 <b>50</b>	13 <b>91</b>	ND	8 <b>77</b>	13 <b>88</b>	1 <b>83</b>	ND	9 <b>88</b>	ND
2c	4 <b>77</b>	ND	3 <b>35</b>	ND	ND	ND	ND	0.4 <b>86</b>	ND	ND	ND	ND
2d	18 <b>86</b>	12 <b>5</b>	44 <b>92</b>	15 <b>43</b>	11 <b>80</b>	10 <b>44</b>	24 <b>91</b>	33 <b>95</b>	7 <b>84</b>	5 <b>15</b>	22 <b>77</b>	7 <b>25</b>
2e	48 <b>7</b>	45 <b>0.3</b>	50 <b>33</b>	43 <b>4</b>	39 <b>11</b>	41 <b>11</b>	45 <b>13</b>	44 <b>26</b>	30 <b>11</b>	40 <b>7</b>	44 <b>11</b>	45 <b>2</b>
2f	12 <b>87</b>	1 <b>57</b>	5 <b>82</b>	3 <b>68</b>	10 <b>89</b>	ND	5 <b>98</b>	12 <b>93</b>	2 <b>83</b>	1 <b>56</b>	3 <b>73</b>	1 <b>70</b>
2g	54 <b>97</b>	13 <b>13</b>	64 <b>95</b>	39 <b>82</b>	41 <b>95</b>	40 <b>87</b>	59 <b>97</b>	62 <b>98</b>	45 <b>96</b>	38 <b>85</b>	51 <b>96</b>	41 <b>86</b>
2h	8 <b>90</b>	4 <b>26</b>	58 <b>98</b>	44 <b>96</b>	30 <b>99</b>	39 <b>94</b>	55 <b>92</b>	51 <b>94</b>	33 <b>99</b>	16 <b>85</b>	53 <b>98</b>	19 <b>83</b>
2i	31 <b>98</b>	4 <b>20</b>	49 <b>98</b>	37 <b>93</b>	19 <b>99</b>	13 <b>96</b>	46 <b>97</b>	51 <b>98</b>	10 <b>94</b>	5 <b>64</b>	38 <b>92</b>	6 <b>61</b>
2j	55 <b>95</b>	7 <b>74</b>	58 <b>96</b>	39 <b>98</b>	40 <b>99</b>	28 <b>94</b>	55 <b>99</b>	61 <b>93</b>	41 <b>98</b>	11 <b>97</b>	39 <b>99</b>	11 <b>88</b>
2k	46 <b>70</b>	17 <b>9</b>	24 <b>52</b>	30 <b>7</b>	33 <b>66</b>	24 <b>14</b>	39 <b>65</b>	52 <b>80</b>	11 <b>19</b>	27 <b>3</b>	29 <b>49</b>	28 <b>2</b>
2l	ND	ND	ND	ND	ND	ND	ND	2 <b>89</b>	ND	ND	ND	ND

ND: not determined; % *ee* are highlighted in bold and % conversion is in plain.



**Table S5:** *At*HNL variants (125 U) catalysed enantioselective synthesis of (*R*)- $\beta$ -nitroalcohols.

R	WT (62.5U)	WT (125U)	F179N (62.5U)	F179N (125U)	F179W (62.5U)	F179W (125U)	Y14M (62.5U)	Y14M (125U)	Y14F (62.5U)	Y14F (125U)
Ph	61 <b>98</b>	-	76 <b>96</b>	82 <b>97</b>	47 <b>97</b>	58 <b>99</b>	75 <b>97</b>	84 <b>93</b>	68 <b>98</b>	75 <b>99</b>
trans cinnamyl	7 <b>82</b>	-	8 <b>91</b>	-	13 <b>91</b>	8 <b>81</b>	8 <b>77</b>	-	13 <b>88</b>	-
4-Fluoro Ph	ND	4 <b>77</b>	ND	3 <b>35</b>	ND	3 <b>56</b>	ND	5 <b>91</b>	ND	0.4 <b>86</b>
4-Chloro Ph	18 <b>86</b>	-	44 <b>92</b>	-	11 <b>80</b>	-	24 <b>91</b>	-	33 <b>95</b>	53 <b>91</b>
4-Nitro Ph	48 <b>7</b>	-	50 <b>33</b>	-	39 <b>11</b>	-	45 <b>13</b>	-	44 <b>22</b>	53 <b>16</b>
2,4-Dimethoxy Ph	12 <b>87</b>	-	5 <b>82</b>	-	10 <b>89</b>	-	5 <b>98</b>	-	12 <b>93</b>	27 <b>98</b>
3-Chloro Ph	54 <b>97</b>	-	64 <b>95</b>	72 <b>98</b>	41 <b>95</b>	-	59 <b>97</b>	-	62 <b>98</b>	-
3-Methyl Ph	8 <b>90</b>	-	58 <b>98</b>	59 <b>98</b>	30 <b>99</b>	-	55 <b>92</b>	-	51 <b>94</b>	-
4-Methyl Ph	31 <b>98</b>	-	49 <b>98</b>	-	19 <b>99</b>	-	46 <b>97</b>	-	51 <b>98</b>	61 <b>99</b>
3-Methoxy Ph	55 <b>95</b>	-	58 <b>96</b>	-	40 <b>99</b>	-	55 <b>99</b>	-	61 <b>93</b>	65 <b>99</b>
3,4,5-Tri methoxy Ph	46 <b>70</b>	-	24 <b>52</b>	-	33 <b>66</b>	-	39 <b>65</b>	-	52 <b>80</b>	67 <b>91</b>
4-Benzyloxy Ph	ND	2 <b>70</b>	ND	3 <b>88</b>	ND	0.2 <b>38</b>	ND	7 <b>95</b>	2 <b>89</b>	5 <b>95</b>

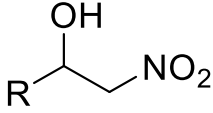
ND: not determined; – mark: not done; % *ee* is highlighted in bold and % conversion is in plain.

**Table S6:** *At*HNL double variants catalyzed enantioselective synthesis of (*R*)- $\beta$ -nitroalcohols.

R	WT (62.5U)	Y14M- F179W (62.5U)	Y14M- F179W (125U)	Y14M- F179N (200U- crude)	Y14F- F179W (200U- crude)	Y14F- F179N (200U- crude)
Ph	61 <b>98</b>	60 <b>98</b>	76 <b>99</b>	4 <b>74</b>	10 <b>18</b>	5 <b>57</b>
trans cinnamyl	7 <b>82</b>	21 <b>95</b>	24 <b>93</b>	ND	ND	ND
4-Fluoro Ph	ND	ND	3 <b>82</b>	ND	ND	2 <b>65</b>
4-Chloro Ph	18 <b>86</b>	45 <b>96</b>	56 <b>97</b>	1 <b>43</b>	2 <b>24</b>	2 <b>56</b>
4-Nitro Ph	48 <b>7</b>	49 <b>37</b>	53 <b>56</b>	24 <b>7</b>	34 <b>10</b>	23 <b>15</b>
2,4-Dimethoxy Ph	12 <b>87</b>	17 <b>97</b>	-	ND	ND	ND
3-Chloro Ph	54 <b>97</b>	52 <b>96</b>	-	4 <b>16</b>	6 <b>13</b>	6 <b>56</b>
3-Methyl Ph	8 <b>90</b>	56 <b>99</b>	-	1 <b>71</b>	2 <b>50</b>	2 <b>85</b>
4-Methyl Ph	31 <b>98</b>	56 <b>98</b>	-	1 <b>48</b>	2 <b>11</b>	1 <b>67</b>
3-Methoxy Ph	55 <b>95</b>	54 <b>99</b>	-	2 <b>61</b>	3 <b>58</b>	3 <b>60</b>
3,4,5-Trimethoxy Ph	46 <b>70</b>	48 <b>84</b>	-	ND	11 <b>86</b>	6 <b>16</b>
4-Benzyloxy Ph	ND	4 <b>78</b>	4 <b>98</b>	ND	ND	ND

ND: not determined; – mark: not done; % *ee* is highlighted in bold and % conversion is in plain.

**Table S7:** HPLC conditions and retention time of 4-methoxybenzaldehyde and racemic 1-(4-methoxyphenyl)-2-nitroethanol.

	HPLC condition	RT of aldehyde (min)	RT of ( <i>R</i> ) and ( <i>S</i> ) BNAs (min)
	<i>n</i> -hexane: 2-propanol (v/v)		
4-methoxy Ph	99:1 for 8 minutes followed by 90:10	12.1	19.7, 21.1

**Table S8:** Steady-state kinetic parameters of purified *At*HNL, Y14M and F179N for the synthesis of **2a** using benzaldehyde as the substrate.

Enzyme	$K_m$ (mM)	$V_{max}$ (U/mg)	$k_{cat}$ ( $\text{min}^{-1}$ )	$k_{cat}/K_m$ ( $\text{min}^{-1}\text{mM}^{-1}$ )
WT	1.73±0.99	1.28±0.06	35.74± 1.74	24.30± 9.73
Y14M	1.26±0.51	4.10±0.85	114.49±23.90	98.00±26.33
F179N	0.72±0.23	4.22±0.25	118.20±7.01	175.29±47.13

**Table S9:** Steady-state kinetic parameters of purified *At*HNL and Y14M-F179W for the synthesis of **2b** using *trans* cinnamaldehyde as the substrate.

Enzyme	$K_m$ (mM)	$V_{max}$ (U/mg)	$k_{cat}$ ( $\text{min}^{-1}$ )	$k_{cat}/K_m$ ( $\text{min}^{-1}\text{mM}^{-1}$ )
WT	12.05±2.09	1.28±0.16	35.84± 4.34	3.03± 0.61
Y14M-F179W	6.90±1.63	4.16±1.25	116.58±34.87	16.70±1.29

**Table S10:** Steady-state kinetic parameters of purified *At*HNL and Y14F for the synthesis of **2d** using 4-chlorobenzaldehyde as the substrate.

Enzyme	$K_m$ (mM)	$V_{max}$ (U/mg)	$k_{cat}$ ( $\text{min}^{-1}$ )	$k_{cat}/K_m$ ( $\text{min}^{-1}\text{mM}^{-1}$ )
WT	4.68±1.10	0.74±0.06	20.79± 1.53	4.63± 1.28

Y14F	1.85±0.29	3.56±0.33	99.65±9.34	55.22±14.89
------	-----------	-----------	------------	-------------

**Table S11:** Steady-state kinetic parameters of purified AtHNL and Y14F for the synthesis of **2f** using 2,4-dimethoxybenzaldehyde as the substrate.

Enzyme	$K_m$ (mM)	$V_{max}$ (U/mg)	$k_{cat}$ (min <sup>-1</sup> )	$k_{cat}/K_m$ (min <sup>-1</sup> mM <sup>-1</sup> )
WT	13.16±0.57	0.68±0.03	18.95± 0.75	1.44± 0.06
Y14F	4.95±0.98	1.48±0.29	41.45±7.98	8.41±0.99

**Table S12:** Steady-state kinetic parameters of purified AtHNL and F179N for the synthesis of **2g** using 3-chlorobenzaldehyde as the substrate.

Enzyme	$K_m$ (mM)	$V_{max}$ (U/mg)	$k_{cat}$ (min <sup>-1</sup> )	$k_{cat}/K_m$ (min <sup>-1</sup> mM <sup>-1</sup> )
WT	1.83±0.35	1.74±0.06	48.68± 1.68	27.31± 5.65
F179N	1.17±0.09	2.72±0.05	76.02±1.37	65.04±5.07

**Table S13:** Steady-state kinetic parameters of purified AtHNL and F179N for the synthesis of **2h** using 3-methylbenzaldehyde as the substrate.

Enzyme	$K_m$ (mM)	$V_{max}$ (U/mg)	$k_{cat}$ (min <sup>-1</sup> )	$k_{cat}/K_m$ (min <sup>-1</sup> mM <sup>-1</sup> )
WT	3.15±0.37	0.97±0.04	27.01± 1.06	8.68± 1.35
F179N	1.71±0.29	4.22±0.06	118.16±1.71	70.47±11.58

**Table S14:** Steady-state kinetic parameters of purified AtHNL and Y14F for the synthesis of **2i** using 4-methylbenzaldehyde as the substrate.

Enzyme	$K_m$ (mM)	$V_{max}$ (U/mg)	$k_{cat}$ (min <sup>-1</sup> )	$k_{cat}/K_m$ (min <sup>-1</sup> mM <sup>-1</sup> )
WT	2.67±0.53	0.71±0.06	19.94± 1.54	7.60± 1.08
Y14F	1.12±0.05	1.82±0.13	50.55±3.54	45.50±4.97

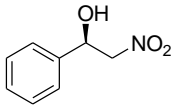
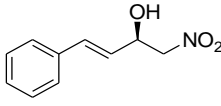
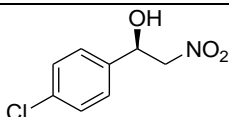
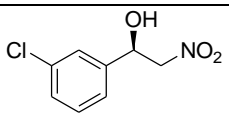
**Table S15:** Steady-state kinetic parameters of purified *At*HNL and Y14F for the synthesis of **2k** using 3,4,5-trimethoxybenzaldehyde as the substrate.

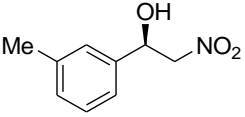
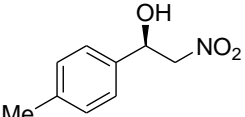
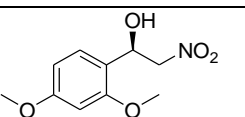
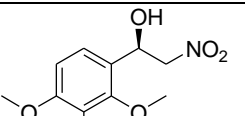
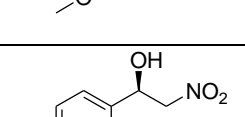
Enzyme	$K_m$ (mM)	$V_{max}$ (U/mg)	$k_{cat}$ ( $\text{min}^{-1}$ )	$k_{cat}/K_m$ ( $\text{min}^{-1}\text{mM}^{-1}$ )
WT	30.21±5.68	4.06±0.24	113.69± 6.61	3.83± 0.56
Y14F	14.71±1.91	6.73±0.58	188.35±16.29	12.86±0.81

**Table S16:** Steady-state kinetic parameters of purified *At*HNL and Y14M-F179W for the synthesis of **2m** using 4-methoxybenzaldehyde as the substrate.

Enzyme	$K_m$ (mM)	$V_{max}$ (U/mg)	$k_{cat}$ ( $\text{min}^{-1}$ )	$k_{cat}/K_m$ ( $\text{min}^{-1}\text{mM}^{-1}$ )
WT	2.10±0.36	6.23±0.81	174.37± 22.78	83.51± 6.25
Y14M-F179W	0.68±0.08	11.97±1.81	335.16±50.72	493.11±19.33

**Table S17:** The fold increase in the catalytic efficiency of the variants in comparison to the wild type.

Products	Variant	Fold increase in the variant's catalytic efficiency than the wild type
	Y14M	4.03
	F179N	7.21
	Y14M-F179W	5.51
	Y14F	11.92
	F179N	2.38

	F179N	8.12
	Y14F	5.99
	Y14F	5.84
	Y14F	3.36
	Y14M-F179W	5.9

**Table S18:** Docking results of **2m** with WT and Y14M-F179W shows the differential interactions and binding energy

Interactions	WT_4-MeONPE docked	Y14M_F179W_4-MeONPE docked
H-bonds	-OH of 4-MeONPE with O $\gamma$ of Ser81: 4.3	--OH of 4-MeONPE with O $\gamma$ of Ser81: 2.7
	-OH of 4-MeONPE with His236-N $\epsilon$ 2: 3.3	-OH of 4-MeONPE with His236-N $\epsilon$ 2: 3.0
	-NO <sub>2</sub> of 4-MeONPE with His236-N $\epsilon$ 2: 3.3	-NO <sub>2</sub> of 4-MeONPE with His236-N $\epsilon$ 2:
	-NO <sub>2</sub> of 4-MeONPE with O $\gamma$ of Ser81: 2.7	-NO <sub>2</sub> of 4-MeONPE with O $\gamma$ of Ser81: 3.0
	-NO <sub>2</sub> of 4-MeONPE with Ala11 main chain NH: 3.7	-NO <sub>2</sub> of 4-MeONPE with Ala11 main chain NH: 3.0
		-NO <sub>2</sub> of 4-MeONPE with Phe82 main chain NH: 3.0

		-NO <sub>2</sub> of 4-MeONPE with ε <sup>1</sup> NH of Trp179: 2.9
Cavity	89 pts, 154 Å <sup>3</sup> (cavity no 10)	69 pts, 135 Å <sup>3</sup> (cavity no 15)
Binding energy	- 6.2 kcal. mol <sup>-1</sup>	- 4.8 kcal. mol <sup>-1</sup>
Explanation	<p>The binding energy suggest a tight binding with the product</p> <p>Bigger cavity size probably lacks specific interaction</p> <p>H-bonding are not strong compared to the variant</p>	<p>Comparatively loose binding with the product perhaps helps in releasing</p> <p>Relatively smaller cavity might be helping in specific interaction with the product</p> <p>H-bonding are strong compared to the wild type.</p> <p>Additional H-bond found between Trp NH with NO<sub>2</sub> of the product</p> <p>The orientation of the product is changed from the WT to the double mutant. The altered orientation of the product shows a new interaction, i.e., H-bond between side chain NH of W179 and the product.</p>

## References

1. B. Vishnu Priya, D. H. Sreenivasa Rao, R. Gilani, S. Lata, N. Rai, M. Akif and S. Kumar Padhi, *Bioorg. Chem.*, 2022, **120**, 105594.
2. D. H. S. Rao and S. K. Padhi, *ChemBioChem*, 2019, **20**, 371–378.
3. Chatterjee, D. H. S. Rao and S. K. Padhi, *Adv. Synth. Catal.*, 2021, 363, 5310–5318
4. R. Boobalan, G. H. Lee and C. Chen, *Adv. Synth. Catal.*, **2012**, 354, 2511–2520
5. Jianyou Mao, Xin Nie, Min Wang, Qian Wang, Bing Zheng, Qinghua Bian and Jiangchun Zhong, *Tetrahedron: Asymmetry*, **2012**, 23, 965–971.
6. K. I. Fuhshuku, Y. Asano, *J. Biotechnol.* **2011**, 153, 153–159
7. Chloe Vovard-Le Bray, Fan Jiang, Xiao-Feng Wu, Jean-Baptiste Sortais and Christophe Darcel, *Tetrahedron Lett.*, **2010**, 51, 4555–4557